

# Proceedings

## Second Webinar

### Expert Talk (Magnetron) & Young Researchers' Talk Series (Reltron and Relativistic BWO)

5 September 2020, Saturday

#### Editors:

Vishal Kesari

B N Basu



**Thinkers in Vacuum Electron Devices Group  
India**

## **Programme of the Webinar**

**Date:** 5 September 2020, Saturday

**Time:** 05:00 – 6:30 pm

**Convener:** Mr. Raj Singh

### **Session 1 - Expert Talk**

**Chair:** Dr. Lalit Kumar

<b>Duration</b>	<b>Topic of deliberation</b>	<b>Speaker</b>
05:00 - 05:05 pm	Opening Remark	Dr. Lalit Kumar
05:05 - 05:40 pm	Past and Present Status of the Magnetron Development in the Country and the Efforts at CSIR-CEERI Leading to the Product Development for the Users	Dr. S Mourya

### **Session 2 – Young Researcher's Talk Series**

#### **Research contributions of younger researchers in VEDs**

**Host:** Dr. N Purushothaman

<b>Duration</b>	<b>Topic of deliberation</b>	<b>Speaker</b>
05:40 - 06:00 pm	Compact and Efficient High Power Microwave Source — Reltron	Dr. Manpuran Mahto
06:00 - 06:20 pm	RF Pulse Shortening Studies of High Power Relativistic BWO Using MAGIC-PIC Simulation	Mr. Mumtaz Ansari
06:20 - 06:30 pm	Vote of thanks	Dr. B K Shukla

## **Organizing Committee**

<b>Name</b>	<b>Designation</b>	<b>Affiliation</b>	<b>Role</b>
Dr. Lalit Kumar	Distinguished Research Advisor	Siddaganga Institute of Technology, Tumkur	Chair
Raj Singh	Scientist	Institute of Plasma Research, Gandhinagar	Convener
Prof. B N Basu	Adjunct Professor	Supreme Knowledge Foundation Group of Institutions	Advisor
Dr. B K Shukla	Scientific Officer G	Institute of Plasma Research, Gandhinagar	Vote of Thanks
Dr. Vishal Kesari	Scientist E	Microwave Tube Research and Development Centre, Bangalore	Editor Proceedings
Dr. Uttam Kumar Goswami	Post-Doctoral Fellow	Institute of Plasma Research, Gandhinagar	Webinar Coordinator
Dr. N Purushothaman	Scientist C	Central Electronics Engineering Research Institute, Pilani	Host

# Session 1

## Expert Talk

### Topic of Deliberation

Past and Present Status of the Magnetron Development in the Country and the Efforts at CSIR-CEERI Leading to the Product Development for the Users

### Speaker

Dr. S Mourya



**Dr. Shivendra Maurya**

Principal Scientist

CSIR- Central Electronics Engineering Research Institute

Pilani-333031, Rajasthan, India

Email: sm.ceeri@gmail.com, smaurya@ceeri.res.in

## **Past and Present Status of the Magnetron Development in the Country and the Efforts at CSIR-CEERI Leading to the Product Development for the Users**

The magnetron is a high-power cross field vacuum tube, that works as self-excited microwave oscillator and finds applications in many fields where high-power microwave is required, such as meteorological radar, marine navigation, particle accelerator and domestic and industrial heating. When the operating frequency is in microwave range and the frequency stability is not of prime concern the magnetron may be the best solution as compared to other microwave tubes. Magnetrons have been the beacon of success for the British armies against the Nazi's attack in the 1940s. Since then, they have continued to be a significant vacuum electron device (VED) whenever portability, efficiency and ease of development are a pre-requisite for any device. The journey has been long and results of numerous efforts from the scientific and research communities from time to time. The pioneering scientific research in magnetron is an outcome of some noteworthy scientists like A W Hull [1] in USA, K Posthumus [2-4] in Holland, E C S Megaw [5-7] and F B Pidduck [8] in Britain, G R Kilgore [9] in US, Hans Erich Hollman in Germany, K Okabe with H Yagi in Japan, and many other researchers almost over

a decade (1929 – 1936). Following the series of developments, the most significant and widespread design breakthrough for high-power magnetron was the modern cavity magnetron structure proposed by J T Randall and H A H Boot in 1940. They united the separate units, namely the resonant circuit and the anode-cathode assembly, into a single unit and placed the construction in a vacuum enclosure.

In India, some work on magnetrons and related technology started with establishment of Institute of Radio Physics under University of Calcutta in early fifties [10]. Later Dr. Amarjit Singh initiated work on multi-cavity magnetron at National Physical Laboratory, New Delhi, prior to joining CEERI, Pilani. As Scientist-in-Charge and later on as Director, of CEERI, he increased the pace of work on Cavity Magnetrons (Hole and Slot type) from early sixties. The first major work was on S-band 500 kW for Indian Navy. They were batch produced at CEERI and about 75 tubes were delivered to Indian Navy. Then came S-band 1.0 MW Magnetron for Air Force. This had six variants in frequency (approx. 2910 to 3100 MHz). The technology was transferred to CEL. Later on, 35 GHz mm-wave magnetron, X-band, 200 kW coaxial magnetron, 1.0/2.0/2.6/3.0 MW S-band Tunable pulse magnetron were also designed and developed. The technical know-how of 2.6 MW S-band magnetron has been shared with M/s Panacea Medical Pvt. Ltd. Bengaluru for production. Currently, low power CW magnetron, spatial harmonics magnetrons, and system based on low power CW magnetrons are also being explored at CSIR-CEERI.

Beside CSIR-CEERI, MTRDC Bengaluru and BARC, Mumbai are also involved in design and development of S-band relativistic magnetrons. Institute like BITS Pilani, Hyderabad campus started research work on phase locking of magnetrons. Recently established SAMEER, Guwahati has also started design and development of S-band 4MW pulse tunable magnetron for their LINAC program.

**References:**

- [1] A. W. Hull, "The Magnetron", Journal of the American Institute of Electrical Engineers, Vol.40, Issue No: 09, pp:715-723, Sept. 1921.
- [2] K. Posthumus, "Magnetron Oscillations of a New Type," Nature, 1934, pp. 179.
- [3] K. Posthumus, "Oscillations in a Split Anode Magnetron," The Wireless Engineer, 12, pp: 126-132, 1935.
- [4] K. Posthumus and E. C. S. Megaw, "Magnetron Oscillations," Nature, 135, 3422, 1935, pp: 914-914.
- [5] E. C. S. Megaw, "Note on the theory of the Magnetron Oscillator", Proceedings of the Institute of Radio Engineers, Vol. 21, Issue. 12, pp: 1749-1751, Dec. 1933.
- [6] E. C. S. Megaw, "Magnetron Oscillations," Nature, pp: 324-325, 1934.
- [7] F. B. Pidduck, "Electrical Notes: Oscillations with a Split-Anode Magnetron", pp: 241-251.
- [8] F. B. Pidduck, "Magnetron Oscillations," Nature, pp: 945-946, June 1936.
- [9] G. R. Kilgore, "Magnetostatic Oscillators for generation of ultra-short waves," Proceedings of the Institute of Radio Engineers, Vol.20, Issue:11, pp: 1741-1751, Nov. 1932.
- [10] Calcutta University Annual report 1956-57, published in 1958.

## **Session 2**

# **Young Researcher's Talk Series**

**Research contributions of younger researchers in VEDs**

### **Topic of Deliberation 1**

Compact and Efficient High Power  
Microwave Source — Reltron

### **Speaker 1**

Dr. Manpuran Mahto

### **Topic of Deliberation 2**

RF Pulse Shortening Studies of High  
Power Relativistic BWO Using  
MAGIC-PIC Simulation

### **Speaker 2**

Mr. Mumtaz Ansari

**Dr. Manpuran Mahto**

Assistant Professor

Department of Electronics & Communication Engineering  
National Institute of Technology (NIT), Patna, Bihar, INDIA

Email: [mmahto@nitp.ac.in](mailto:mmahto@nitp.ac.in)

## **Compact and Efficient High Power Microwave Source — Reltron**

Reltron is a narrowband megawatt (MW) HPM source, which is compact and efficient. Reltron fulfils the vital requirements of a high-efficiency microwave source, such as, intense electron bunching, least energy spread and efficient RF extraction without breakdown. It is developed through the exploration of the cavity of the split-cavity oscillator (SCO), which is comparable to the klystron cavity in nature. Its operating principle is also similar to that of the conventional klystron where the RF power is coupled out through a series of output cavities from the intense electron bunches. However, it is primarily distinct in two ways: (i) the bunching process is different and (ii) the intense electron bunches are reaccelerated to the higher energy by applying an additional DC potential. The external DC magnetic field is not required in a reltron and the self-magnetic field developed in the RF interaction cavity is used to focus the electrons in the longitudinal direction. Long pulses, upto microsecond duration can be generated, which enables it to radiate both high RF peak power and high RF energy per pulse. The other features of the tube include its frequency tunability and inherent energy storage capability and its compatibility with the external power conditioning elements and pulse forming networks.

**M. A. Ansari**

Research Scholar, Center of Research in Microwave Tubes  
Department of Electronics Engineering  
Indian Institute of Technology (BHU), Varanasi  
Varanasi-221005, Uttar Pradesh, INDIA  
Email: mumtazaa.rs.ece15@itbhu.ac.in

## **RF Pulse Shortening Studies of High Power Relativistic BWO Using MAGIC-PIC Simulation**

The MAGIC-PIC simulation studies were performed to examine the beam-wave interaction behavior of a high power X-band relativistic backward-wave oscillator (RBWO) operating at low guiding magnetic field and to understand the causes of RF pulse shortening therein. The various possible causes of RF pulse shortening such as beam degradation, high electric field electron emission, secondary electron emission and collector plasma formation were analyzed first individually and then combined. The saturated RF power of  $\sim 0.80$  GW was generated only for 50 ns degrading after  $\sim 73$  ns by the effect of beam degradation at the typical low guiding magnetic field of 0.61 T. The RF power was additionally suppressed to  $\sim 0.775$  GW and terminated after  $\sim 65$  ns due to the electrons emitted in high RF electric field from the surfaces of RR and SWS. The secondary emitted electrons did not affect the RF power, while the RF power pulse duration was reduced by  $\sim 3$  ns in addition to the beam degradation. Finally, the collector plasma further shortened the RF power pulse duration by  $\sim 9$  ns and stopped generating the RF signal by  $\sim 64$  ns. At last, the combined study, including all the causes under consideration, additionally showed the RF

output power generation reduced by ~100 MW to ~0.70 GW at ~9.52 GHz for ~40 ns with the power conversion efficiency ~21.3 % and the RF pulse duration terminated after ~63 ns.

The presentation is based on:

M. A. Ansari and M. Thottappan, "Studies of pulse shortening phenomena and their effects on the beam-wave interaction in an RBWO operating at low Magnetic field," *IEEE Transactions on Plasma Science*, vol. 48, no. 2, pp. 0426-0432, Feb. 2020.

## **Topic of Deliberation**

Vote of Thanks

## **Proposed by**

Dr. B K Shukla



**Dr. Braj Kishore Shukla**

Scientific Officer – G  
(Head, High Power ECRH systems Division)  
Institute for Plasma Research  
Bhat, Gandhinager – 382428, Gujarat, INDIA  
Email: [shukla@ipr.res.in](mailto:shukla@ipr.res.in), [shukla.ipr@gmail.com](mailto:shukla.ipr@gmail.com)

Dear All,

It's my pleasure to deliver the vote of thanks to the second webinar of Vacuum Electron Devices - VED (September 05, 2020).

First of all I would like to thank Professor BN Basu for proving an excellent platform to discuss on the technology of vacuum tubes. In fact this platform has enormous potential for researcher, young researcher and participating industries. This platform provides the opportunity to everyone to discuss the ideas and technical developments on vacuum tubes in country. I thank you Basu ji for his remarkable effort.

On today's webinar-2, I would like to thank Dr. Lalit Kumar for chairing first session. I thank Dr. Shivendra Maurya from CEERI-Pilani for his excellent talk on "Past and present status of the magnetron development in the country and the efforts of CSIR-CEERI". He presented very professionally on the magnetron from the history to current status and future of advance magnetron. I thank Dr. Maurya ji for his presentation.

I thank Dr. N. Purushothaman for hosting the second session of webinar. I thank Dr. Manpuran Mahto for delivering an interesting talk on Compact and efficient high power microwave source – Reltron. A detailed simulation have been presented with the explanation on formation of the virtual cathode. I thank Dr. Mahto for his talk. I thank Mr. Mumtaz Ali Ansari for presenting his research work on BWO.

I thank Dr. S.N. Joshi, Prof. BN Basu, Dr. L M Joshi, Dr. Lalit Kumar, Dr. K P Ray, Dr. KS Bhat, and others for providing valuable technical inputs after the presentations.

I thank Mr. Raj Singh, Dr. Vishal Kesari and their team for organizing the second webinar successfully. Finally I thank all the participants including

**Proceedings Second Webinar**

**Expert Talk (Magnetron) & Researchers' Talk Series (Reltron and Relativistic BWO)**

engineers from M/s Panacea Medical Technologies Pvt. Ltd. for attending the webinar and participated in the technical discussion.

Thanks one and all!

**Annexure I:**  
**Expert Talk Slides**



INNOVATE

DEVELOP

DELIVER

# **Past and Present Status of the Magnetron Development in the Country and the Effort at CSIR-CEERI leading to the Product Development for the users**

**Shivendra Maurya**

sm.ceeri@gmail.com

**Vacuum Electron Devices Design Group  
CSIR-Central Electronics Engineering Research  
Institute Pilani, Rajasthan, India**



INNOVATE

DEVELOP

DELIVER

**“A life of  
Joy and happiness  
is possible only  
on the basis of  
knowledge and science.”**

*Dr. Sarvepalli Radhakrishnan*



**Happy teacher's day!!**



# Outline

INNOVATE

DEVELOP

DELIVER

- **Introduction**
- **Evolution of magnetron in the country**
- **Past achievements of CSIR-CEERI**
- **Research and Development status in the country**
- **Effort toward product/system development**
- **Bottleneck**
- **Acknowledgement**

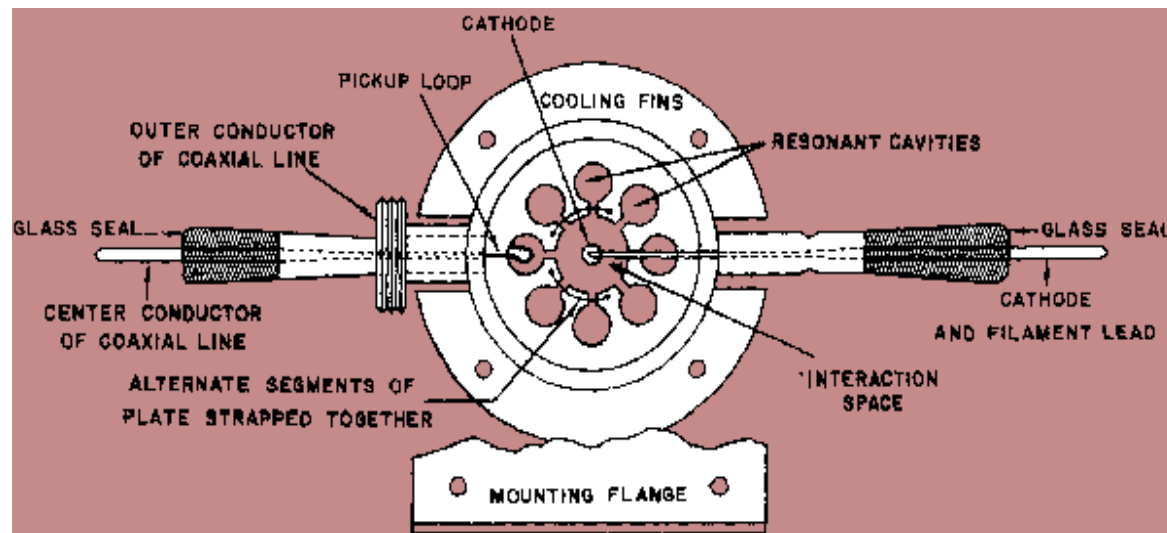
# Introduction

INNOVATE

DEVELOP

DELIVER

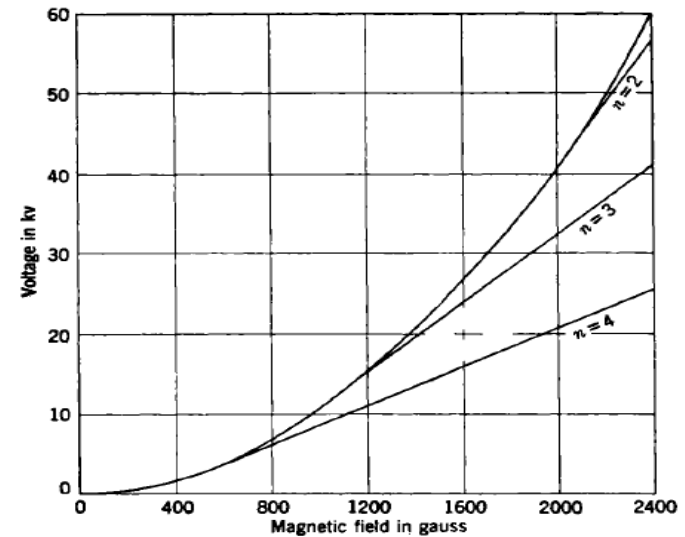
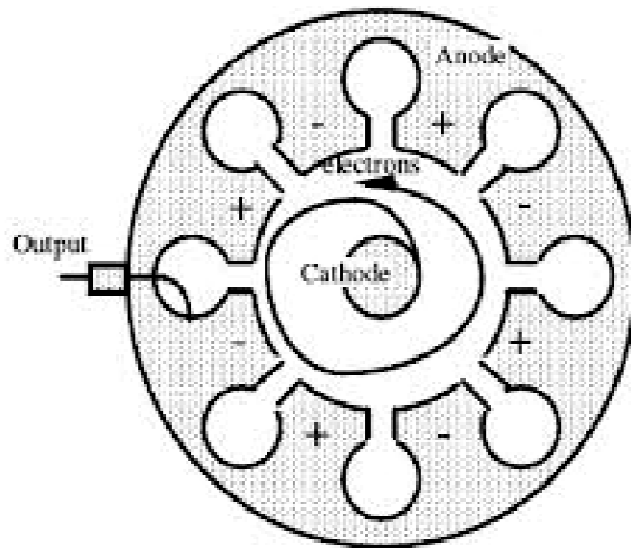
- ✓ Magnetrons are self-excited oscillators.
- ✓ Potential Energy of electron is converted into RF output power.
- ✓ Conversion takes place in the interaction space
- ✓ Crossed field
- ✓ Highly efficient



INNOVATE

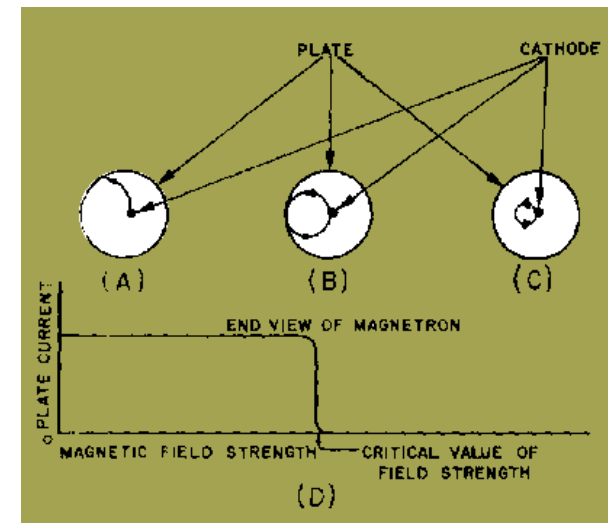
DEVELOP

DELIVER



$$V_c = \frac{eB^2 r_a^2}{8m} \left[ 1 - \left( \frac{r_c}{r_a} \right)^2 \right]^2$$

$$V_T = \frac{\pi c r_a^2}{n\lambda} \left( 1 - \frac{r_c^2}{r_a^2} \right) B - \left( \frac{2\pi^2 c^2 r_a^2 m}{e\lambda^2 n^2} \right)$$



[1] Samuel Y. Liao "Microwave Electron-Tube Devices" Prentice-Hall Inc., New Jersey, 1988.

[2] R.S.H. Boulding, "The Resonant Cavity Magnetron", Chapter 7, New York, NY, USA, D. Van Nostrand company Inc., 1952.



## History of Magnetron (contd...)

INNOVATE

DEVELOP

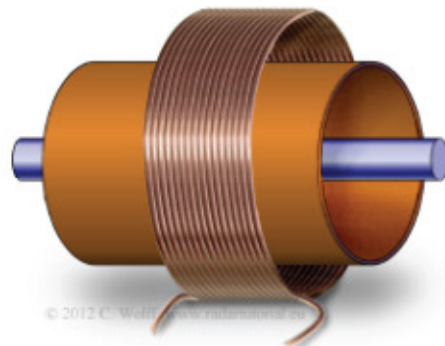
DELIVER

1921: Heinrich Greinacher tried to use a cylindrical arrangement of anode with co-axial cathode and magnetic field to measure  $e/m$  ratio.

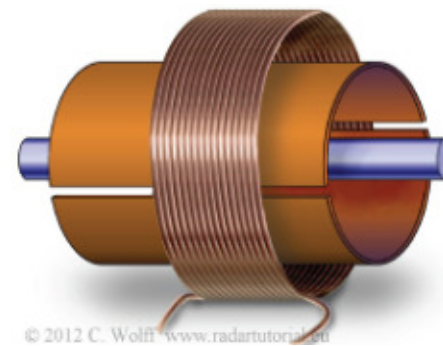
Initial device failed due to poor vacuum and cathode

1921: Albert W. Hull at General Electric company used this experimental setup, investigated the motion of electron under axial magnetic field and noticed the possibility of RF generation. He called his novel device “MAGNETRON”

1924: Erich Habann investigated independently the magnetron for high frequency oscillation and used multi-segment anode.



Model of Hull's anode magnetron



Model of Habann's split magnetron

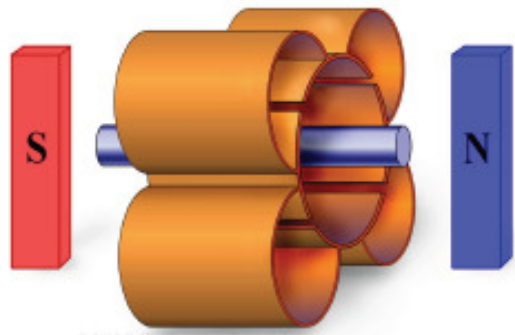
INNOVATE

DEVELOP

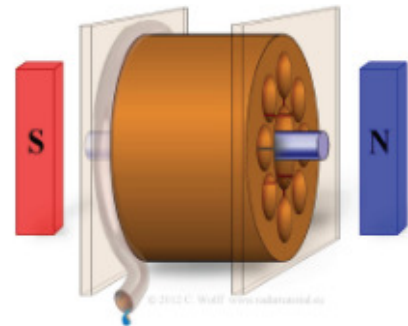
DELIVER

1935: Hans Erich Hollmann filed a patent on magnetron in 1935, and US patent was granted in 1938, well ahead of John Randall and Boot's work in 1940

1940: The modern multi-cavity magnetron built by two engineers from the University in Birmingham, John Randall and Henry Boot. They used more than four cavities to increase the effectiveness of RF generation. It was a milestone in the sub-marine war against Germany by mid-1940



Model of Hollmann's multi-cavity magnetron



Model of multi-cavity magnetron by Randall and Henry Boot

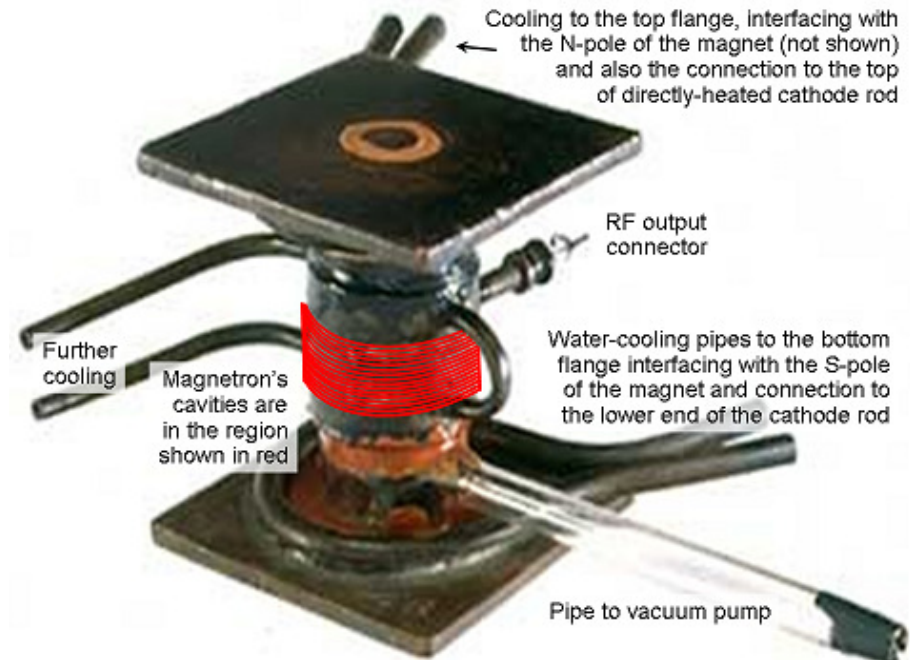
INNOVATE

DEVELOP

DELIVER



Figure 1. H. A. H. Boot (l) and J. T. Randall in their laboratory after WW II. Boot has in his hands a six-cavity anodic block.



## Abstract

It is a common belief by many people that the resonant-cavity magnetron was invented in February 1940 by Randall and Boot from Birmingham University. In reality, this is not the full story. Rather, it is a point of view mostly advocated by the winners of the Second World War, who gained a great benefit from this microwave power tube (thanks to a two-orders-of-magnitude increase of power) in the Battle of the Atlantic, in night bombing until the final collapse of the German Reich, and in many other operations. This paper discusses the contributions by other nations, mainly France, but also Germany, Japan, The Netherlands, the Czech Republic, the USSR, and even more, to the cavity magnetron and to its roots.

*Yves Blanchard, Gaspare Galati, and Piet van Genderen, Consulting engineer and historian, retired from Thales (France), "The Cavity Magnetron: Not Just a British Invention" IEEE Antennas and Propagation Magazine, Vol. 55, No. 5, October 2013*



# Potential application of different types of magnetrons



INNOVATE

DEVELOP

DELIVER

## L Band

0.8 – 2 GHz

Freq: 890 – 930 MHz  
Power: 30 -100 kW (p)

### Applications

- Radar systems
- Air Traffic Control

Freq: 915 MHz  
Power: 75 -100 kW (CW)

### Applications

- Industrial Heating

## S Band

2 – 4 GHz

Freq: 2.45 GHz  
Power: 1 kW (CW)

### Applications

- Domestic Oven

Freq: 2.45 GHz  
Power: 3 – 15 kW (CW)

### Applications

- Industrial Heating

Freq: 2.45 GHz  
Power: 30 – 750 kW (p)

### Applications

- Air Traffic control
- Weather Radars
- Surveillance Radars

Freq: 2.9 – 3.0 GHz  
Power: 1.0 – 5.5 MW (p)

### Applications

- Medical LINAC
- Scanning LINAC

## C Band

4 – 8 GHz

Freq: 4.5 – 5.7 GHz  
Power: 0.25 – 2.5 MW

### Applications

- Compact LINAC system

Freq: 5.2 – 5.9 GHz  
Power: 0.7 – 800 kW

### Applications

- Air Traffic control
- Weather Radars
- Beacon Transponder
- Threat Detector
- Surveillance Radars
- Frequency Agile
- Tracking Radars

## X Band

8 – 12 GHz

Freq: 9.38 – 9.44 GHz  
Power: 4.0 – 50 kW

### Applications

- Marine Radars
- Spectrum Control

Freq: 9.28 – 9.3 GHz  
Power: 0.4 – 2.7 MW

### Applications

- LINAC systems

Freq: 8.5 – 9.7 GHz  
Power: 70 – 325 kW

### Applications

- Air Traffic control
- Weather Radars
- Beacon Transponder
- Threat Detector

## Ku Band

12 – 18 GHz

Freq: 11.9 – 17.5 GHz  
Power: 2.5 – 250 kW

### Applications

- Air Traffic control

Freq: 12.8 – 16.5 GHz  
Power: 0.5 – 250 kW

### Applications

- Threat Detector



## Potential application of different types of magnetrons



INNOVATE

DEVELOP

DELIVER

- Naval Radar
- Missile Guidance Radar
- Police Radar
- Domestic oven
- Water Based Adhesive Drying
- Ore Processing
- Waste Treatment
- ATC Radars
- Industrial Heating
- Medical
- Autoclave
- Microwave assisted plasma generation
- MPCVD -diamond growth
- Space solar power station



# Current Research Issues on different types of magnetron

INNOVATE

DEVELOP

DELIVER

By Steve Bush 22nd January 2016

## The future of microwave cooking is solid-state

Microwave cookers are about to change as magnetrons are replaced by more flexible solid-state energy sources – or so says [RF power transistor maker Ampleon](#), which was part of NXP until last year.

## Replacing the magnetron with solid-state devices in microwave ovens

29 May 2019 Telecoms, Datacoms, Wireless, IoT

By Mark Patrick, Mouser Electronics.

### Magnetron vs. SSRFE Transistor

**DIFFICULT TO CONTROL:** Intermediate energy levels are created between alternating full and zero power. Also, absorbed energy cannot be discerned from reflected power, which makes it impossible to control the overall amount of energy delivered. Consequently, food is not uniformly cooked.

**BULKY / HIGH VOLTAGE:** Large size and energy intensive operation limits innovative design options for next gen microwave ovens.

**INEFFICIENT:** Power is increasingly lost as the magnetron ages, so it takes longer to cook the same dish as time goes on.

**DEGRADES OVER TIME:** Over three to four years the output power of a magnetron will reduce by as much as 30%.

**INCONSISTENT:** The magnetron lacks the ability to sense changing load conditions and energy absorption from food, resulting in similar dishes being cooked differently each time.



**PRECISE:** Ability to tailor the frequency, phase and output power to suit cooking a specific food, or even multiple foods placed in the cavity.

**SMALL FORM FACTOR/ LOW VOLTAGE:** Transistor size and low power requirements enable innovative designs and easy integration.

**EFFICIENT:** Device monitors the amount of power being absorbed and reflected throughout the cooking processes, delivering only the necessary amount of energy required.

**DURABLE:** Designed for 20 years of continuous operation without degradation of power.

**REPEATABLE:** Systems controller determines the precise load conditions via feedback, adjusting frequency as needed. This allows for the same cooking result to be reproduced each time, every time.



## Current Research Issues on different types of magnetron



INNOVATE

DEVELOP

DELIVER

1. “Metamaterial Cathodes in Multi-cavity Magnetrons” Andrey D. Andreev\* and Kyle J. Hendricks High-Power Microwave Division, Directed Energy Directorate, Air Force Research Laboratory 3550 Aberdeen Ave, Kirtland Air Force Base, NM 87117-5776, USA
2. “Application of Meta materials in Spatial Harmonic Magnetrons,” Nasrin Nasr Esfahani and Klaus Schiinemann Institute fur Hochfrequenztechnik, Tech. Univ. Hamburg Harburg Denickestrasse 22,21073 Hamburg, Germany
3. Phase and frequency locking in high power CW magnetrons (>100 kW in L-band)
4. Power and efficiency enhancement by priming techniques
5. Stacking of magnetrons
6. Cold cathode for THz magnetron and thermal management in high power CW magnetrons



## Evolution of Electron tube & magnetron in the country



INNOVATE

DEVELOP

DELIVER

- ✓ Institute of Radio Physics was established in early fifties.
- ✓ “Work on electron tubes has been intensified since **September 1956**, when the **UNESCO Expert, Dr. H. F. Steyskal** joined the Institute.

The aim of the work was to improve research facilities involved in the electron tube making, especially with regard to all metal tubes, including microwave tubes, e.g., **magnetron**.

The equipment in the lab has been enriched by the following items:

- ✓ High vacuum pumping units with provision for measuring pressures of 10<sup>-7</sup> mm Hg.
- ✓ Hydrogen Furnace up to 1000<sup>0</sup> C.
- ✓ Chamber for heat treatment in protective atmosphere at temp. up to 1200<sup>0</sup> C.
- ✓ Ball Mill for powdering chemicals.
- ✓ Apparatus for spraying insulating coatings and emission pastes.
- ✓ 6 KW RG heating unit (Gift from UNESCO).
- ✓ Glass lathe (Gift from UNESCO).

*CU Annual Report: 1956-57 published in 1958*





# Evolution of Electron tube & magnetron in the country



INNOVATE

DEVELOP

DELIVER

## Process developed:

- ✓ Glass to metal sealing ( Kovar and Copper)
- ✓ Vacuum tight brazing of metals in protective atmospheres and in vacuum
- ✓ Fabrication of special brazing alloy, electroplating, machining of **magnetron** parts,
- ✓ Development, activation and characterization of oxide cathodes and their filaments

1961-62

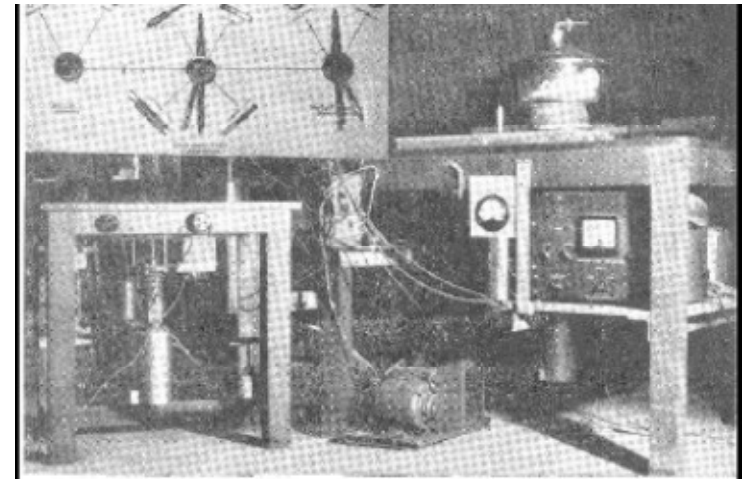
Work is also in progress towards better design and performance of **10 cm multi-cavity CW magnetron**.

Courtesy : Prof. PK Basu (Calcutta University)

: Prof. BN Basu

: CU Annual Report: 1956-57 published in 1958

1. N. B. Chakraborty, "Lower frequency pumping of electron beam parametric amplifiers," *Int. J. Electron.*, vol. 8, no. 3, 161-165 (1960).
2. N. B. Chakraborty, "Analysis of fast-wave amplifiers for transverse field parametric amplifiers," *Int. J. Electron.*, vol. 10, no. 2, 147-151 (1961).



Setup (1956) at Institute of Radio physics and Electronics, Calcutta University



## Magnetron : CSIR-CEERI



INNOVATE

DEVELOP

DELIVER

- **Dr Amarjit Singh** initiated some work on Multi-cavity Magnetron at National Physical Laboratory, prior to joining CEERI.
- As Scientist-in - Charge and later on as Director, of CEERI, he increased the pace of work on Cavity Magnetrons ( Hole and Slot configuration) from early sixties.
- The first major work was on S- band 500 kW magnetrons. They were batch produced in CEERI and about 75 tubes were delivered to Indian Navy.



Courtesy : Dr. SN Joshi  
: KRC, CSIR-CEERI Pilani



# Magnetron: Past Achievements



INNOVATE

DEVELOP

DELIVER

Developed Magnetrons	Frequency (GHz)	Application
500 kW and 1 MW Pulse Magnetron	S-Band	Naval Radar, 75 nos. were supplied to Indian Navy
800 kW/1MW Pulse Tunable Magnetron	S-Band	Ground Missile Guidance Radar ToT to CEL Shahibabad
200 kW Pulse Tunable Co-axial Magnetron	X-Band	Fire control Radars
400 W Ka-Band Magnetron	Ka-Band	Proximity Fuse
2.0 MW Pulse Magnetron	2.998/2.856	Medical Linac (Radiotherapy) Delivered to RRCAT, BARC
3.0 MW Pulse Magnetron	2.998	Medical Linac (Radiotherapy)
2.6 MW Pulse Magnetron	2.998 GHz	Medical Linac ToT to M/s Panacea Medical
3.0 MW Pulse Magnetron	2.856	Cargo Scanning
Electromagnet	-	For testing of 3 MW S-band Magnetron



# Magnetron: Past Achievements (contd...)



INNOVATE

DEVELOP

DELIVER

## 500 kW S-Band Pulse Magnetron

### SPECIFICATIONS:

Peak Power (peak)	:	500 kW
Frequency	:	S-Band (2.950-3.060 GHz) (four versions)
Year of completion	:	~1960
Application	:	Navel Radars
Tubes were batch produced and supplied to Indian Navy (~75 nos.)		



## 800 kW/ 1 MW S-Band Pulse Magnetron (Tunable/fixed frequency)

### SPECIFICATIONS:

Peak Power	:	800 kW/1MW
Frequency	:	S-Band (2.8-31.GHz)
Year of completion	:	1968-70
Application	:	Navel Radars

Know-how was transferred to CEL Sahibabad.



INNOVATE

DEVELOP

DELIVER

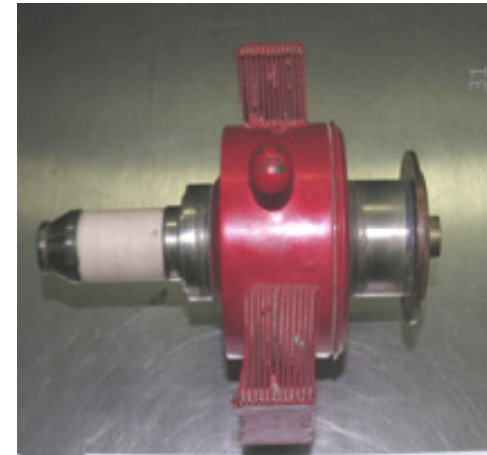
## 200 kW X-Band Pulse Magnetron

### SPECIFICATIONS:

Peak Power	:	200 kW
Frequency	:	X-Band (8.5-9.6 GHz)
Project duration	:	1974-83
Application	:	Fire control Radars

Tubes were developed in limited numbers (~11 nos.)

<b>Features</b>	:	Fully ceramic metal window
	:	Mechanically tunable (~11% bandwidth)
	:	Indirectly heated S-type dispenser cathode
	:	Packaged magnet



## 400 W Ka-Band miniature fast warm-up Magnetron

### SPECIFICATIONS:

Peak Power	:	200 W
Frequency	:	Ka-Band (35 GHz)
Project duration	:	--?
Application	:	Guided missile system
Achievement	:	Design and fabrication of magnetron assembly
	:	Development of fast warm up cathode using nimonic-80 A alloy
	:	Segment technique for fabrication of anode



1. Dr. Lalit Kumar, "An Amazing world of Microwave-Terawave", 37 Ram Lal Wadhwa Award Lecture
2. Sirapa Mutyala Rao, "Design and experimental evaluation of the coaxial cavity or circular electric mode magnetron", M.Tech. dissertation, IT-BHU guided by Dr. NC Vaidya and Dr. Lalit Kumar, 1981.
3. "Thermal Design Consideration for Fast Warm-up Cathodes in MM Wave Magnetrons", HK Dwivedi and DS Venkatswarlu, IEEE Transactions on Electron Devices (USA), 2011-2018, 43, 11, November 1996.



INNOVATE

DEVELOP

DELIVER

## 2 MW S-Band tunable Pulse Magnetron

### SPECIFICATIONS:

Peak Power	:	2 MW
Frequency	:	S-Band (2998 ± 5 MHz) (2856 ± 5 MHz)
Project duration	:	1999-2005
Application	:	Microtron and LINAC
Sponsorer	:	BRNS, DAE

Tubes were developed in limited numbers (~10 nos.)

<b>Features</b>	:	Glass window and cathode support
	:	Mechanically tunable
	:	Indirectly heated S-type dispenser cathode
	:	Un –packaged (Electromagnet)

7 nos. of tube were supplied to RRCAT, Indore and 3 nos. were supplied to BARC, Mumbai



## 3MW S-Band tunable pulse Magnetron

### SPECIFICATIONS:

Peak Power	:	3 MW
Frequency	:	S-Band (2998±5 MHz)
Project duration	:	1999-2005
Sponsorer	:	BRNS, DAE
Application	:	LINAC/Microtron
Achievement	:	Developed two numbers of lab prototypes and supplied to RRCAT, Indore



INNOVATE

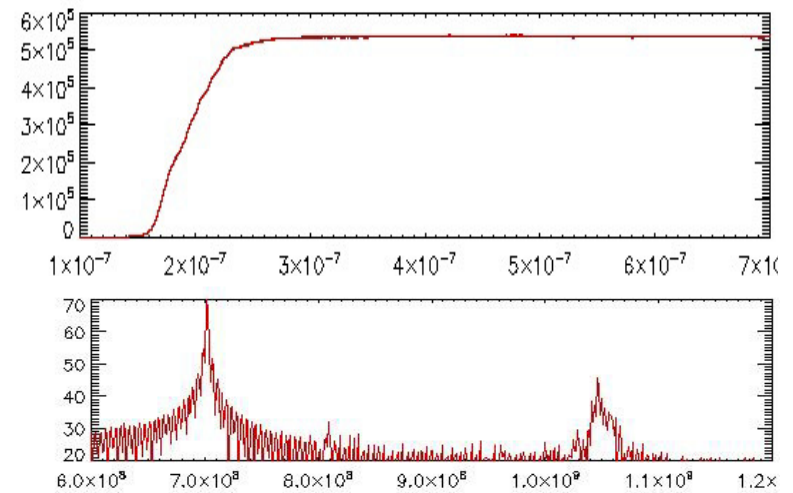
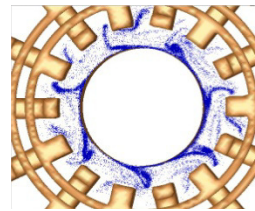
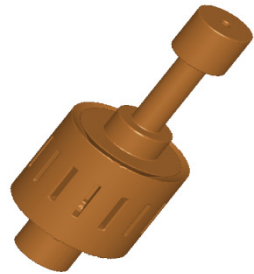
DEVELOP

DELIVER

## Design of 704 MHz, 500 kW magnetron for Proton Accelerator

### SPECIFICATIONS:

Parameters	Values
Frequency	704 MHz
Power (Peak)	200kW-1 MW
Pulse Length	5 $\mu$ s-5ms
Efficiency	>90%
Magnet	NyFeB
External Q	~50
Maximum	100 kW



## 3MW S-Band tunable pulse Magnetron

### SPECIFICATIONS:

Peak Power	:	3 MW
Frequency	:	S-Band (2998 $\pm$ 5 MHz)
Project duration	:	1999-2005
Sponsorer	:	BRNS, DAE
Application	:	LINAC/Microtron
Achievement	:	Developed two numbers of lab prototypes and supplied to RRCAT, Indore

INNOVATE

DEVELOP

DELIVER



2.6 MW S-Band Magnetron

**FEATURES :**

- Water cooled
- Glass window

## 2.6 MW S-Band tunable Pulse Magnetron

**SPECIFICATIONS:**

Peak Power	:	2.6 MW
Frequency	:	2998 MHz
Tuning range (Min.)	:	2992 to 3002 MHz
Magnetic field	:	1550 ± 25 Gauss
Pulse duration (Max.)	:	4.5 μS
Pulse repetition rate (Max.)	:	250 PPS



Acceptance test at CSIR-CEERI



INNOVATE

DEVELOP

DELIVER

## 2.6 MW S-Band tunable Pulse Magnetron

- Tested in actual LINAC System at SAMEER, Mumbai
- Produced the desired X-Ray dose



### LPT - 06 Testing Record on Linac

Magnetron Filament Voltage - 9.0 Volt  
 Magnetron Filament Current - 7.9 Amps.  
 Gun Filament Voltage- 6.3 Volts  
 Gun injection voltage - 13.5KV

Sl.No	Variac	PRF (HZ)	I mag	Electromagnet current (A)	Duration (sec)	X Ray Dose (rads/mint)	Remarks
1	86	50	92.8	19.00	60	51	
2	86	50	92.8	19.00	60	50	
3	86	100	91.2	19.50	60	111	
4	86	150	86.4	20.50	60	202	
5	86	150	86.4	20.40	60	200	
6	86	200	84.0	21.00	60	226	

*M. Kumar*  
*N. Venugopal*

*Abh*

Testing on LINAC system at SAMEER, Mumbai

Approved results and X-ray doses using  
 CEERI developed Magnetrons

INNOVATE

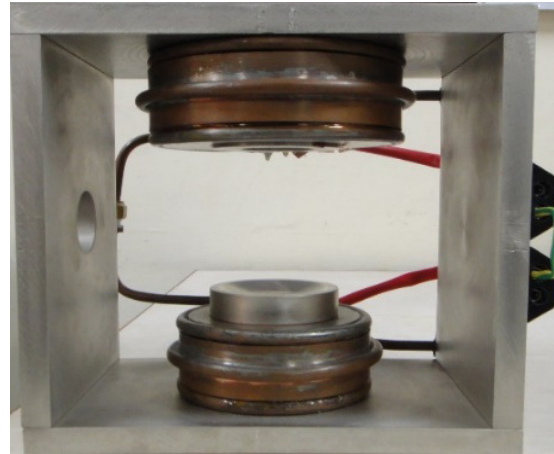
DEVELOP

DELIVER

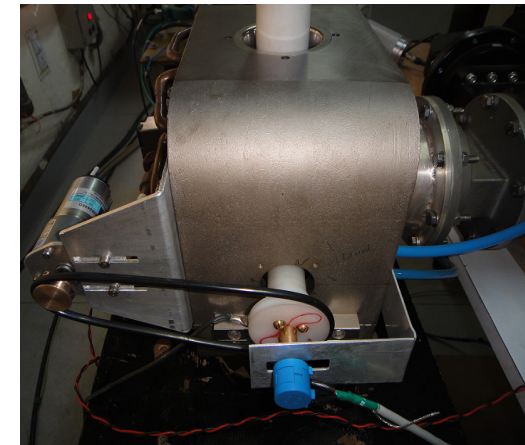
## 3 MW S-Band tunable Pulse Magnetron



3 MW S-Band Magnetron



Electromagnet



Motorized tuning system

### SPECIFICATIONS:

Peak Power	:	3 MW
Frequency	:	2856 MHz
Tuning range (Min.)	:	2851 to 2861 MHz
Magnetic field	:	$1650 \pm 25$ Gauss
Pulse duration (Max.)	:	4.5 $\mu$ S
Pulse repetition rate (Max.)	:	250 PPS

### FEATURES :

- Water cooled
- Robust ceramic cathode support

### APPLICATION :

- Industrial LINAC

The magnetrons were developed under the sponsored project by BARC, Mumbai.





# Magnetron: Recent Achievements



INNOVATE



DEVELOP

DELIVER

3 nos. of developed magnetrons were tested as per specifications and delivered to BARC, Mumbai (in 2018) with electromagnet, motorized tuning mechanism and know-how documents



Delivery of developed magnetrons to BARC, Mumbai

भा.प.अ.के.  
BARC  
भारत सरकार  
सरलमेव जयते  
भारत सरकार

आर. के. राजावत  
R.K. Rajawat  
सह निदेशक, बीटीडीजी एवं  
अध्यक्ष, एपीपीडी, भापअ केंद्र  
Associate Director,  
BTDG & Head, APPD  
e-mail id: [rkraj@barc.gov.in](mailto:rkraj@barc.gov.in)  
Mobile/मोबाइल: 9757000361

इंजीनियरी हॉल नं.4, ट्रांबे,  
Engg. Hall - 4, Trombay,  
Mumbai/मुंबई-400085  
टेलि/Tel.: (+9122)25593619  
फैक्स/Fax: (+9122)25505151

Government of India  
भाभा परमाणु अनुसंधान केंद्र  
Bhabha Atomic Research Centre  
किरणपुंज प्रौद्योगिकी विकास वर्ग  
Beam Technology Development Group  
त्वरक एवं स्पंद शक्ति प्रभाग  
Accelerator & Pulse Power Division

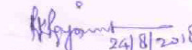
To,  
The Director  
CSIR-CEERI, Pilani-333031  
Rajasthan

Subject : Delivery of 3 MW S-Band Pulse Tunable Magnetron lab prototypes and its accessories to EBC Kharghar, BARC Mumbai

Name of the Project : Design and Development of 3.0 MW S-Band Tunable Pulse Magnetron

MoU no. : BARC/Accts./Works/MoU/326/2011/395

This is to bring your kind notice that CSIR-CEERI, Pilani has delivered 3 Nos. of magnetron prototypes, one no. of electromagnet with power supply, motorized tuning mechanism along with know-how document and other accessories as per deliverable mentioned in above MoU between CSIR-CEERI and BARC, Mumbai, after successful completion of the project. Before delivery, the prototypes have been tested at CSIR-CEERI Pilani by BARC officials.

Yours Sincerely  
  
(R.K. Rajawat) 24/8/2018

cc : Head PMBD, CSIR-CEERI, Pilani  
Area coordinator, MWD Area CSIR-CEERI, Pilani

# Magnetron: Recent Achievements

INNOVATE

DEVELOP

DELIVER

## 10 kW S-Band CW Magnetron

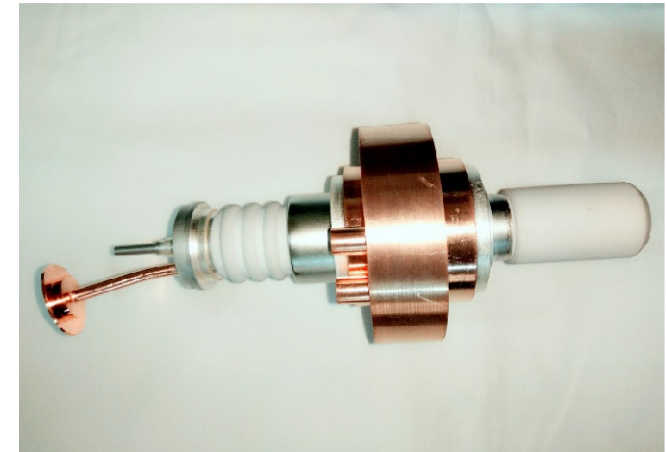
### SPECIFICATIONS:

Peak Power	:	10 kW
Frequency	:	S-Band (2450 ± 50 MHz)
Application	:	Industrial heating
Sponsorer	:	CSIR New Delhi

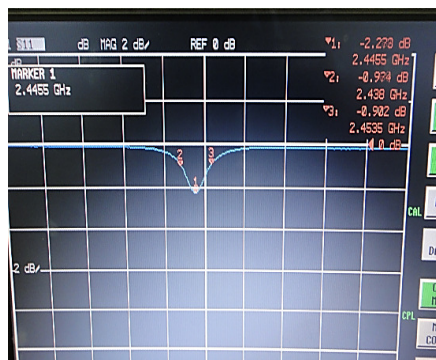
One tube was developed and limited testing was carried out

### Features:

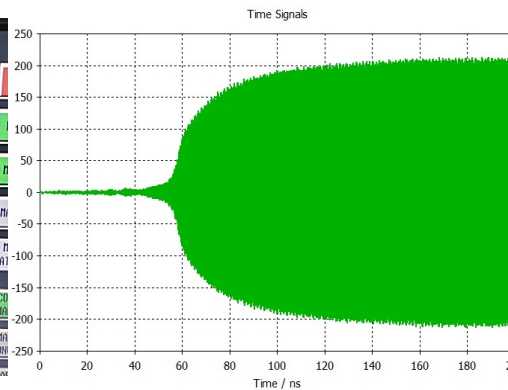
- : Ceramic window
- : Fixed frequency
- : Directly heated filamentary cathode



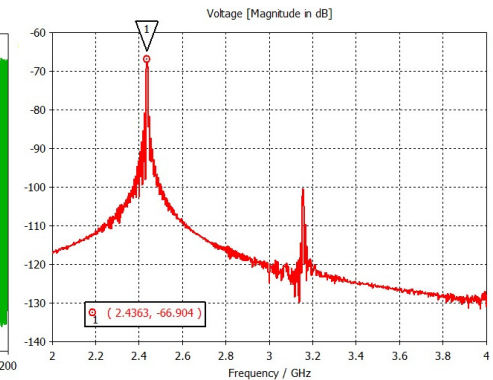
Anode block



S<sub>11</sub> parameters



Output signal



Oscillation spectrum

1. Sandeep Kumar Vyas, Shivendra Maurya, Rajendra Kumar Verma and Vindhyaasini Prasad Singh, "Synthesis and Simulation studies of a 10 kW, 2.45 GHz CW Magnetron". Published in IEEE Tran. on Plasma science Vol. 43, No. 10, pp. 3615-3619, Oct., 2015.

# Magnetron: Simulation work

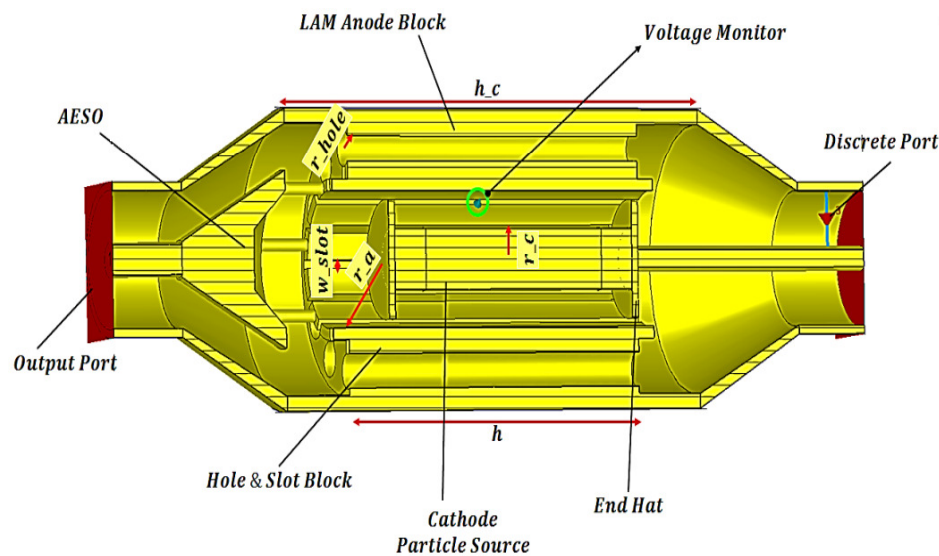
INNOVATE

DEVELOP

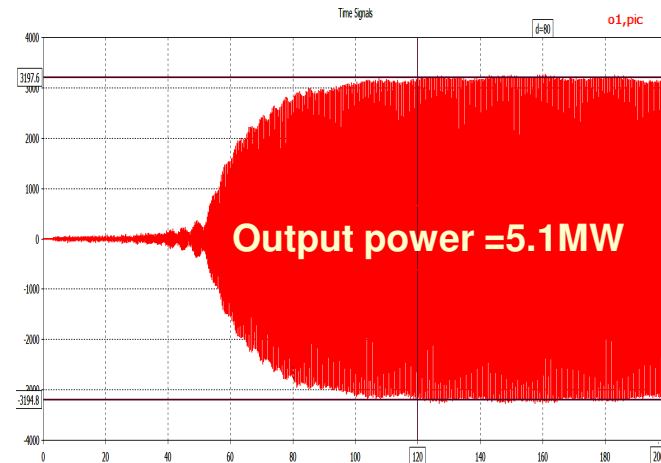
DELIVER

## 5 MW Long Anode Magnetron

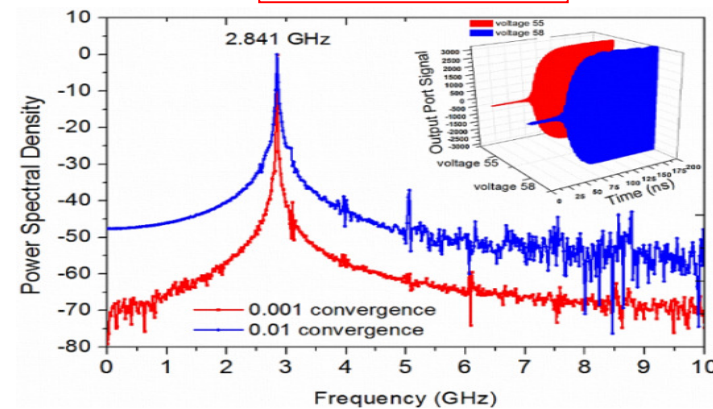
- Longer cathode / Longer anode block
- High thermal capabilities / High power capabilities



3D simulation model with output coupler



Output signal



Oscillation Spectrum

1. Rajendra Kumar Verma, Shivendra Maurya and Vindhyaasini Prasad Singh. "Study of Mode Control in Long-Anode High Power Pulse Magnetron". Published in IEEE Tran. on Plasma science Vol. 42, Issue 12, pp. 4010-4014, December, 2014.



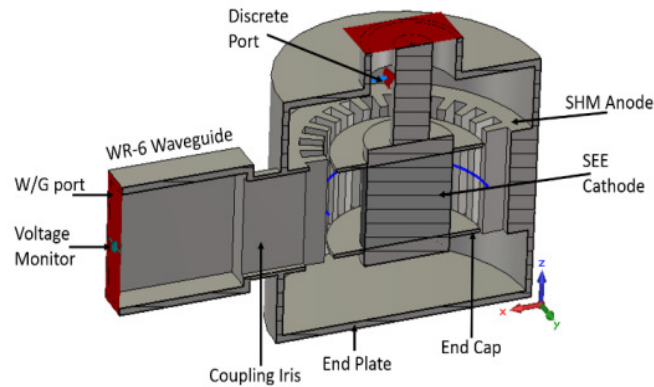
# Magnetron: Simulation work

INNOVATE

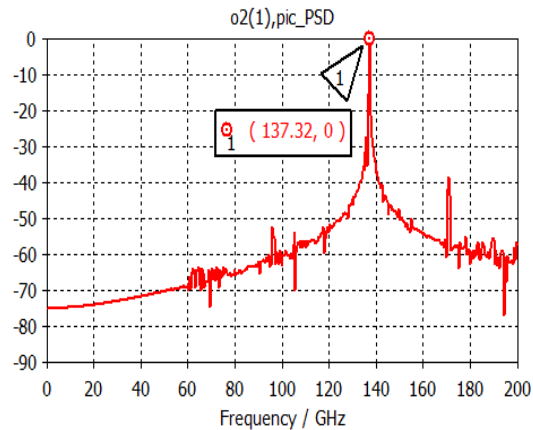
DEVELOP

DELIVER

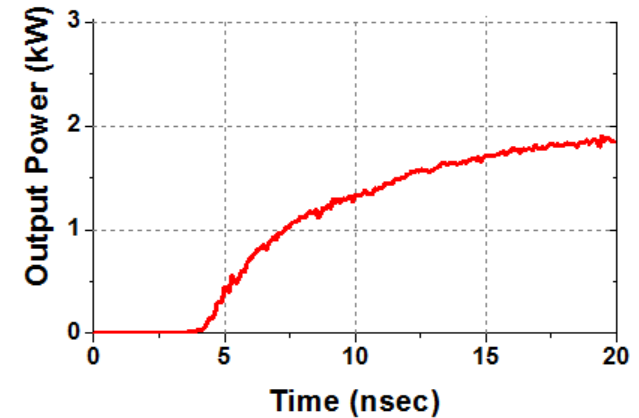
## 140 GHz Spatial Harmonic Magnetron



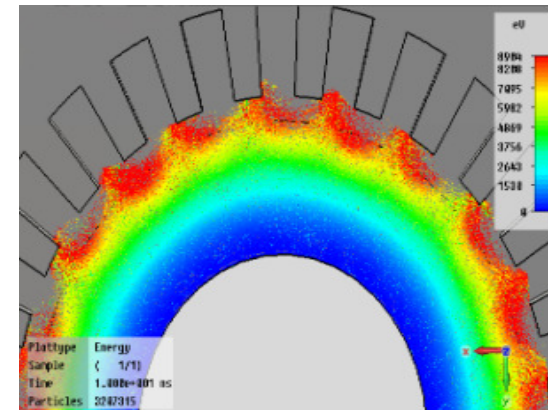
3D simulation model with output coupler



Oscillation spectrum



Output power



Formation of spokes

1. Rajendra Kumar Verma, S. Maurya, "Effect of Operating Region on the Performance of a Spatial Harmonic Magnetron," published in IEEE Transactions on Plasma Science, Vol. 57, No. 10, October 2019.

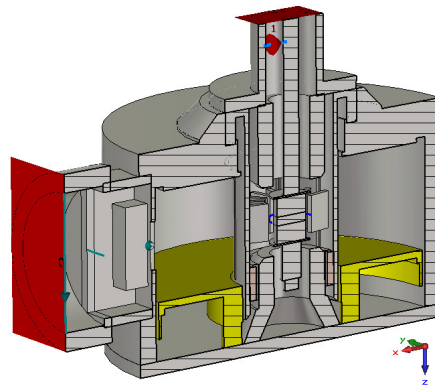
# Magnetron: Simulation work

INNOVATE

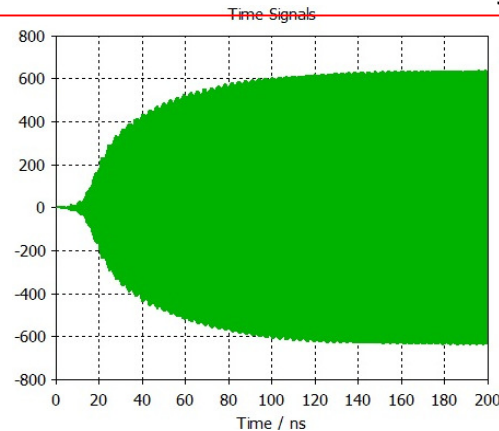
DEVELOP

DELIVER

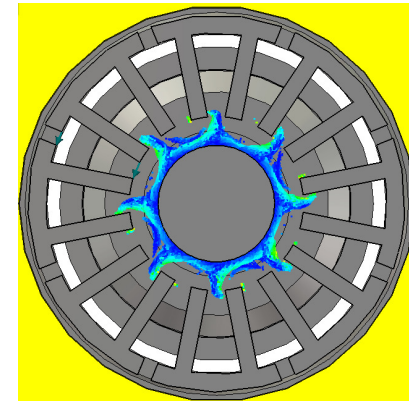
## Simulation study of X-Band / 200KW Tunable Pulsed Coaxial magnetron



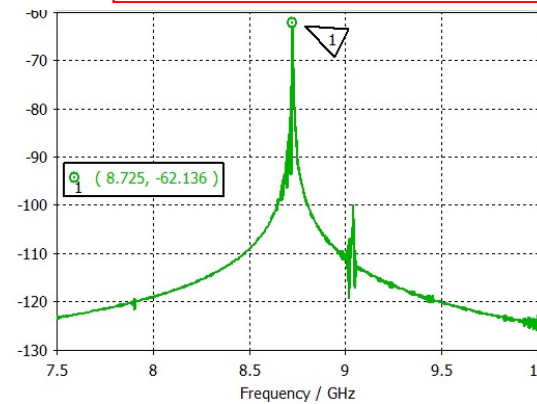
Resonant structure with outer cavity



Output signal



Formation of spokes



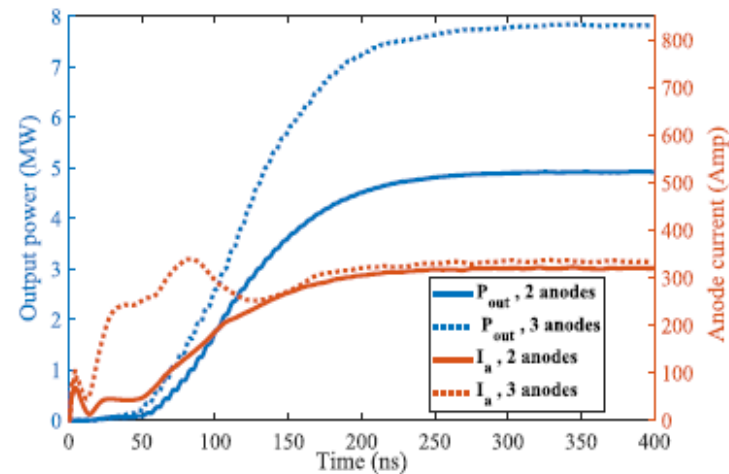
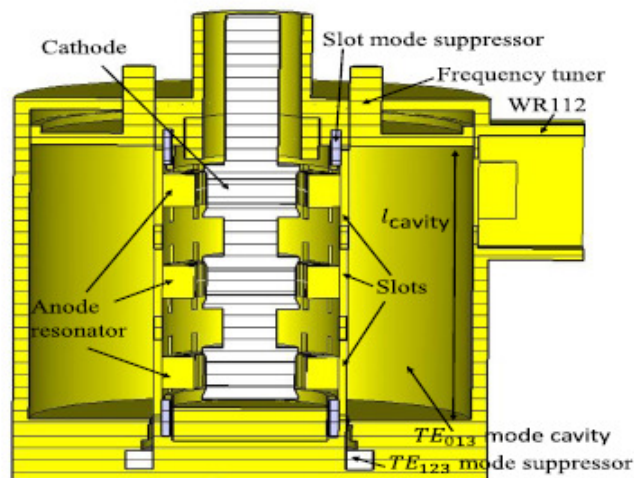
Oscillation spectrum

Journal Publication : 18 (IEEE Trans. 11 / IJMWA-3 / Springer-1)  
 Conference Publication : 35 (Two best paper award)  
 Ph.D. : 03  
 Award/Fellowship : 03

## SAMEER -Centre for High Power Microwave Tube and Component Technology (CHMTCT) Guwahati

### Equipped with simulation software and development facilities

- Design and development of 4.0 MW S-Band tunable pulse magnetron
- Simulation studies on X-band coaxial pulse tunable magnetron
- Stack anode resonators in coaxial magnetron



1. Mohit Kumar Joshi, Sandeep Kumar Vyas, Tapeshwar Tiwari, and Ratnajit Bhattacharjee, "Particle-in-Cell Simulation and Analysis of 28-Vane Megawatt-Class Pulsed Power Coaxial Magnetron in X-Band" IEEE Trans. on Plasma Science, April-2020
2. Mohit Kumar Joshi, Sandeep Kumar Vyas, Tapeshwar Tiwari, and Ratnajit Bhattacharjee, "A New Approach for High-Power Coaxial Magnetron Using Stacked Anode Resonators IEEE ED, February-2020





# Research and development work in the Country



INNOVATE

DEVELOP

DELIVER

## BARC Mumbai

- Design and simulation studies on relativistic magnetron (A6- $\pi$  mode) and related power supply and magnet

## MTRDC, DRDO Bengaluru

- Design and development of relativistic magnetron (A6- $\pi$  mode) with diffraction output

## BEL, Bengaluru

- To cater the requirement of strategic sector microwave tube plant was established in 1969.
- Production of L, S and X-band magnetrons in different frequency and power levels for military and Navy radars.
- Production of modified X-band coaxial magnetron for power improvement  
(Dr. Kiran Visweswaraiah , Dr. Sanjay Ghosh and Team)

1. Romesh Chandra et. al . APPD, BARC Mumbai, " Design of Relativistic magnetron for high power microwave generation", Proceedings of LINAC 2014, Geneva, Switzerland
2. Suvadeep Choudhury, Ajay Kumar Saini, and SK Chhotray , " Three Dimensional Particle-In-Cell Simulation Study of Relativistic Magnetron with Diffraction Output in CST " <https://ieeexplore.ieee.org/stamp/stamp.jsp?arnumber=6733494>
3. <https://www.thehindubusinessline.com/companies/kiran-visweswaraiah-is-new-gm-of-bharat-electronics/article7281933.ece>
4. <http://www.vedas.org.in/22-creation-of-vedas.html>



# Research and development work in the Country



INNOVATE

DEVELOP

DELIVER

## **BITS-Pilani, Hyderabad Campus**

- Design and simulation studies on phase locking of magnetrons
- Power improvement study in magnetrons
- Design of 3.7 GHz, 20 kW CW magnetrons

**Few other academic Institutes : As a part of student B.Tech./M.Tech project**

1. Aviraj R. Jadhav, Joseph John1 , Kushal Tuckley , Harish V. Dixit , P. K. Sharma, " Conceptual RF design of 3.7 GHz 20 kW CW Magnetron for LHCD system of Tokamaks" IVEC-2019, South Korea



## Effort toward product/system development



### INNOVATE

### DEVELOP

### DELIVER

- Transferred the know-how document of 2.6 MW S-band tunable pulse magnetron to M/s Panacea medical Pvt. Ltd. Bengaluru
- Discussion with M/s Panacea for magnetron production based on design of CSIR-CEERI for other user agencies.
- Interaction with M/s VEM Technology Pvt. Ltd. Hyderabad for development of magnetron jointly.
- Discussion with M/s SS Medical System (India) Pvt. Ltd. Bhimtal, Uttarakhand



# Bottleneck

INNOVATE

DEVELOP

DELIVER

- **Unrealistic time line**
- **Quality control and characterization of sub-assemblies**
- **Development yield**
- **Industrial partner should be involved from beginning of the R&D for system level development.**
- **Documentation and failure analysis**



# Acknowledgement



INNOVATE

DEVELOP

DELIVER

- **Director, CSIR-CEERI**
- **All the past team members of magnetron**
- **My colleagues and friends**
- **Dr. RK Sharma- for fruitful iteration with industries**
- **All those who have provided information**





INNOVATE

DEVELOP

DELIVER

# THANKS



**Annexure II:**  
**Young Researcher's Talk-1 Slides**

## **Encouraging Words**

“I congratulate two M’s (Mumtaz and Manpuran) for presenting their brilliant work. I have enhanced my knowledge from your talks. I believe you have also learnt from the interaction with the group following your talks. I hope more and more young researchers would come forward to showcase their work on the platform of this group in similar webinar programmes in future.”

**-B. N. Basu**



# Compact and Efficient High Power Microwave Source- Reltron



**Dr. Manpuran Mahto**

**Assistant Professor**

**Department of Electronics and Communication Engineering**

**National Institute of Technology (NIT)**

**Patna 800005**

# Contents

2

- 1: Introduction of Reltron**
- 2: Contribution I: Analytical Fundamentals of Reltron**
- 3: Contribution II: Design and Simulation Study of Reltron**
- 4: Contribution III: Electron Beam and Electromagnetic Waves Interaction Analysis**
- 5: Contribution IV: Virtual Cathode Formation Mechanism in the Reltron**
- 6: Research Publications**

# Introduction of Reltron

- ❖ Reltron is similar to klystrons in that microwave power is extracted from a bunched beam using a set of output cavities; however, it is unique in two respects
  - ❖ The bunching mechanism differs from that in a klystron.
  - ❖ The bunched beam is reaccelerated to higher energy to increase the energy withdrawn in the output cavities.
- ❖ It grew out through the investigation of split cavity oscillator (SCO).

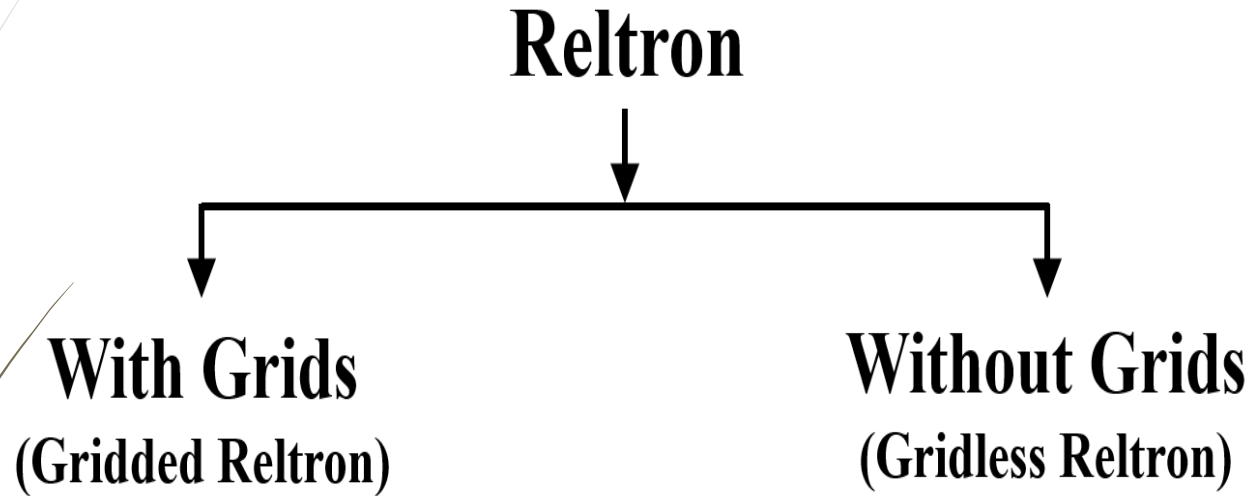


**Figure :** Classification of reltron.

## Attractive Features

- **High power, highly efficient, and compact high power microwave (HPM) source.**
- **External magnetic field is not required.**
- **No need of mode converter.**
- **Pulsed power in excess of 100ns duration.**
- **Frequency tuning is very easy.**
- **Efficiency of the device can reach upto 50%.**

## Possible Applications

- **Nonlethal HPM weapon.**
- **HPEM simulator.**
- **Electronic warfare.**
- **Directed energy weapon.**
- **Other possible applications in radar, imaging, material processing and plasma science.**

# Contribution I

## Analytical Fundamentals of Reltron\*

\*The work has been published as:

**Manpuran Mahto** and Pradip Kumar Jain, “Oscillation Condition and Efficiency Analysis of the Reltron,” *IEEE Transactions on Plasma Science*, vol. 44, pp. 1056–1062, 2016.

# Device Description and Operating Principle of the Reltron

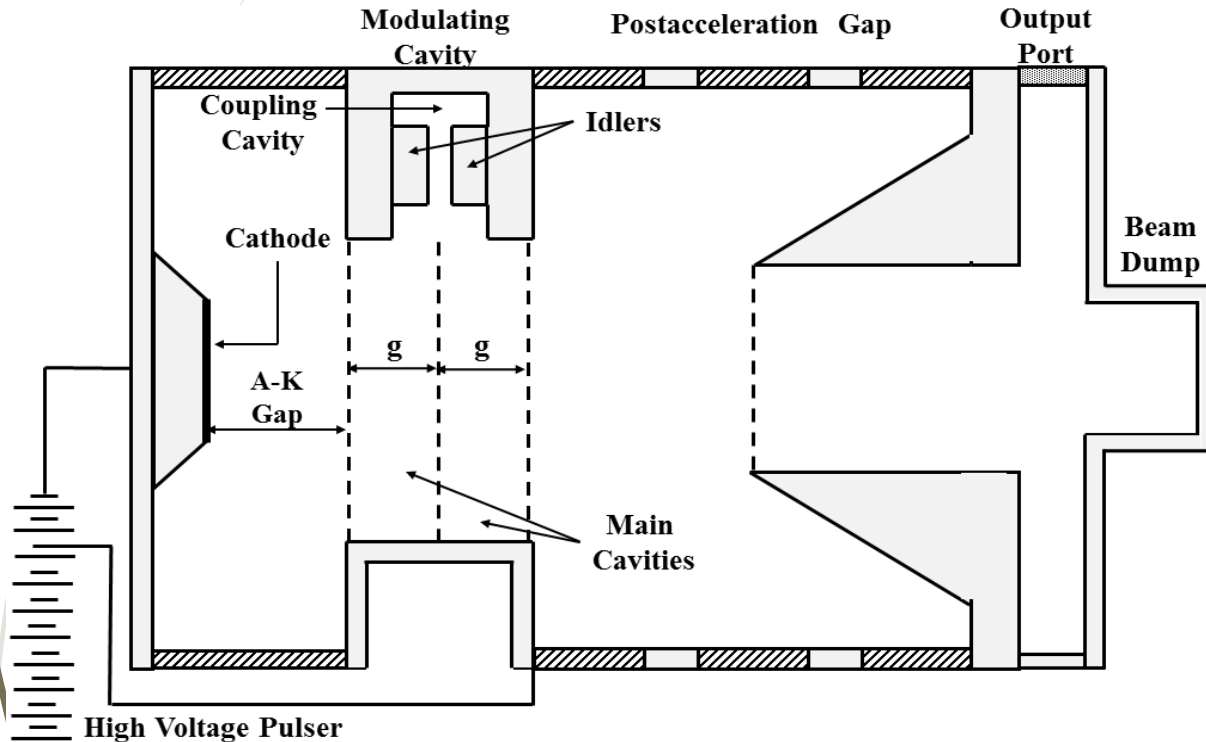


**Figure:** Schematic diagram of a reltron.

## Elements of Reltron

- Power Supply
- Cathode
- Modulation Cavity
- Post acceleration Gap
- Extraction Cavity
- Beam Dump



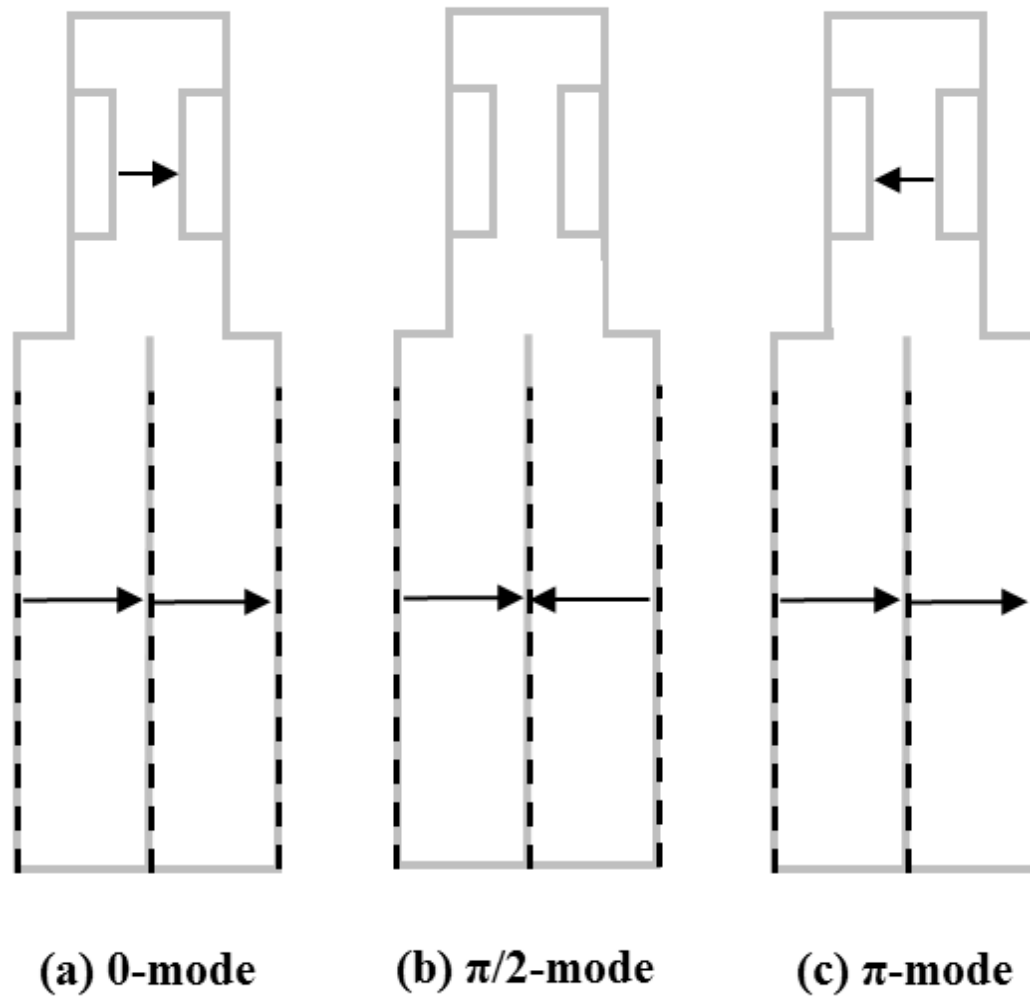


**Figure:** Electric field amplitudes of (a) 0-mode, (b)  $\pi/2$ -mode, and (c)  $\pi$ -mode in the side coupled modulation cavity.

# Oscillation Condition

- **The electron beam is pre-modulated at the first grid spacing of the modulation cavity and then enters into the second grid spacing to excite it.**
- **As the induced gap voltage in the first grid spacing (between the first and second grids) is high enough, it forms a virtual cathode in the second grid spacing (between the second and third grids).**
- **Once the virtual cathode is formed, results into two processes**
  - (1) **the virtual cathode oscillates in between the first and second grid spacing, and**
  - (2) **some of the electrons are reflected back towards the cathode, and they are then again reflected back due to the cathode potential towards the virtual cathode. This phenomena sets up an oscillation in the cavity, known as reflexing.**

- Total current  $I_t$  flowing in the circuit can be written as:

$$I_t = \frac{V}{R} + \frac{1}{L} \int V dt + C \frac{dV}{dt}$$

- Differentiating the above expression and rearranging the terms yield:

$$\omega^2 \frac{d^2V}{d\bar{t}^2} + \frac{\omega}{RC} \frac{dV}{d\bar{t}} + \frac{1}{LC} V = \frac{\omega}{C} \frac{dI_t}{d\bar{t}} \quad (2.1)$$

$$\omega = 1/\sqrt{LC}, \quad Q = \omega RC = R/\omega L, \quad \bar{t} = \omega t$$

- The total current  $I_t$  can be expressed as [Uhm *et al.* (1993)]:

$$I_t(\bar{t}) = sI_0 F(\psi, \bar{t}) \quad (2.2)$$

$I_0$  is the initial beam current,  $s$  is the form factor

- The normalized beam current at a location  $\psi$  in the first grid spacing is given by

$$F(\psi, \bar{t}) = \frac{\sqrt{1 - \psi^2}}{1 + \psi \cos \bar{t} + \psi A\{\bar{t}\} \cos(\bar{t} - \varphi\{\bar{t}\} + \alpha)} \quad (2.3)$$

- **Considering  $\psi \ll 1$ , equation (2.3) becomes:**

$$F(\psi, \bar{t}) = 1 - \psi \cos \bar{t} - \psi A\{\bar{t}\} \cos(\bar{t} - \varphi\{\bar{t}\} + \alpha) \quad (2.4)$$

- **The total induced gap voltage in the first grid spacing can be obtained from (2.1), (2.2) and (2.4) as**

$$\frac{d^2V}{d\bar{t}^2} + \frac{1}{Q} \frac{dV}{d\bar{t}} + V = \frac{1}{Q} \phi_w \sin \bar{t} + I_s A\{\bar{t}\} \sin(\bar{t} - \varphi\{\bar{t}\} + \alpha) \quad (2.5)$$

$\phi_w (= sRI_0\psi)$  =Steady state value to saturate the induced voltage

$I_s (= \omega sI_0\psi / C)$  =Intensity of the return current from virtual cathode

- **Suppose, the induced gap voltage in the first grid spacing can be expressed in the form**

$$V\{t\} = A\{\bar{t}\} \sin(\bar{t} - \varphi\{\bar{t}\}) \quad (2.6)$$

- **The amplitude and phase shift of the induced voltage at the modulation cavity can be given as**

$$\frac{d A}{d \bar{t}} = \sin \varphi + (h \sin \alpha - 1) A \quad (2.7)$$

$$\frac{d \varphi}{d \bar{t}} = \frac{\cos \varphi}{A} + h \cos \alpha \quad (2.8)$$

where the term  $h$  is defined for  $I_s Q$

- **To solve these equations, it is assumed that the electrons enter the modulation cavity at time  $\bar{t} = 0$ .**
- **The initial conditions for the amplitude and phase are thus given by  $A\{0\} = 1$  and  $\varphi\{0\} = \pi/2$ . This gives a homogeneous solution of amplitude ( $A$ ), which increases exponentially, provided**

$$h \sin \alpha > 1 \quad (2.9)$$

This is the self-oscillation condition of the device.

- As long as, the return current from the virtual cathode is much less than the forward beam current, the modulation cavity is excited linearly. Once the return current becomes significant fraction of the forward beam current, modulation cavity starts saturating.
- **And when the nonlinear saturation condition is considered, expressions (2.7) and (2.8) get modified as**

$$\frac{d A}{d \bar{t}} = \sin \varphi + [h(1 - \kappa A^2) \sin \alpha - 1] A \quad (2.10)$$

$$\frac{d \varphi}{d \bar{t}} = \frac{\cos \varphi}{A} + h(1 - \kappa A^2) \cos \alpha \quad (2.11)$$

where the nonlinear saturation coefficient  $\kappa \ll 1$ .

- **In (2.11), the term  $\kappa A^2$  denotes the saturation amplitude and is given by**

$$A_s = \sqrt{\frac{h \sin \alpha - 1}{\kappa h \sin \alpha}} \quad (2.12)$$

$A_s \gg 1$  for self-oscillation condition

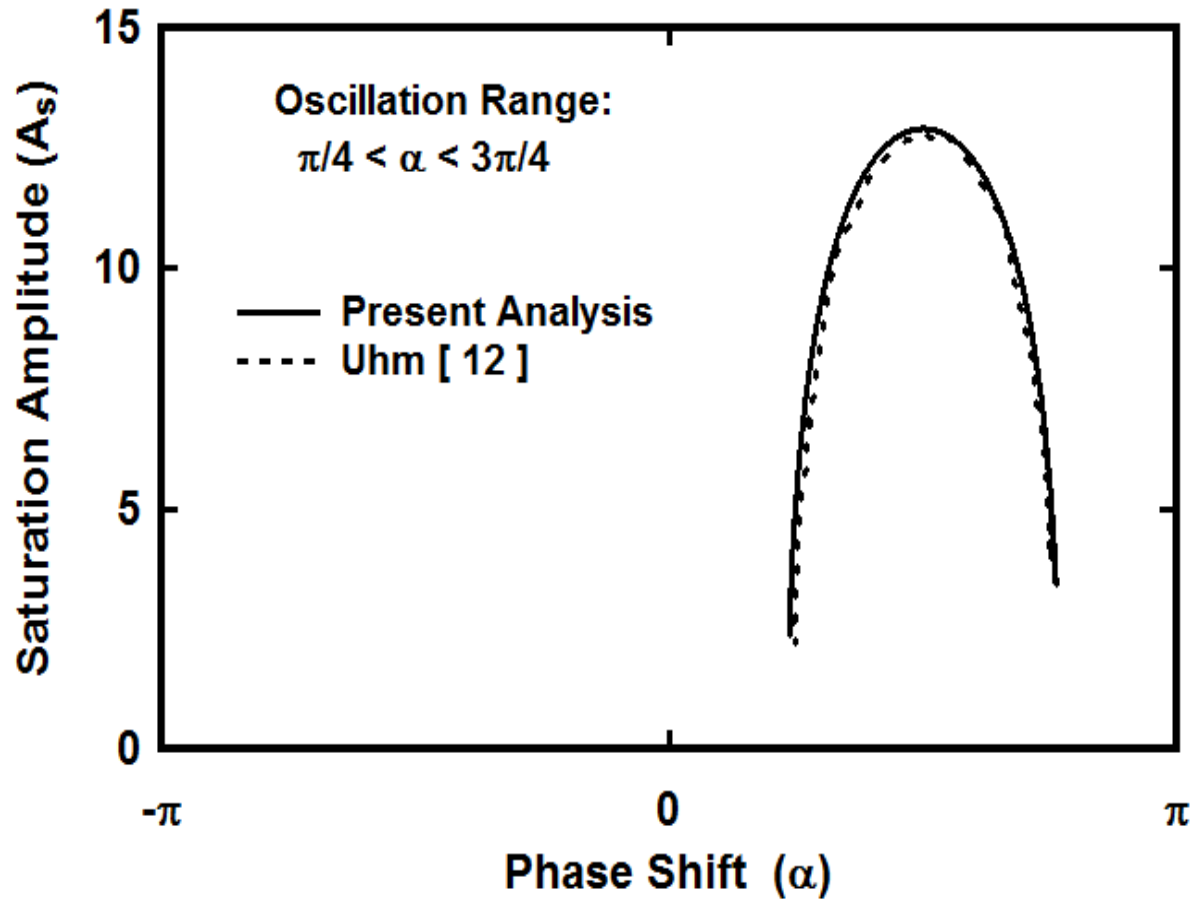


**Figure:** Plot of the normalized saturation amplitude ( $A_s$ ) versus phase shift ( $\alpha$ ) from expression (2.12).

# Efficiency Analysis

- **The electronic efficiency of the reltron is obtained by taking the ratio of the average kinetic energy (converted into the RF energy) to the initial electron beam energy.**
- **Kinetic energies are calculated by numerically integrating the relativistic electron motion expressions.**
- **The Lorentz force equation in the cylindrical coordinate system, in terms of electron momentum  $p$  can be written as:**

$$\frac{d p}{d t} = -e (E + v \times B) \quad (2.13)$$



- The RF electric field ( $E$ ) is generated due to the induced gap voltage  $V\{t\}$  inside the modulation cavity which can be approximated by the  $\pi/2$  mode of operation as:

$$E = \begin{cases} -E_0 \sin(\omega t + \theta) & 0 < z < g \\ E_0 \sin(\omega t + \theta) & g < z < 2g \end{cases} \quad (2.14)$$

- In the first grid spacing  $0 < z < g$  the force equation can be written as

$$\frac{dp}{dt} = -eE_0 \sin(\omega t + \theta)$$

- Integrating the above expression provides the momentum in the 1<sup>st</sup> grid spacing

$$p(t, \theta) = p_0 \{1 + \zeta [\cos(\omega t + \theta) - \cos \theta]\} \quad (2.15)$$

$$\zeta = eE_0 / \omega p_0$$

- Here,  $p_0$  is initial momentum defined by

$$p_0 = \gamma_0 m v_0 \quad (2.16)$$

- The relativistic mass factor ( $\gamma_0$ ) has the form:

$$\gamma_0 = 1 / \sqrt{1 - v_0^2 / c^2} \quad (2.17)$$

- Substituting equation (2.17) in (2.16), the expression for initial momentum can be expressed as:

$$p_0^2 = m^2 c^2 / \sqrt{1 - v_0^2 / c^2}$$

- Then, solving the above expression for  $(v_0/c)^2$  and substituting it in (2.17) provides  $\gamma_0$  in the form:

$$\gamma_0 = \sqrt{1 - (p_0 / mc)^2} \quad (2.18)$$

- The axial position of electrons can be obtained from (2.16) as:

$$\frac{dz}{dt} = \frac{p_0}{\gamma_0 m}$$

- Putting the value of  $\gamma_0$  in the above expression becomes:

$$\frac{dz}{dt} = \frac{c p_0}{\sqrt{m^2 c^2 + p_0^2}} \quad (2.19)$$

- Suppose at time  $t = T_0$ , the electrons enter the second gap, then equation (2.15) at the exit of the first gap gets modified as:

$$p\{T_0, \theta\} = p_0 \{1 + \zeta [\cos(\omega T_0 + \theta) - \cos \theta]\} \quad (2.20)$$

- The force equation in the second grid spacing of the modulation cavity  $g < z < 2g$ , can now be written in the form as

$$\frac{dp}{dt} = e E_0 \sin(\omega t + \theta)$$

- Again, integrating the above expression provides the electrons momentum in the 2<sup>nd</sup> grid spacing as:

$$p\{t, \theta\} = p\{T_0, \theta\} - p_0 \zeta [\cos(\omega t + \theta) - \cos(\omega T_0 + \theta)] \quad (2.21)$$

- **Substituting the value of  $p\{T_0, \theta\}$  into (2.21) becomes:** (2.22)

$$p\{t, \theta\} = p_0 \{1 + \zeta [2 \cos(\omega T_0 + \theta) - \cos(\omega t + \theta) - \cos \theta]\}$$

- **The normalized electrons momentum after the post-acceleration can be written in the form:**

$$\frac{d\bar{p}}{d\bar{t}} = \xi \zeta [2 \cos(\omega T_0 + \theta) - \cos(\bar{t} + \theta) - \cos \theta] \quad (2.23)$$

where  $\xi = V_{pa}/V_{ak}$  is the ratio of post-acceleration voltage to the cathode voltage.

**The trajectory of electron position can be obtained using (2.23) in (2.19) as:**

$$\frac{dz}{dt} = \frac{c\bar{p}}{\sqrt{m^2 c^2 - \bar{p}^2}} \quad (2.24)$$

- The kinetic energy  $W_f$  can be expressed as the difference between the total electron energy and the energy at rest, which is given by

$$W_f\{\tau, \theta\} = (\gamma - \gamma_0)mc^2 \quad (2.25)$$

- The kinetic energy of the spent beam can be obtained by averaging the electron energies of each electron over the phase angle  $\theta$  as

$$\langle W_B \rangle = \frac{1}{2\pi} \int_0^{2\pi} W_f\{\tau, \theta\} d\theta \quad (2.26)$$

- The electronic efficiency of the device can also be estimated as the average loss of the electron energy from their initial value given as:

$$\eta = 1 - \frac{\langle W_B \rangle}{W_{beam}} \quad (2.27)$$

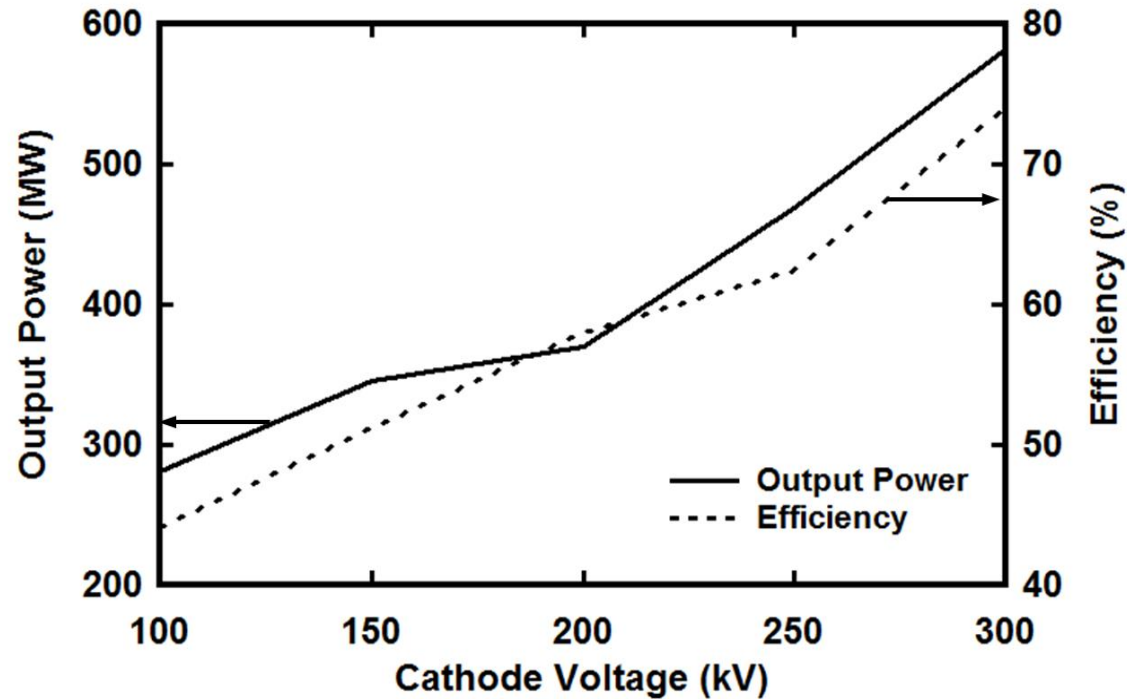


**Figure:** RF Output power and efficiency as function of cathode voltage (current = 750 A, and post-acceleration voltage 750 kV)

	RF Output Power	Efficiency
Miller et al. (1992)	235 MW	37 %
Present Analysis	280 MW	44 %

# Contribution II

## Design and Simulation Study of Reltron\*

\*The work has been published as:

**Manpuran Mahto** and Pradip Kumar Jain, “Design and Simulation Study of the HPM Oscillator—Reltron,” *IEEE Transactions on Plasma Science*, vol. 44, pp. 743–748, 2016.

# Design Methodology

24

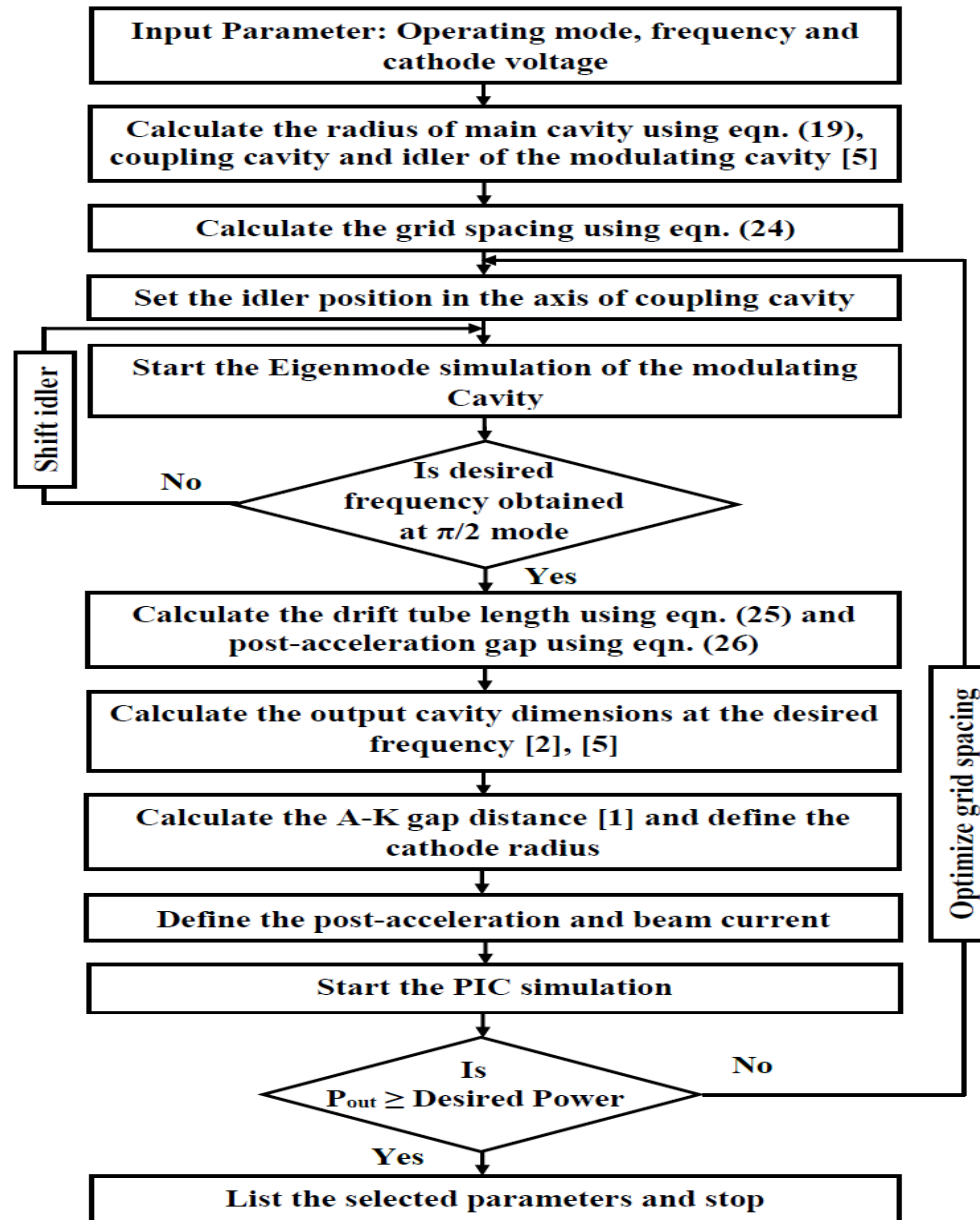


**Figure:** Flowchart describing the relatron design procedure.



# Device Simulation

**Table:** Design specifications of the reltron [Miller *et al.* (1992)]

(a) Device electrical specification	
Operating frequency ( $f$ )	2.75 GHz
Total beam voltage ( $V_{\text{beam}}$ )	850 kV
Cathode voltage ( $V_{\text{ak}}$ )	100 kV
Post-acceleration voltage ( $V_{\text{pa}}$ )	750 kV
Beam Current ( $I_b$ )	750 A
(b) Structural Parameters	
Main cavity radius ( $r_m$ )	38.27 mm
Coupling cavity radius ( $r_r$ )	25.51 mm
Idler radius	12.75 mm
Grid spacing ( $g$ )	18.70 mm
A-K gap spacing ( $d_{\text{ak}}$ )	20.50 mm
Drift tube length ( $L_{\text{DT}}$ )	44.80 mm
Post-acceleration gap ( $L_{\text{PA}}$ )	53.30 mm

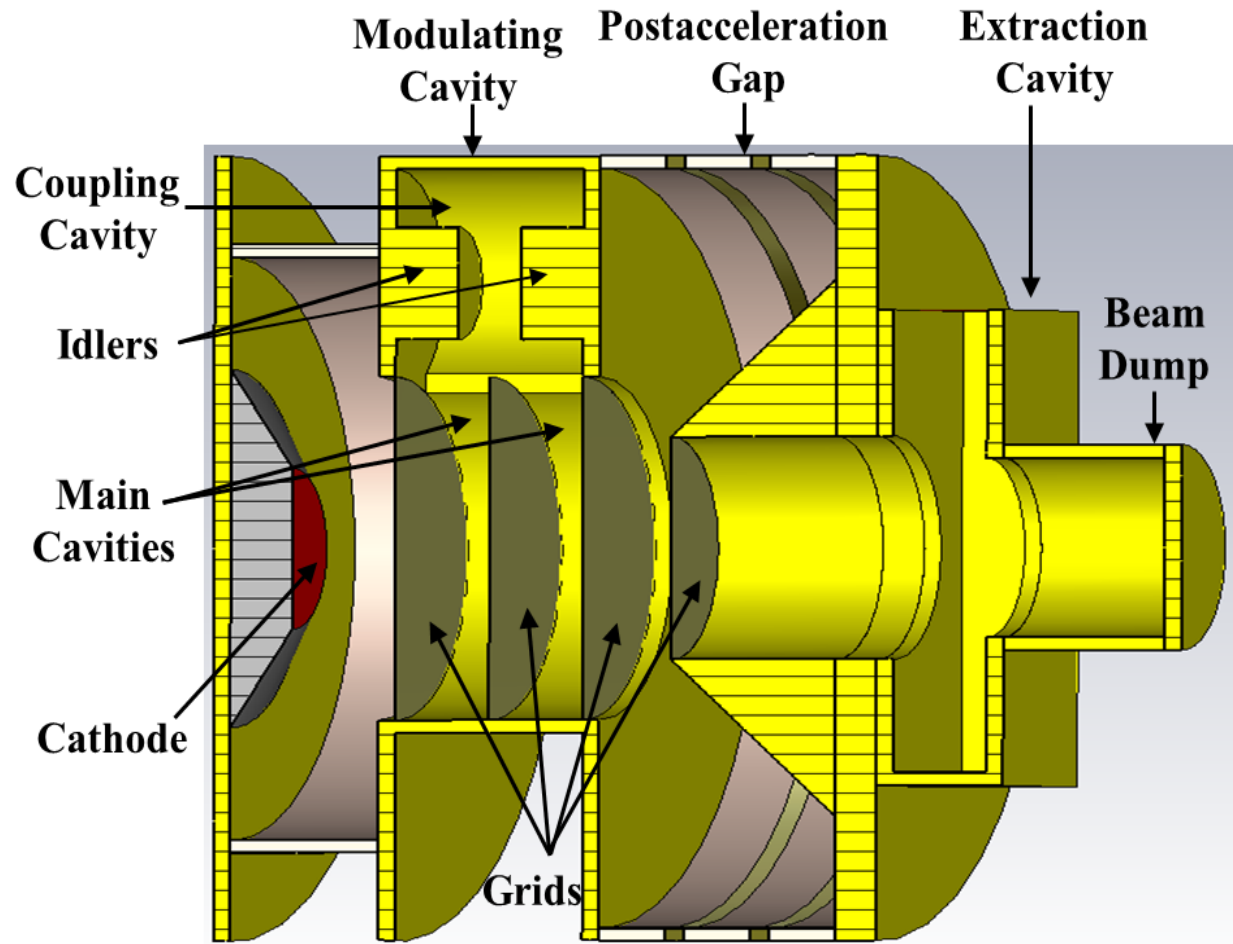
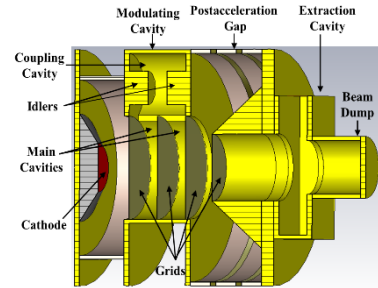
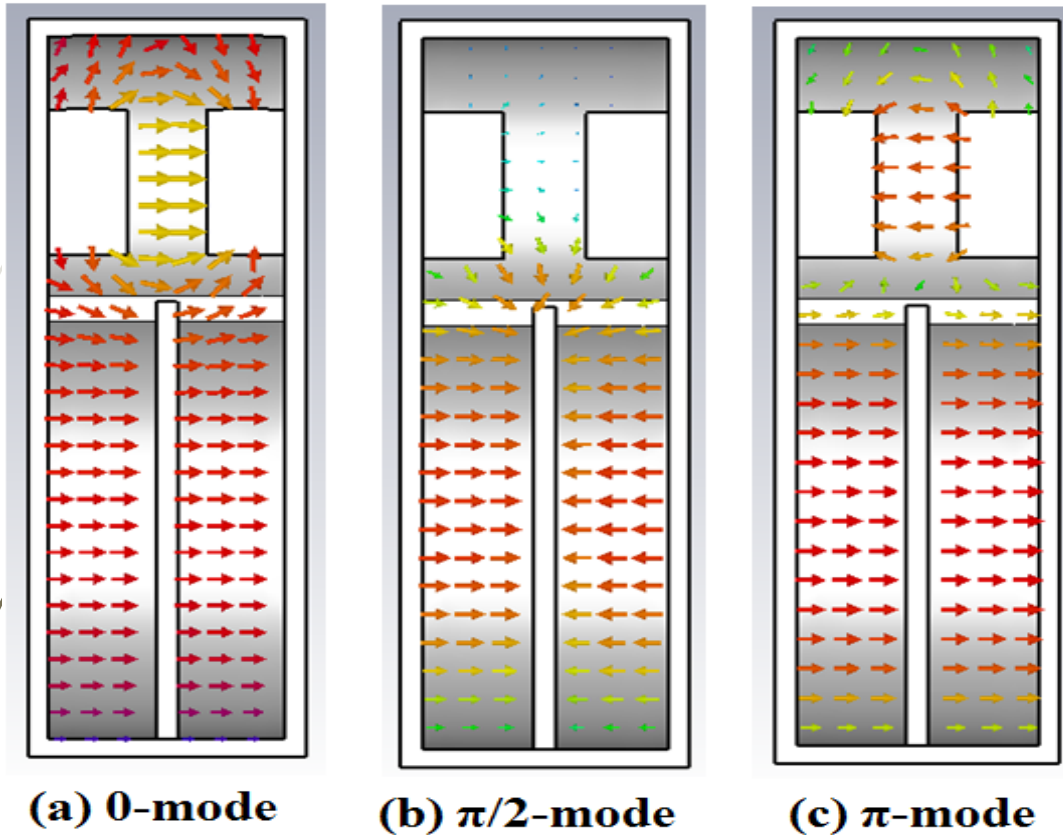


**Figure:** 3D schematic diagram of a reltron.



# Eigenmode Simulation



Mode	Frequency
0	2.57 GHz
$\pi/2$	2.76 GHz
$\pi$	2.96 GHz

**Figure:** Electric field patterns in (a) 0-mode (b)  $\pi/2$ -mode (c)  $\pi$ -mode conditions.

# PIC Simulation

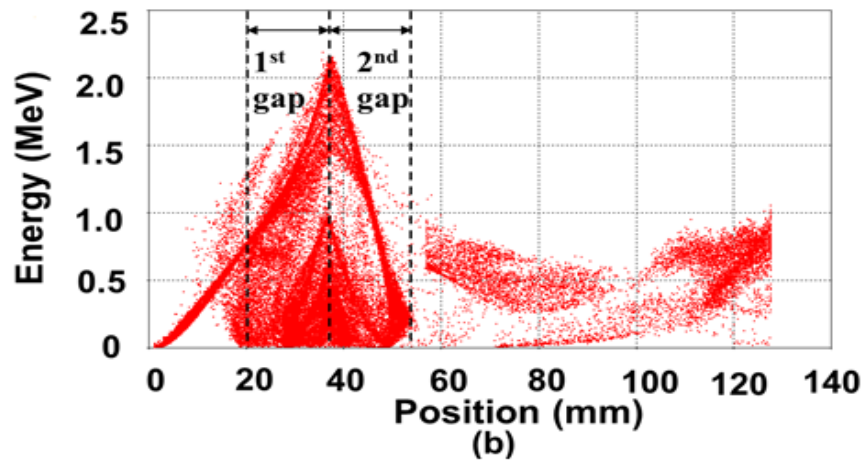
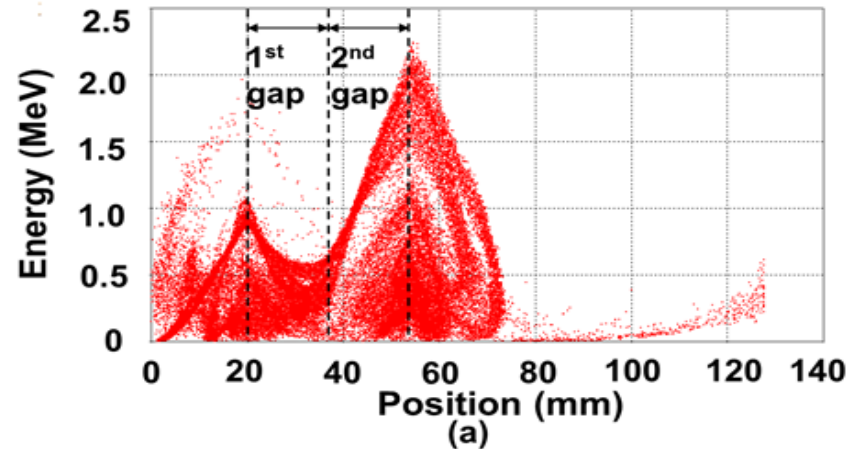
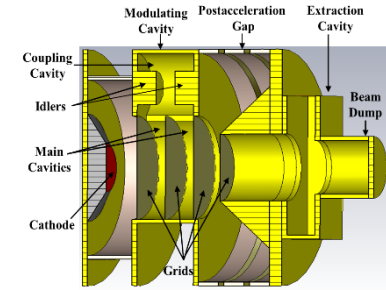


**Figure :** Plot of electron's phase space (a) first half cycle (b) second half cycle.

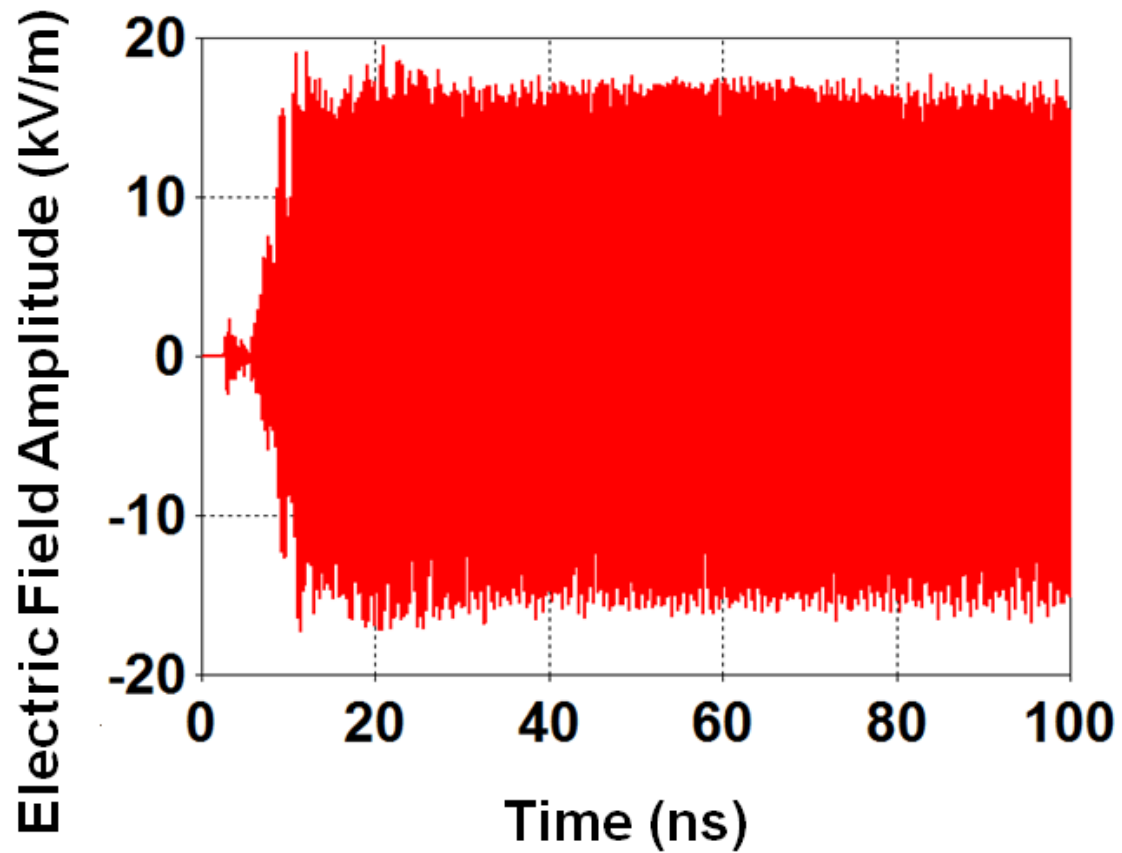


**Figure :** Electric field amplitude versus time plot at the output port.

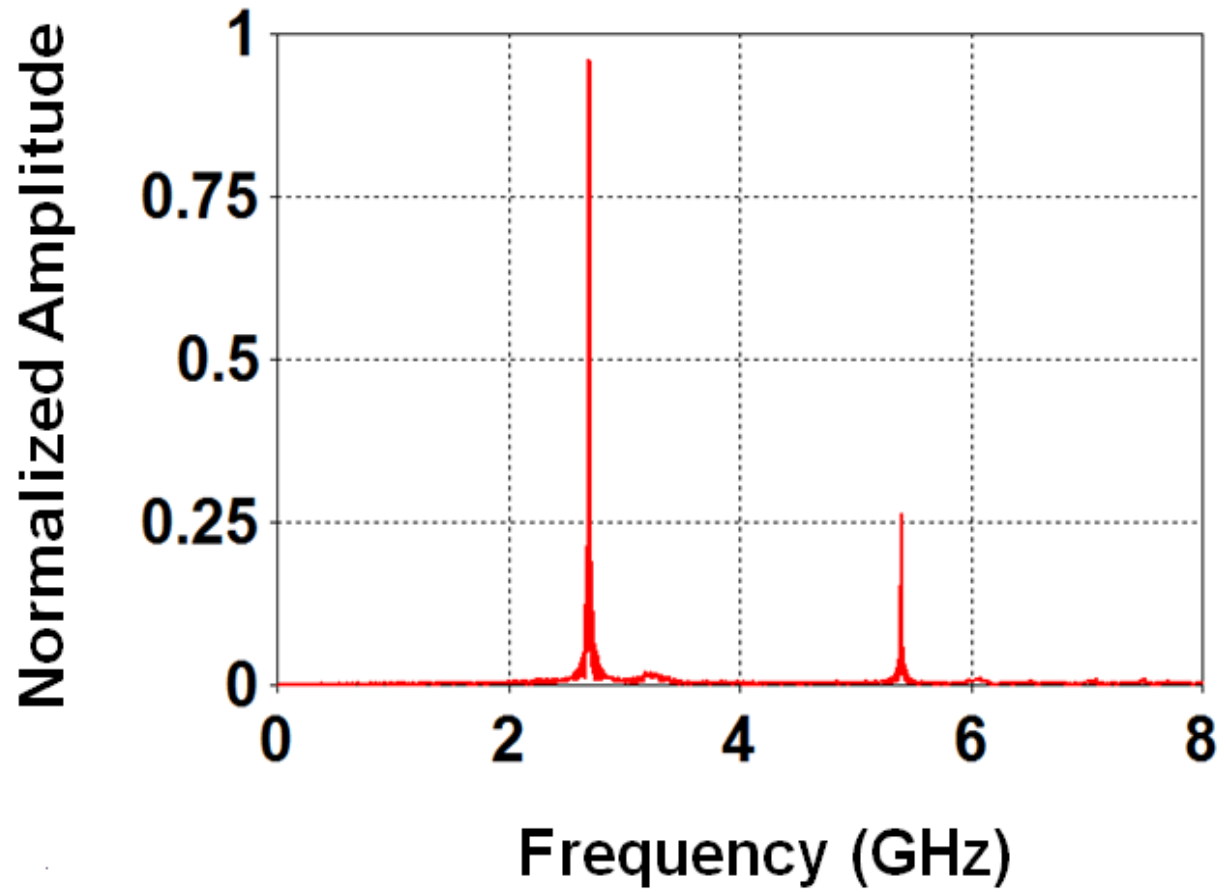


**Figure:** Frequency spectrum of electric field amplitude.

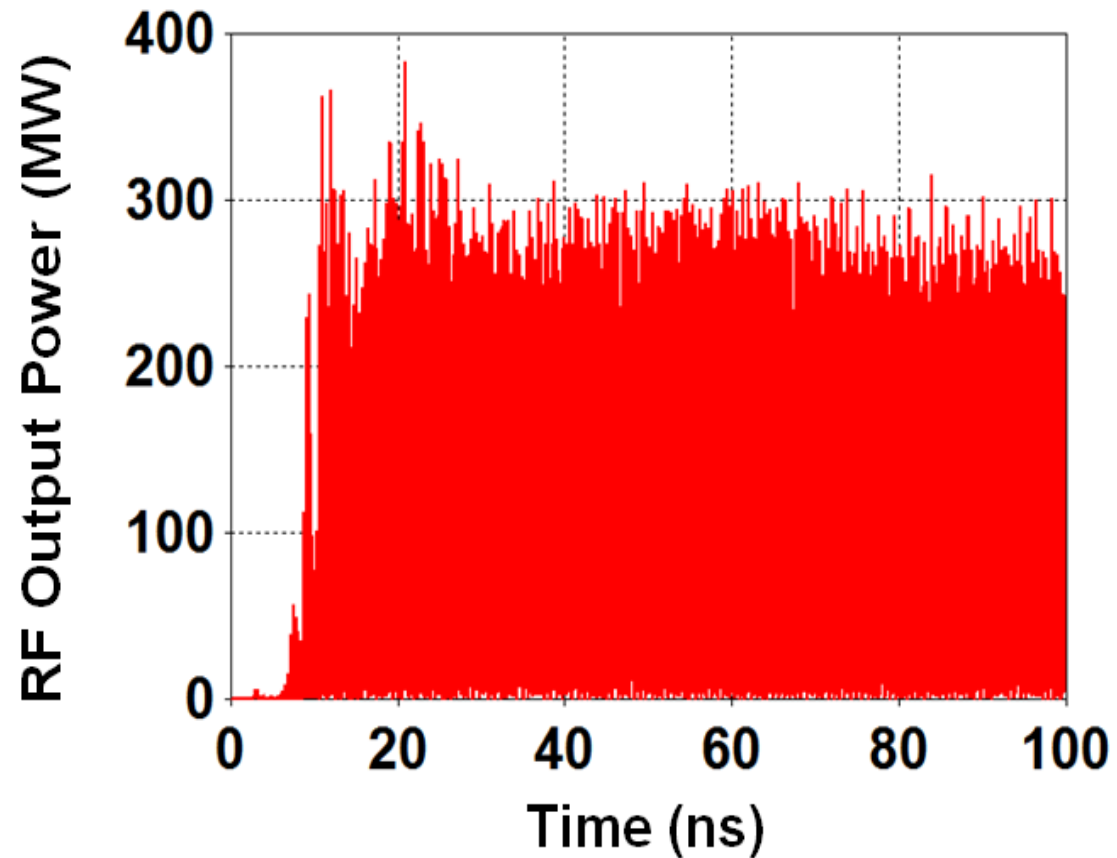


**Figure:** RF output power developed at the output port.

	RF Output Power	Efficiency
Miller et al. (1992)	~200 MW	~32 %
PIC Simulation	~225 MW	~36 %

# Contribution III

## Electron Beam and Electromagnetic Waves Interaction Analysis\*

\*The work has been published as:

**Manpuran Mahto** and P. K. Jain, “Electromagnetic Analysis of the HPM Oscillator — Reltron,” *AIP Physics of Plasmas*, vol. 23, p. 093118, 2016.



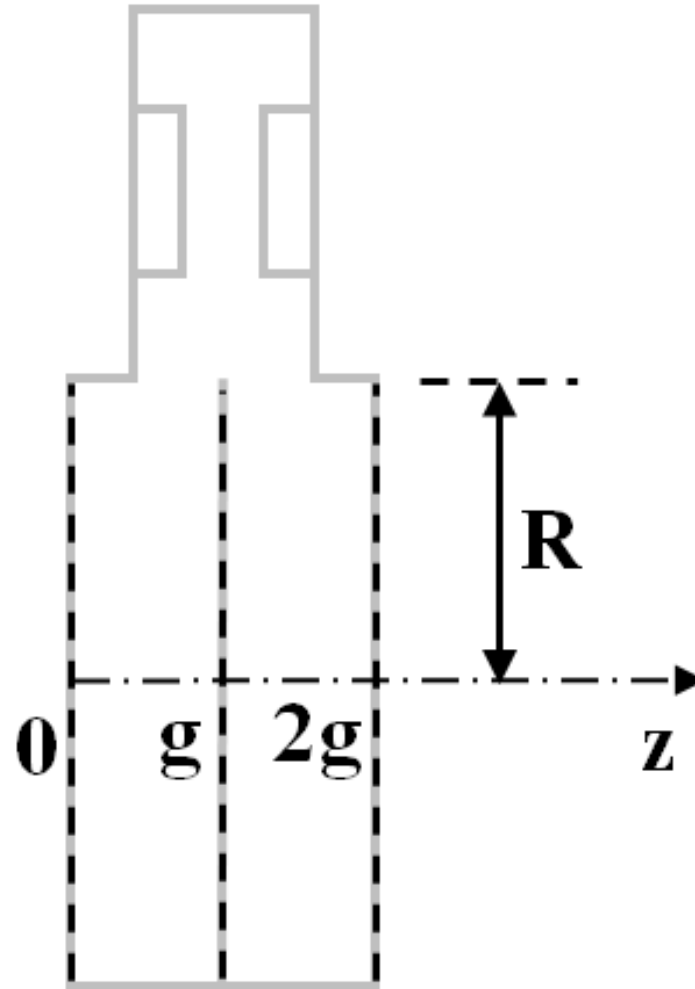
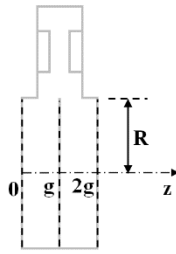


**Figure :** Basic schematic diagram of the modulation cavity of a reltron.

# Bunching Field



- The RF electric field generated inside the modulation cavity in  $\pi/2$  mode can be written as

$$E = \begin{cases} -E_0 \sin(\omega t + \theta) & 0 < z < g \\ E_0 \sin(\omega t + \theta) & g < z < 2g \end{cases} \quad (4.1)$$

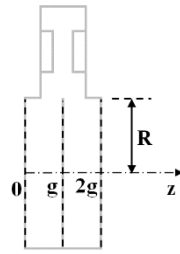
- The metal grids in the modulation cavity allow the electrons to pass through and confine the RF waves in between.
- Due to the reflections of the RF wave from the metal grids, only standing waves exist in between the metal grids and therefore, the axial electric field can be expressed as [Lemke (1992)]:

$$E_z = \sum_{n=1}^{\infty} E_{zn} = \sum_{n=1}^{\infty} [A_n J_0\{\Gamma_n r\} + B_n Y_0\{\Gamma_n r\}] e^{i(\omega t - \beta_n z)} \quad (4.2)$$

$\Gamma_n^2 (= 2\pi / \beta_n)$  is the radial propagation constant .

$\beta_n (= n\pi/g)$  is the axial propagation constant.

$n (= 1, 2, 3\dots)$  represents the stationary wave modal number.



- The axial electric field ( $E_z$ ) consists of forward and backward waves of the standing wave and expressions for these two waves can be written as:

$$E_z^f = \sum_{n=1}^{\infty} E_{zn}^f = \sum_{n=1}^{\infty} [A_n^f J_0\{\Gamma_n r\} + B_n^f Y_0\{\Gamma_n r\}] e^{i(\omega t - \beta_n z)} \quad (4.3)$$

$$E_z^b = \sum_{n=1}^{\infty} E_{zn}^b = \sum_{n=1}^{\infty} [A_n^b J_0\{\Gamma_n r\} + B_n^b Y_0\{\Gamma_n r\}] e^{i(\omega t + \beta_n z)} \quad (4.4)$$

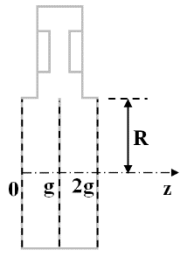
where the superscript  $f$  and  $b$  refer to the forward and backward components of the RF wave, respectively.

- The net axial electric field can be written as:

$$E_{zn} = E_{zn}^f + E_{zn}^b \quad (4.5)$$

- The axial electric field becomes null at the metal grid boundaries ( $z = 0, g, 2g$ ) and  $z = 0$  corresponds to the right face of the first grid and the wave equation can be written in the following form:

$$(E_{zn}^f + E_{zn}^b)_{z=0} = (A_n^f + A_n^b) J_0\{\Gamma_n r\} + (B_n^f + B_n^b) Y_0\{\Gamma_n r\} = 0$$



- Inside the main cavities when  $J_0\{\Gamma_n r\}$  and  $Y_0\{\Gamma_n r\}$  are assumed to have finite values, then:

$$A_n^b = -A_n^f \quad \text{and} \quad B_n^b = -B_n^f$$

- Further, the field components also become null at  $r = R$  which refer to the metallic surface of the RF cavities enabling us to write:

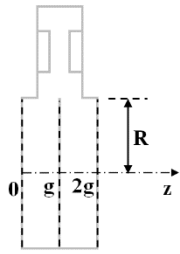
$$B_n^f = -A_n^f \frac{J_0\{\Gamma_n R\}}{Y_0\{\Gamma_n R\}} \quad (4.6)$$

- Substituting (4.3) and (4.4) in (4.5) gives:

$$E_{zn} = -2i \sin(\beta_n z) [A_n^f J_0\{\Gamma_n r\} + B_n^f Y_0\{\Gamma_n r\}] e^{i\omega t} \quad (4.7)$$

- Again substituting (4.6) in (4.7) yields:

$$E_{zn} = \sum_{n=1}^{\infty} A_n^* G_n\{\Gamma_n r\} \sin(\beta_n z) e^{i\omega t} \quad (4.8)$$



Here,

$$A_n^* = \frac{-2iA_n^f}{Y_0\{\Gamma_n R\}}$$

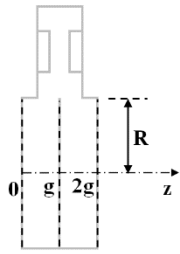
$$G_n\{\Gamma_n r\} = [J_0\{\Gamma_n r\}Y_0\{\Gamma_n R\} - J_0\{\Gamma_n R\}Y_0\{\Gamma_n r\}]$$

- The axial electric field including the effect of space charge wave can be written as

$$E_{zn} = \begin{cases} \frac{1}{2}[G_n\{\Gamma_n r\} \zeta\{z, t\} + E_{scz}] \sin(\beta_n z) e^{i\omega t} & 0 \leq z \leq g \\ -\frac{1}{2}[G_n\{\Gamma_n r\} \zeta\{z, t\} + E_{scz}] \sin(\beta_n z) e^{i\omega t} & g \leq z \leq 2g \end{cases} \quad (4.9)$$

$\zeta\{z, t\}$  is the slowly varying amplitude of the RF wave.

- It is assumed that the slowly varying function varies in the axial direction and vanishes on the metal grid boundaries ( $z = 0, g, 2g$ ).



- The axial electric field of space charge wave  $E_{scz}$  in the individual cavities of the modulation cavity can be expressed as:

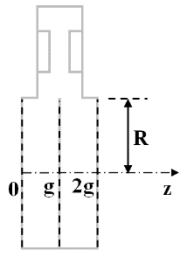
$$E_{scz} = \frac{\gamma^3 / \omega_p^2 (\beta_n v - \omega)^2}{1 - \gamma^3 / \omega_p^2 (\beta_n v - \omega)^2} G_n \{ \Gamma_n r \} \zeta \{ z, t \}$$

- For the side coupled modulation cavity, the above expression modifies as:

$$E_{scz} = (\psi - 1) G_n \{ \Gamma_n r \} \zeta \{ z, t \} \quad (4.10)$$

Here,

$$\psi = \frac{\gamma^3}{\omega_p^2} \left( \frac{1}{(\beta_n v - \omega)^2} + \frac{1}{(\beta_n v + \omega)^2} \right)^{-1}$$



- Putting this value of space charge wave  $E_{scz}$  in equation (4.9) and  $E_{zn}$  becomes:

$$E_{zn} = \begin{cases} \frac{\psi}{2} G_n \{\Gamma_n r\} \zeta \{z, t\} \sin(\beta_n z) e^{i\omega t} & 0 \leq z \leq g \\ -\frac{\psi}{2} G_n \{\Gamma_n r\} \zeta \{z, t\} \sin(\beta_n z) e^{i\omega t} & g \leq z \leq 2g \end{cases} \quad (4.11)$$

- The above expression for the axial stationary harmonic electric field is a combination of the standing and space-charge waves generated inside the cavity, thereby denotes the bunching field in the modulation cavity.

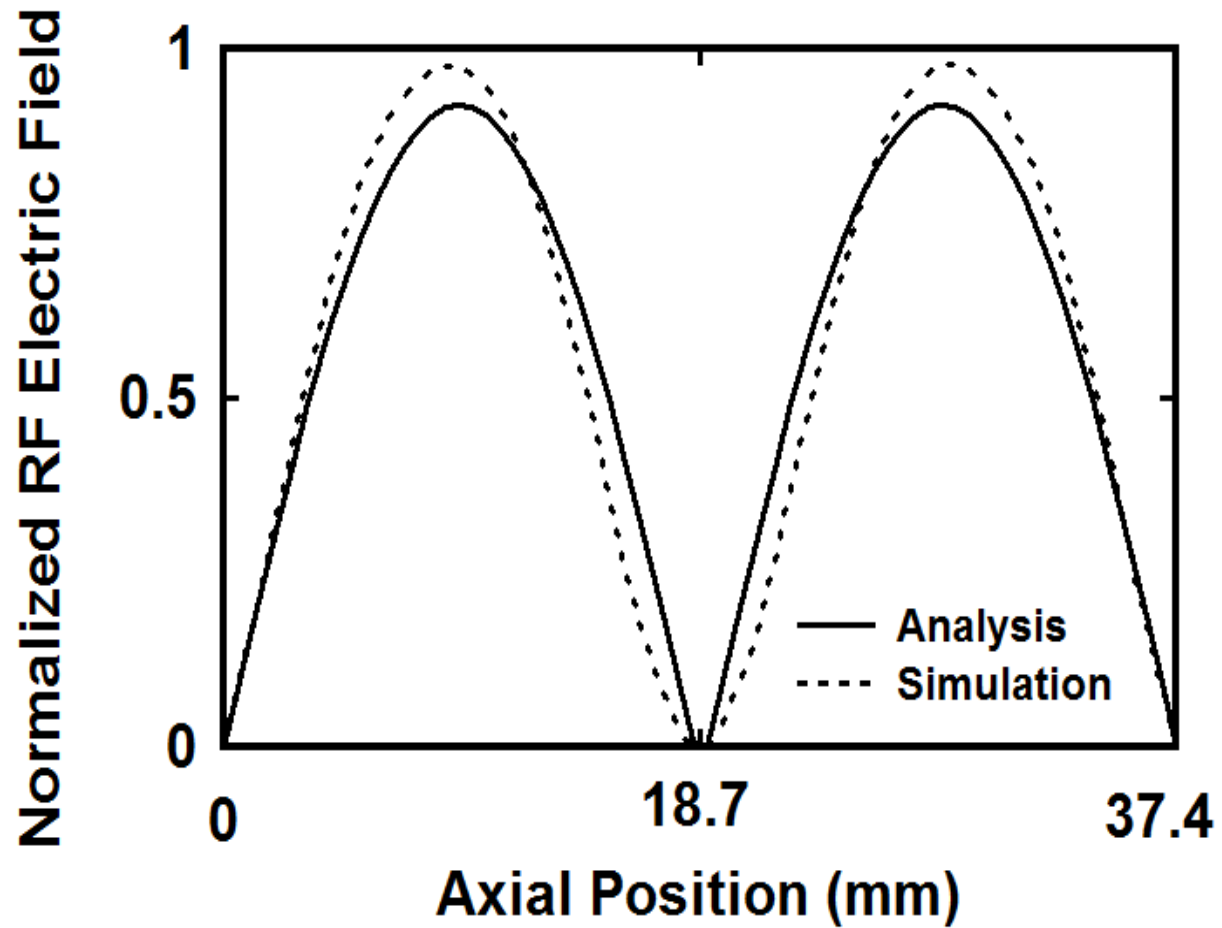


**Figure:** Variation of the normalized RF electric field along the axial direction in the side-coupled modulation cavity.



# Modulation Process

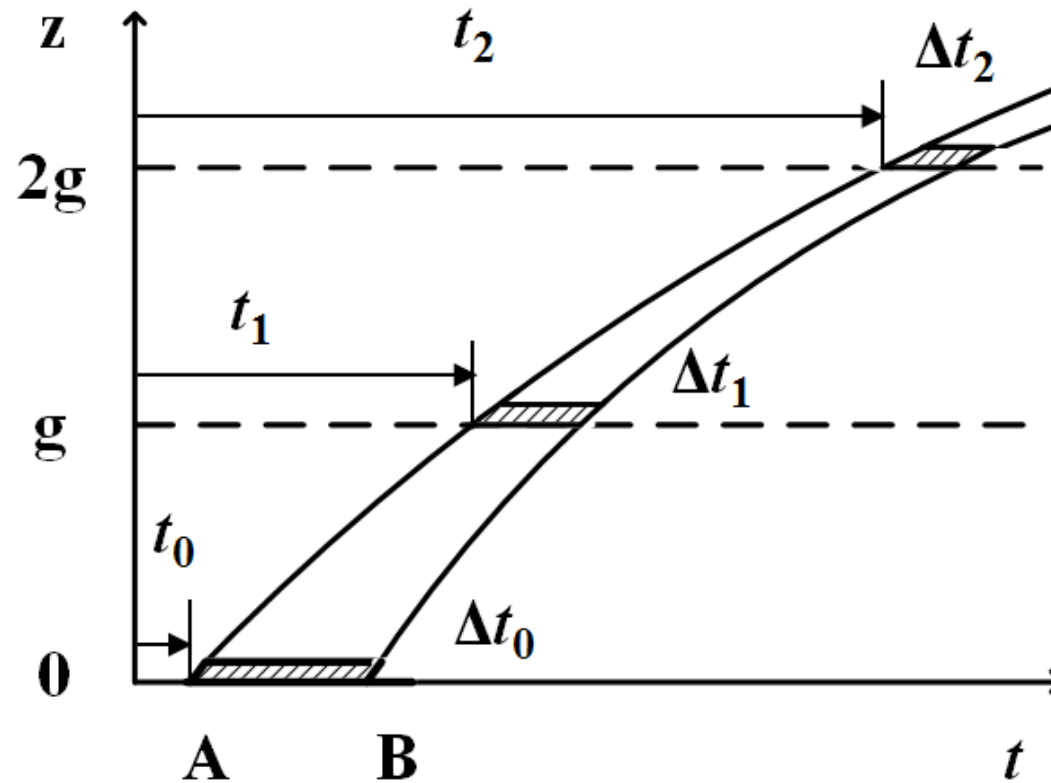
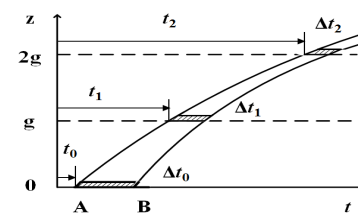


**Figure:** Electron Trajectories of two electrons A and B in presence of DC potential in the modulation cavity.



- Considering an electron A, shown in Fig. 4.3, enters the modulation cavity  $z = 0$  at time  $t_0$  with initial velocity  $v_0$  and leaves the first gap at time  $t_1$  with the velocity

$$v_1 = v_0 \left[ 1 + \frac{MV_{gap1}}{2V_{ak}} \sin(\beta_n z - \omega t_1) \right] \quad (4.12)$$

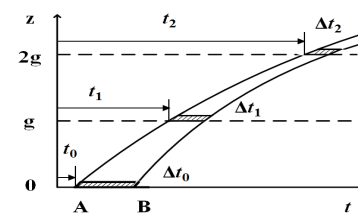
$V_{ak}$  is the cathode voltage

$M (= \sin(\omega g / v_0) / (\omega g / v_0))$  is the coupling coefficient

$V_{gap1}$  is the RF potential developed across the the first grid spacing

- Then, from the conservation of energy the electron A will leave the second gap at time  $t_2$  with velocity:

$$v_2 = v_1 \left[ 1 + \frac{MV_{gap2}}{2(V_{ak} + V_{gap1})} \sin(\beta_n z - \omega t_2) \right] \quad (4.13)$$

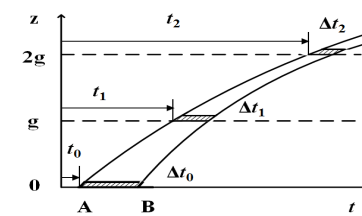


- As the bunched electrons come out from the modulation cavity and enters in the post acceleration gap, due to the applied acceleration potential  $V_{pa}$  in this region, the electrons bunches get re-accelerated and moves toward the extraction cavity with the velocity  $v_{pa}$ :

$$v_{pa} = v_2 \left( 1 + \frac{V_{pa}}{V_{ak} + V_{gap1} + V_{gap2}} \right)^{1/2} \approx v_2 \left( 1 + \frac{V_{pa}}{V_{ak}} \right)^{1/2}$$

- Now, considering an electron beam which is velocity modulated in the 1<sup>st</sup> and 2<sup>nd</sup> grid spacings with velocities  $v = v_0 + v_1\{t\}$  and  $v = v_1 + v_2\{t\}$ .
- In the first grid spacing  $0 < z < g$  the deceleration ( $d_0$ ) is given as

$$d_0 \cong - \left| \frac{eE_{zn}}{\gamma^3 m} \right|$$



- The electron A reaching  $z = 0$  at time  $t_0$  will arrive  $z = g$  at time  $t_1$  which can be obtained from:

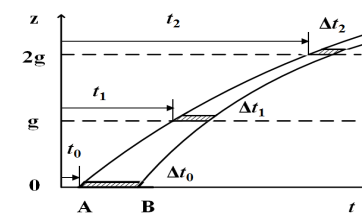
$$g = [v_0 + v_1\{t_0\}](t_1 - t_0) - \frac{1}{2}d_0(t_1 - t_0)^2 \quad (4.14)$$

- Now considering further, another electron B, will arrive  $z = g$  at time  $t_1 + \Delta t_1$  which is to be computed from:

$$g = [v_0 + v_1\{t_0 + \Delta t_0\}][(t_1 + \Delta t_1) - (t_0 + \Delta t_0)] - \frac{1}{2}d_0[(t_1 + \Delta t_1) - (t_0 + \Delta t_0)]^2 \quad (4.15)$$

- Equation (4.14) and (4.15), yields:

$$\Delta t_1 = \Delta t_0 \left( 1 + \frac{g}{v_0^2} \mathcal{F} \frac{\partial v_1\{t_0\}}{\partial t_0} \right) \quad (4.16)$$



- **Considering now the charge conservation in the 1<sup>st</sup> grid spacing**

$$I_0 \Delta t_0 = (I_0 + I_1) \Delta t_1 \quad (4.17)$$

- **Using (4.16) in (4.17) becomes:**

$$I_1 \cong -\frac{I_0 g}{v_0^2} \mathcal{F} \frac{\partial v_1 \{t_0\}}{\partial t_0} \quad (4.18)$$

which is the current modulation at  $z = g$  under the influence of retarding potential.

- **Since, both the main cavities of the modulation cavity are identical in nature, therefore, in the second grid spacing  $g < z < 2g$ .**
- **There is an accelerating electric field of same magnitude that of the retarding field as in case of first grid spacing. Hence, the current modulation at  $z = 2g$  becomes:**

$$I_2 \cong -\frac{I_1 g}{\tilde{v}_0^2} \mathcal{F} \frac{\partial v_2 \{t_1\}}{\partial t_1} \quad (4.19)$$

This equation represents the conversion of velocity modulation into current modulation in the side coupled modulation cavity.

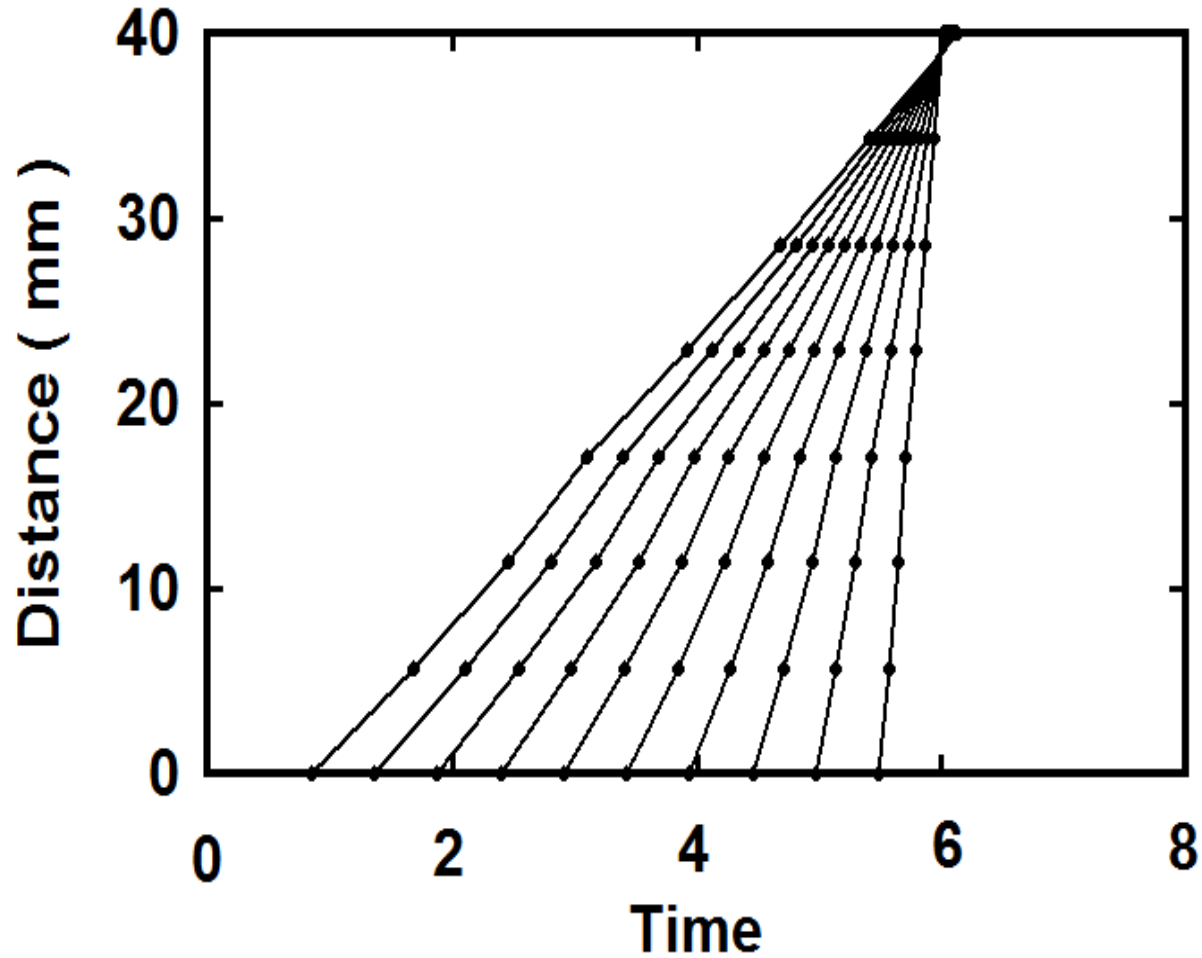


**Figure:** Distance-time graph for the electron beam movement in the side-coupled modulation cavity.

## Associated RF Energy

- All the electrons in the beam is assumed to have the same constant values of energy ( $H$ ) and canonical momentum  $\widehat{p}_z$ .
- The corresponding electric field profile distribution function is defined as

$$f_0\{r, p\} = \eta\{r\} \delta\{H - mc^2 + c\widehat{p}_z\} \delta\{p_r\} \delta\{p_\theta\} \quad (4.20)$$

where  $\eta\{r\}$  represents the charged particle density and  $\delta$  represents the Dirac delta function

The terms  $p_r$  and  $p_\theta$  are the radial and azimuthal component of the momentum ( $p$ ), respectively.

- Using the law of conservation of energy, the total sum of the charge particles energies becomes zero and can be expressed as

$$H = c\{p_z^2 + m^2c^2\}^{1/2} - e\phi\{r\} \quad (4.21)$$

where  $\phi\{r\}$  is the electrical potential.



- **In case of reltron, the canonical momentum can be obtained as**

$$\hat{p}_z = p_z - e B_z \{r\} / c$$

where  $p_z$  is the axial momentum and  $B_z \{r\}$  represents the equilibrium magnetic potential.

- **The density of charged particles can be expressed in the form**

$$\eta \{r\} = K^2 (mc^3 / 4\pi e^2) (r_c / r)^K / r^2$$

$$K = I_A / (\gamma I_\alpha) \quad \text{and} \quad I_\alpha = mc^3 / 2e$$

- **The electric and magnetic potentials, in terms of second order differential equations are defined as:**

$$\frac{\partial^2}{\partial r^2} \phi \{r\} = -4\pi \rho \{r\} \tag{4.22}$$

$$\frac{\partial^2}{\partial r^2} B_z \{r\} = -\frac{4\pi}{c} j_z \{r\} \tag{4.23}$$

- The terms  $\rho\{r\}$  and  $j_z\{r\}$  are the space charge and current densities, and defined by

$$\rho\{r\} = -e \int_{-\infty}^{\infty} \int_{-\infty}^{\infty} \int_{-\infty}^{\infty} dp_z dp_\theta dp_r f_0\{r, p\} \quad (4.24)$$

$$j_z\{r\} = -e \int_{-\infty}^{\infty} \int_{-\infty}^{\infty} \int_{-\infty}^{\infty} dp_z dp_\theta dp_r v_z f_0\{r, p\} \quad (4.25)$$

- Substituting (4.20) in (4.24) and (4.25) provides:

$$\rho\{r\} = -(mc^2 / 4\pi e)(K / r)^2 \cosh(\chi) \quad (4.26)$$

$$j_z\{r\} = -(mc^3 / 4\pi e)(K / r)^2 \sinh(\chi) \quad (4.27)$$

where  $\chi = \ln[(r_m / r_c)^K]$

- The corresponding equilibrium potentials of the cavity can be obtained using equations (4.22) - (4.25) as:

$$e\phi\{r\} = mc^2 [\cosh(\chi) - 1] \quad (4.28)$$

$$eB_z\{r\} = mc^2 \sinh(\chi) \quad (4.29)$$

- The above values can be substituted to the equations (4.20) and (4.21) which will provide the energy developed the reltron.

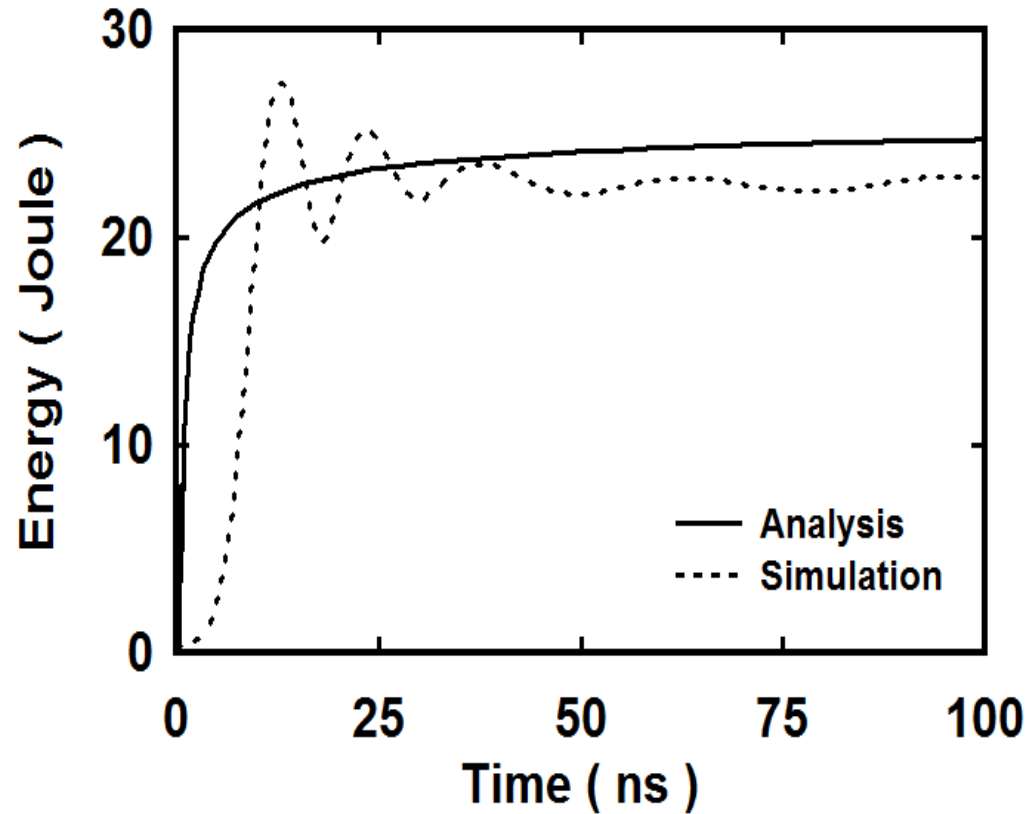


**Figure:** RF energy developed in the reltron, for the typically selected device parameters.

	Pulse width	RF Energy
Analysis	100 ns	~ 24 J
Simulation	100 ns	~ 22.5 J

# Contribution IV

## Virtual Cathode Formation Mechanism in the Reltron\*

\*The work has been published as:

- ❖ **Manpuran Mahto** and P. K. Jain, “Study of Virtual Cathodes Formation during Beam-Wave Interaction in the Reltron Oscillator,” *AIP Physics of Plasmas*, vol. 24, p. 093107, 2017.
- ❖ **Manpuran Mahto** and Pradip Kumar Jain, “PIC Simulation Study of the Formation Mechanism of Periodic Virtual Cathodes in the Reltron,” *IEEE Transactions on Plasma Science*, vol. 46, pp. 518 - 523, 2018.

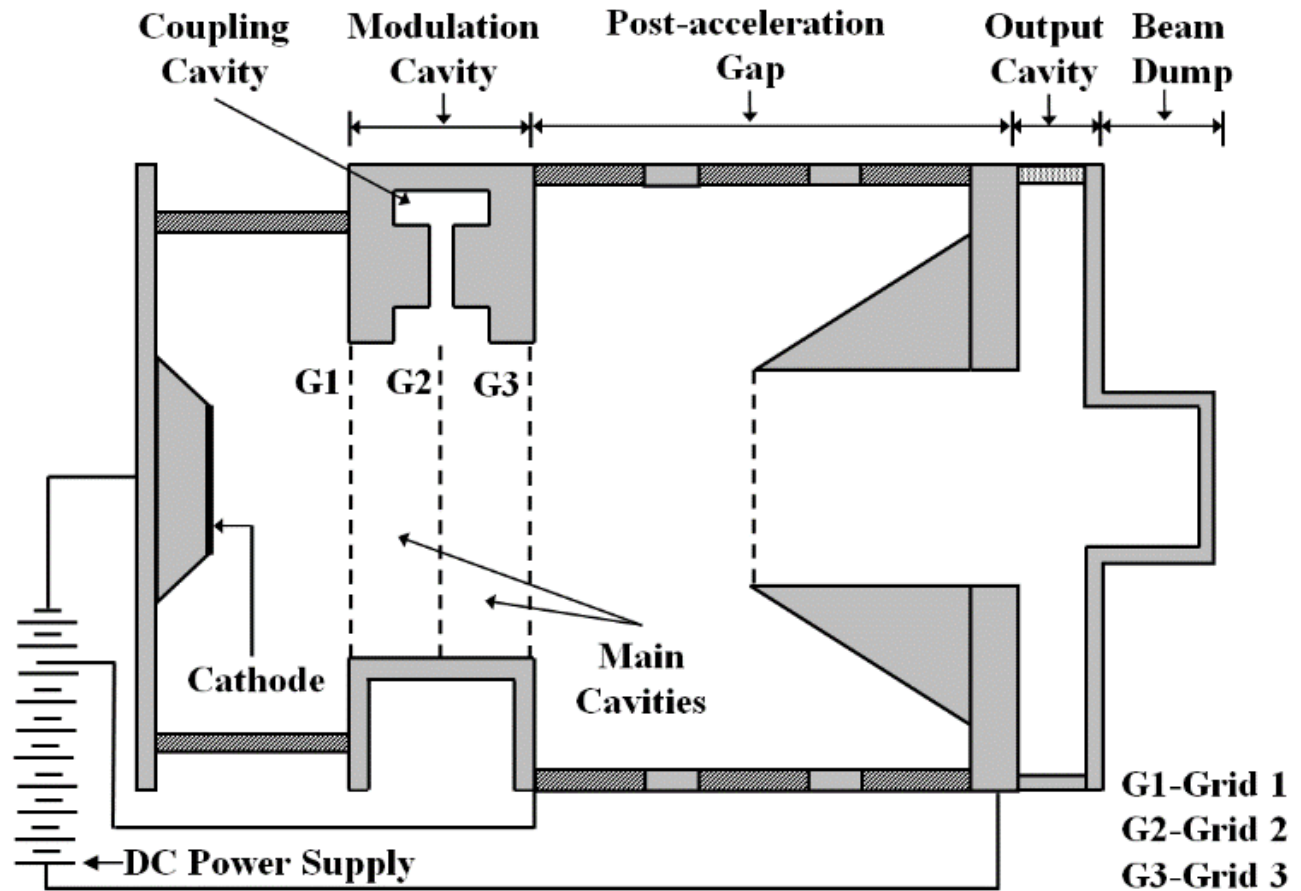


**Figure:** Basic schematic diagram of a reltron.

# Space Charge Limiting Current

- In relatron, the IREB currents lie close to the space charge limiting current.
- At this point, the potential depression starts, and the kinetic energy drops to  $\gamma = \gamma_0^{1/3}$
- The axial beam velocity governed by the Lorentz force equation gives the relation as [Friedman *et al.* (1988)]:

$$\gamma^3 \left( \frac{\partial}{\partial t} + v \frac{\partial}{\partial z} \right) v = \frac{e}{m} E\{z, t\} \quad (5.1)$$

- The surface density of the beam  $\sigma\{z, t\}$  can be expressed as:

$$\frac{\partial \sigma\{z, t\}}{\partial t} + \frac{\partial}{\partial z} (v \sigma\{z, t\}) = 0 \quad (5.2)$$

- With perfect conductor boundary conditions under the assumption of long wave approximation, below differential equation can be obtained as [Friedman *et al.* (1988)]:

$$-\frac{\epsilon_0}{r_c \ln(r_m / r_c)} \frac{\partial E\{z, t\}}{\partial z} = \left( \frac{\partial^2}{\partial z^2} - \frac{1}{c^2} \frac{\partial^2}{\partial t^2} \right) \sigma\{z, t\} \quad (5.3)$$

- In the steady state condition expression (5.1) becomes:

$$\gamma^3 v \frac{\partial v}{\partial z} = c^2 \frac{\partial \gamma}{\partial z} = \frac{e}{m} E\{z, t\} = -\frac{e}{m} \frac{\partial \phi}{\partial z} \quad (5.4)$$

where the term  $\phi$  is the electrostatic potential.

- From conservation of energy, we have the relation:

$$\gamma mc^2 + e\phi = \gamma_{inj} mc^2 \quad (5.5)$$



- From conservation of charge the product of the beam surface density and axial beam velocity becomes constant, *i.e.*:

$$\sigma v = \text{const} \quad (5.6)$$

- The beam surface density is defined by:

$$\sigma = \frac{\epsilon_0}{r_c \ln(r_m / r_c)} \phi \quad (5.7)$$

- Combining equations (5.5), (5.6) and (5.7) we can simplify the relationship as:

$$\gamma_{inj} = \gamma + \frac{I_0}{I_s \beta} \quad (5.8)$$

- The normalized threshold current ( $I_s$ ) is the current developed in the cavity before the space charge potential is set up and it is defined as:

$$I_s = \frac{2\pi\epsilon_0 mc^3}{e \ln(r_m / r_c)} \quad (5.9)$$

- From (5.5) and (5.8), it can be observed that the kinetic energy of the electrons reduces as the IREB current increases and the largest permissible current known as space charge limiting current ( $I_{sc}$ ) is given by:

$$I_{sc} = \frac{8.5(\gamma_{inj}^{2/3} - 1)^{3/2}}{\ln(r_m / r_c)} \text{ kA} = I_s (\gamma_{inj}^{2/3} - 1)^{3/2} \text{ kA} \quad (5.10)$$

When the beam current exceeds this space charge limiting current, the incident electrons split into two different parts:

1. transmitted electrons which cross the virtual cathode, and
2. reflected electrons which propagate in the reverse direction towards the physical cathode.

# Steady State Condition

- In the steady state condition, the total current density is the sum of the transmitted and reflected current densities.
- The electrons propagate in the longitudinal direction and the electric field developed due to the space charge waves can be expressed as:

$$\frac{dE\{z,t\}}{dz} = -\frac{d^2\phi}{dz^2} = -\frac{\sigma\{z,t\}}{\epsilon_0} \quad (5.11)$$

- The above expression can be rewritten as:

$$dE\{z,t\} = -\frac{J}{\epsilon_0 v} dz = -\frac{J}{\epsilon_0 v} \frac{d\phi}{E\{z,t\}} \quad (5.12)$$

- Integrating equation (5.12) and solving yields:

$$E\{z,t\} = \sqrt{-\frac{2Jmc}{e\epsilon_0}} (\gamma^2 - 1)^{1/4} \quad (5.13)$$

- **The expression (5.13) represents the electric field profile between the injection position and the virtual cathode.**
- **The time required to reach the electrons from the virtual cathode to the injection position is known as the time of flight or transit time  $\tau$  which can be found as:**

$$\tau = \int_0^{\tau} dt = - \int_{z_{vc}}^0 \frac{dz}{v} = - \int_{z_{vc}}^0 \frac{en}{J} dz = \int_0^{E(0)} \frac{\epsilon_0}{J} dE \{z, t\} \quad (5.14)$$

where  $z_{vc}$  is the position of the virtual cathode in the longitudinal direction.

- **Solving equation (5.14), transit time  $\tau$  can be written as:**

$$\tau = \sqrt{\frac{2\epsilon_0 m \gamma}{ne^2}} = \frac{\sqrt{2}}{\omega_p} \quad (5.15)$$

- **Expression (5.15) shows that the electrons transit time is inversely proportional to the plasma frequency.**

# RF Interaction Process

60

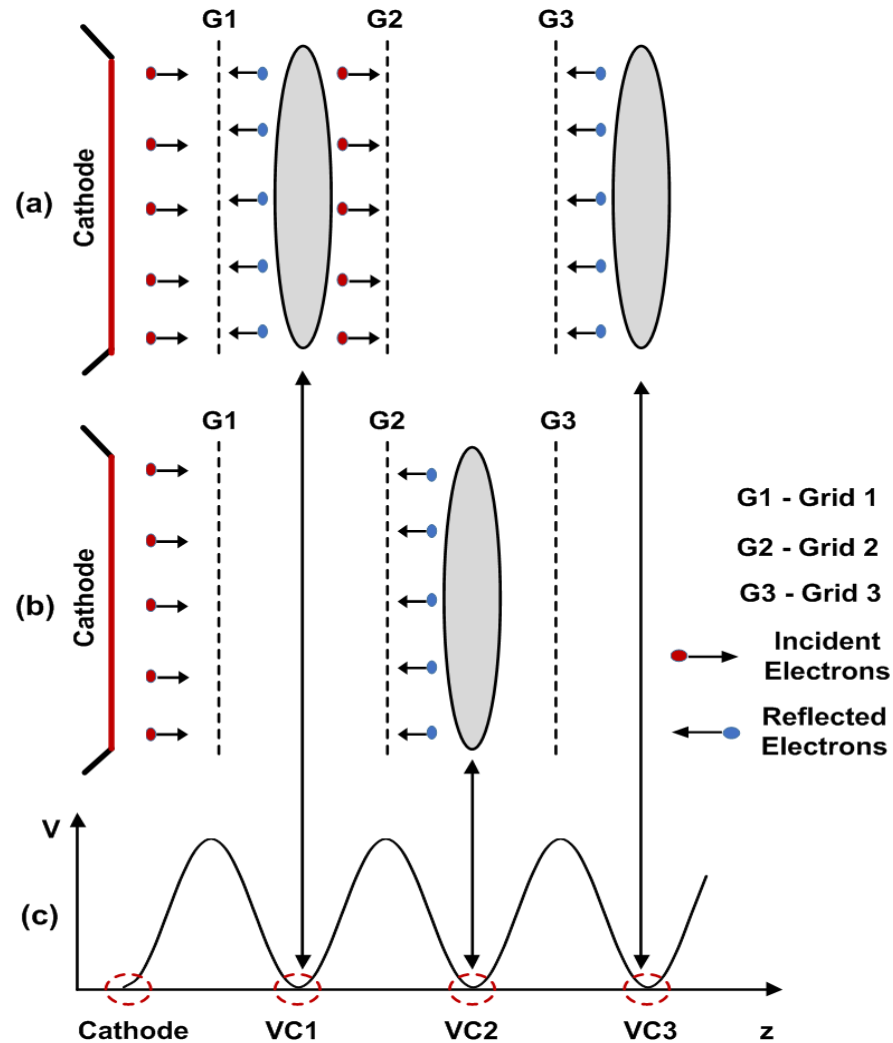
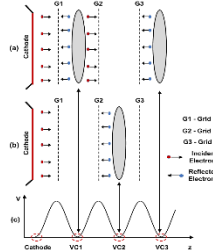


**Figure:** Behaviour of virtual cathode in relatron (a) double virtual cathode condition, (b) single virtual cathode condition (c) axis representation.



- The RF electric field generated due to the beam space charge can be expressed as:

$$E_{mc} = E_0 \sin \omega t \quad (5.16)$$

- The oscillating electric field due to the virtual cathode VC1 can be represented as:

$$E_{VC1} = E'_0 \sin \omega t \quad (5.17)$$

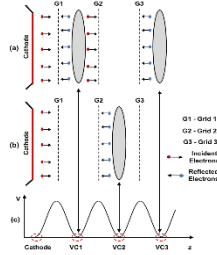
- The net momentum  $p$  is given by the RF electric field and oscillating electric field of VC1 as:

$$\frac{dp}{dt} = e(E_0 + E'_0) \sin \omega t$$

- Suppose the incident electrons enter the injection point (first grid G1), at time  $t_0$  and as it propagates to the virtual cathode VC1, the kinetic energy of the electrons start decreasing.

- After some time  $t = t_0 + \tau_1$  the electrons reach at the virtual cathode VC1 where its velocity drop to zero; then we can represent the relation for the injected electrons as

$$P_{i1} = \int_{t_0}^{t_0 + \tau_1} e(E_0 + E'_0) \sin \omega t dt \quad (5.18)$$



- Solving the expression (5.18) provides:

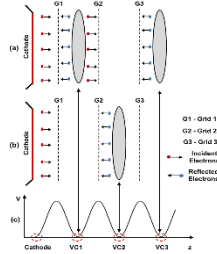
$$p_{i1} = \frac{2e(E_0 + E'_0)}{\omega} \sin \omega \left( t_0 + \frac{\tau_1}{2} \right) \times \sin \omega \left( \frac{\tau_1}{2} \right) \quad (5.19)$$

- The reflected electrons from the virtual cathode VC1 will reach the injection position G1 at a particular time  $t = t_0 + \tau_1 + \tau_2$  ; then the electron momentum can be expressed as

$$p_{r1} = \int_{t_0 + \tau_1}^{t_0 + \tau_1 + \tau_2} e(E_0 + E'_0) \sin \omega t dt \quad (5.20)$$

- The above expression can be written in the form:

$$p_{r1} = \frac{2e(E_0 + E'_0)}{\omega} \sin \omega \left( t_0 + \tau_1 + \frac{\tau_2}{2} \right) \times \sin \omega \left( \frac{\tau_2}{2} \right) \quad (5.21)$$



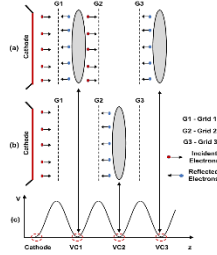
- The average momentum is the difference between the momentums caused by the incident electrons ( $p_{i1}$ ) and reflected electrons ( $p_{r1}$ ):

$$p_{av1} = \frac{\overline{p_{i1} - p_{r1}}}{p_{i1}} = \frac{2e(E_0 + E'_0)}{\omega T p_{i1}} \int_0^T \left[ \sin \omega \left( t_0 + \frac{\tau_1}{2} \right) \times \sin \omega \left( \frac{\tau_1}{2} \right) - \sin \omega \left( t_0 + \tau_1 + \frac{\tau_2}{2} \right) \times \sin \omega \left( \frac{\tau_2}{2} \right) \right] dt_0 \quad (5.22)$$

- If transit time of the electrons do not depend on the direction of propagation, then  $\tau' = \tau_1 = \tau_2$  and the expression (5.22) can be rewritten as:

$$p_{av1} = \frac{2e(E_0 + E'_0)}{\omega T p_i} \int_0^T \left[ \sin \omega \left( t_0 + \frac{\tau'}{2} \right) - \sin \omega \left( t_0 + \frac{3\tau'}{2} \right) \right] \times \sin \omega \left( \frac{\tau'}{2} \right) dt_0 \quad (5.23)$$





- **If the derivative of the time of flight with respect to its average value is represented as**

$\delta_1 = \tau' - \bar{\tau}$  **then equation (5.23) can be written as:**

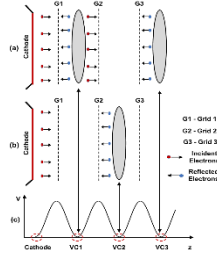
$$p_{av1} = -\frac{4e(E_0 + E'_0)}{\omega T p_{i1}} \int_0^T \left[ \sin^2 \omega \left( \frac{\bar{\tau} + \delta_1}{2} \right) \times \cos \omega \left( t_0 + \bar{\tau} + \delta_1 \right) \right] dt_0 \quad (5.24)$$

- **Expression (5.18) can be modified in the form:**

$$p_{i1} = e(\bar{\tau} + \delta_1) E_{mc} + e \int_{t_0}^{t_0 + \tau} e E'_0 \sin \omega t dt \quad (5.25)$$

- **Then expression (5.25) provides the relation:**

$$\omega \delta_1 = -2 \frac{E'_0}{E_{mc}} \sin \omega \left( \frac{\bar{\tau}}{2} \right) \sin \omega \left( t_0 + \frac{\bar{\tau}}{2} \right) \quad (5.26)$$



- When the phase shift is very less then the amplitude of the oscillation becomes also very low and in this situation expression (5.23) can be modified as:

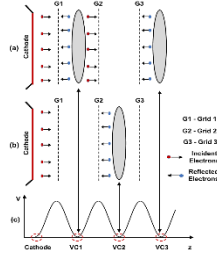
$$P_{av1} = -\frac{e(E_0 + E'_0)}{\omega T P_{i1}} \int_0^T \left[ \omega \delta_1 \times \sin \omega \bar{\tau} \times \cos \omega (t_0 + \bar{\tau}) \right] dt_0 \quad (5.27)$$

- Substituting (5.26) in (5.27) and solving yields:

$$P_{av1} = \left( \frac{E'_0}{E_{mc}} \right)^2 F\{\omega \bar{\tau}\} \quad (5.28)$$

- The amplitude of the oscillating electric field is very high, and therefore, the function  $F\{\omega \bar{\tau}\}$  is defined as:

$$F\{\omega \bar{\tau}\} = -\frac{1}{\omega \tau} \sin^2 \left( \frac{\omega \bar{\tau}}{2} \right) \sin \omega \bar{\tau} \quad (5.29)$$



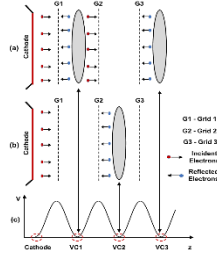
- Consider the situation when the phase shift becomes large enough. For this situation consider the notations:

$$s_1 = \omega \bar{\tau} \quad , \quad A_1 = \frac{E'_0}{E_{mc}} \quad , \quad \theta = \omega t_0 \quad (30)$$

- Using the notations mentioned in (5.30) and substituting (5.26) in (5.24) provides the relation:

$$p_{av1} = -\frac{2A_1}{s_1\pi} \int_0^{2\pi} \left[ \begin{array}{l} \sin^2 \left( \frac{s_1}{2} - A_1 \sin \left( \frac{s_1}{2} \right) \sin \left( \theta + \frac{s_1}{2} \right) \right) \times \\ \cos \left( \theta + s_1 - 2A_1 \sin \left( \frac{s_1}{2} \right) \sin \left( \theta + \frac{s_1}{2} \right) \right) \end{array} \right] d\theta \quad (5.31)$$

Expression (5.31) indicates the momentum relationship when the virtual cathode VC1 is formed. When a single virtual cathodes VC2 is formed in the condition will be similar to the expression (5.31).



- Now, we analyze the effect of second virtual cathode VC3 which will also exert an oscillating electric field. The oscillating electric field of VC3 can be represented as:

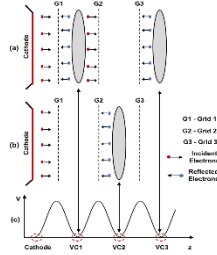
$$E_{VC3} = E_0'' \sin \omega t \quad (5.32)$$

- Suppose the incident electrons from VC1 starts at a time  $t = t_0 + \tau_1$  and reach the VC3 at time  $t = t_0 + \tau_1 + \tau_3$  where the velocity of the electrons again drops to zeros and we can represent the momentum of the injected electrons as:

$$p_{i2} = \int_{t_0 + \tau_1}^{t_0 + \tau_1 + \tau_3} e(E_0 + E_0'') \sin \omega t dt \quad (5.33)$$

- Solving the above yields:

$$p_{i2} = \frac{2e(E_0 + E_0'')}{\omega} \sin \omega \left( t_0 + \tau_1 + \frac{\tau_3}{2} \right) \times \sin \omega \left( \frac{\tau_3}{2} \right) \quad (5.34)$$



➤ **If the reflected electrons from VC3 reach to VC1 at a particular time**

**$t = t_0 + \tau_1 + \tau_3 + \tau_4$  then the momentum of the reflected electrons become:**

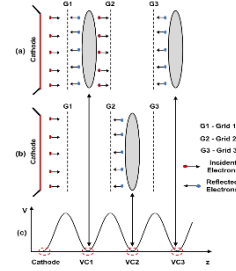
$$p_{r2} = \int_{t_0 + \tau_1 + \tau_3}^{t_0 + \tau_1 + \tau_3 + \tau_4} e(E_0 + E_0'') \sin \omega t dt \quad (5.35)$$

➤ **The above expression can be expressed in the form:**

$$p_{r2} = \frac{2e(E_0 + E_0'')}{\omega} \sin \omega \left( t_0 + \tau_1 + \tau_3 + \frac{\tau_4}{2} \right) \sin \omega \left( \frac{\tau_4}{2} \right) \quad (5.36)$$

➤ **The average momentum due to the virtual cathode VC3 is determined by the momentums caused by the incident electrons ( $p_{i2}$ ) and reflected electrons ( $p_{r2}$ ) as:**

$$p_{av2} = \frac{\overline{p_{i2} - p_{r2}}}{p_{i2}} = \frac{2e(E_0 + E_0'')}{\omega T p_{i2}} \int_0^T \left[ \begin{array}{l} \sin \omega \left( t_0 + \tau_1 + \frac{\tau_3}{2} \right) \times \sin \omega \left( \frac{\tau_3}{2} \right) - \\ \sin \omega \left( t_0 + \tau_1 + \tau_3 + \frac{\tau_4}{2} \right) \times \sin \omega \left( \frac{\tau_4}{2} \right) \end{array} \right] dt_0 \quad (5.37)$$



- Assumed that the transit time of the electrons between VC1 and VC3, does not depend on the direction of propagation, than  $\tau'' = \tau_3 = \tau_4$ , (5.37) becomes:

$$p_{av2} = \frac{2e(E_0 + E_0'')}{\omega T p_{i2}} \int_0^T \left[ \sin \omega \left( t_0 + \tau' + \frac{\tau''}{2} \right) - \sin \omega \left( t_0 + \tau' + \frac{3\tau''}{2} \right) \right] \times \sin \omega \left( \frac{\tau''}{2} \right) dt_0 \quad (5.38)$$

- The derivative of the time of flight with respect to its average value can be represented as  $\delta_2 = \tau'' - \bar{\tau}$ , then equation (5.38) can be written as:

$$p_{av2} = \frac{2e(E_0 + E_0'')}{\omega T p_{i2}} \int_0^T \left[ \sin \omega \left( t_0 + \tau' + \frac{\tau''}{2} \right) - \sin \omega \left( t_0 + \tau' + \frac{3\tau''}{2} \right) \right] \times \sin \omega \left( \frac{\tau''}{2} \right) dt_0 \quad (5.39)$$

- Expression (5.33) can be rewritten as:

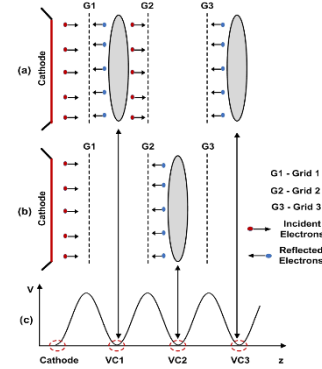
$$p_{i2} = e(\bar{\tau} + \delta_2) E_{mc} + e \int_{t_0 + \tau_1}^{t_0 + \tau_1 + \tau_3} e E_0'' \sin \omega t dt \quad (5.40)$$

➤ **Equation (5.40) provides the relation:**

$$\omega\delta_2 = -2 \frac{E_0''}{E_{mc}} \sin \omega \left( \frac{\tau}{2} \right) \sin \omega \left( t_0 + \bar{\tau} + \frac{\tau}{2} \right) \quad (5.41)$$

➤ **Substituting (5.41) in (5.39) provides the relation:**

$$p_{av2} = -\frac{2A_2}{s_1\pi} \int_0^{2\pi} \left[ \begin{array}{l} \sin^2 \left( \frac{s_2}{2} - A_2 \sin \left( \frac{s_2}{2} \right) \sin \left( \theta + s_1 + \frac{s_2}{2} \right) \right) \times \\ \cos \left( \theta + s_1 + s_2 - 2A_1 \sin \left( \frac{s_1}{2} \right) \sin \left( \theta + \frac{s_1}{2} \right) \right) \\ - 2A_2 \sin \left( \frac{s_2}{2} \right) \sin \left( \theta + s_1 + \frac{s_2}{2} \right) \end{array} \right] d\theta \quad (5.42)$$



➤ **The above expression deals with the momentum when the two virtual cathodes VC1 and VC2 are formed simultaneously.**

➤ **This two stage virtual cathode formation is periodic in nature which occurs one after another.**

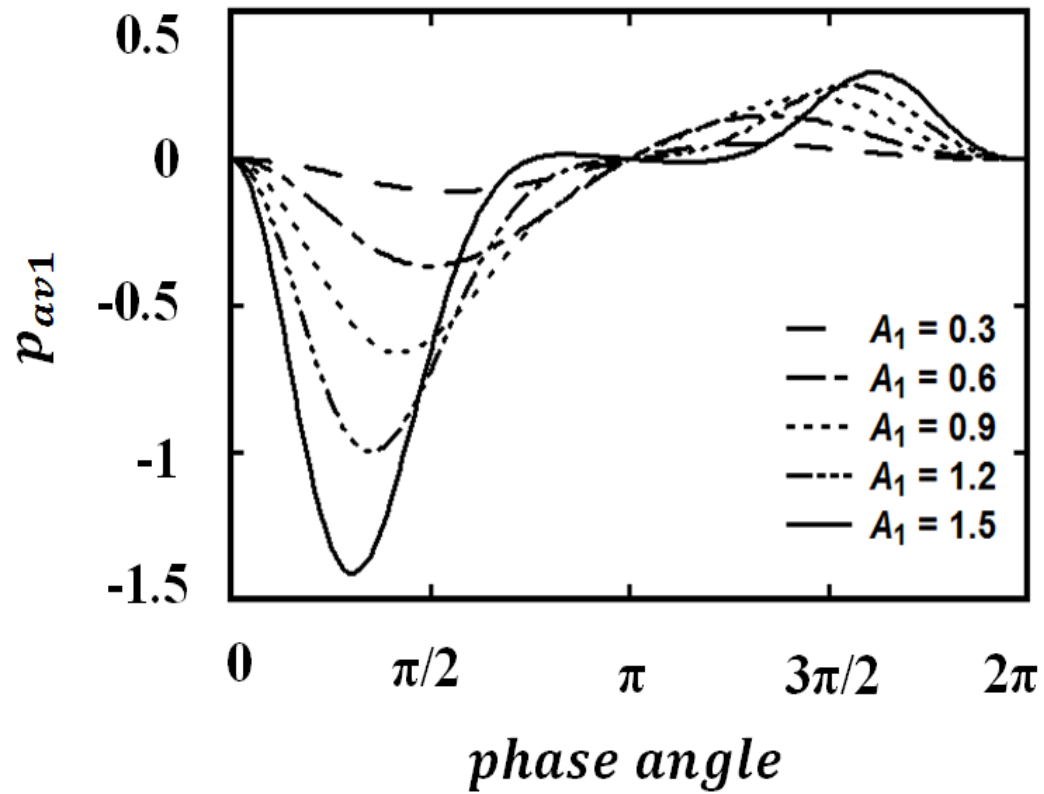


**Figure:** Plot of average momentum ( $p_{av1}$ ) versus phase angle ( $s_1 = \omega \bar{\tau}$ ) for different value of  $A_1 (= E'_0 / E_{mc})$



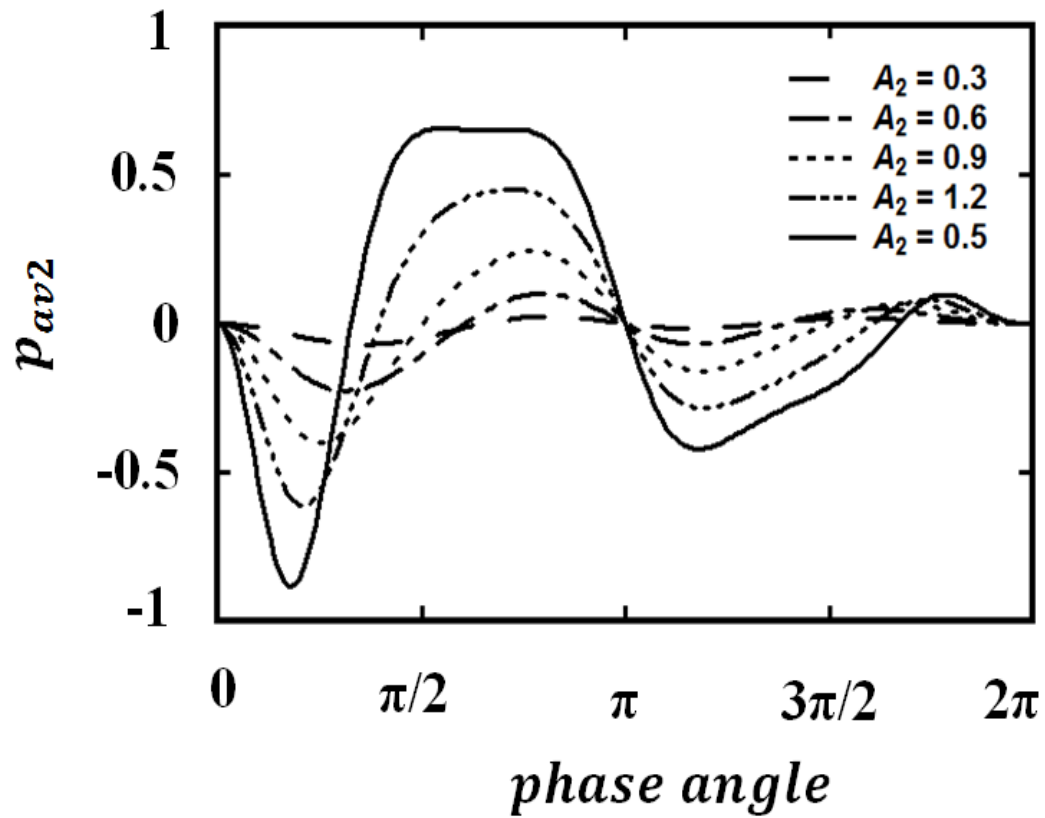


**Figure :** Plot of average momentum ( $p_{av1}$ ) versus phase angle when two virtual cathodes are formed simultaneously.

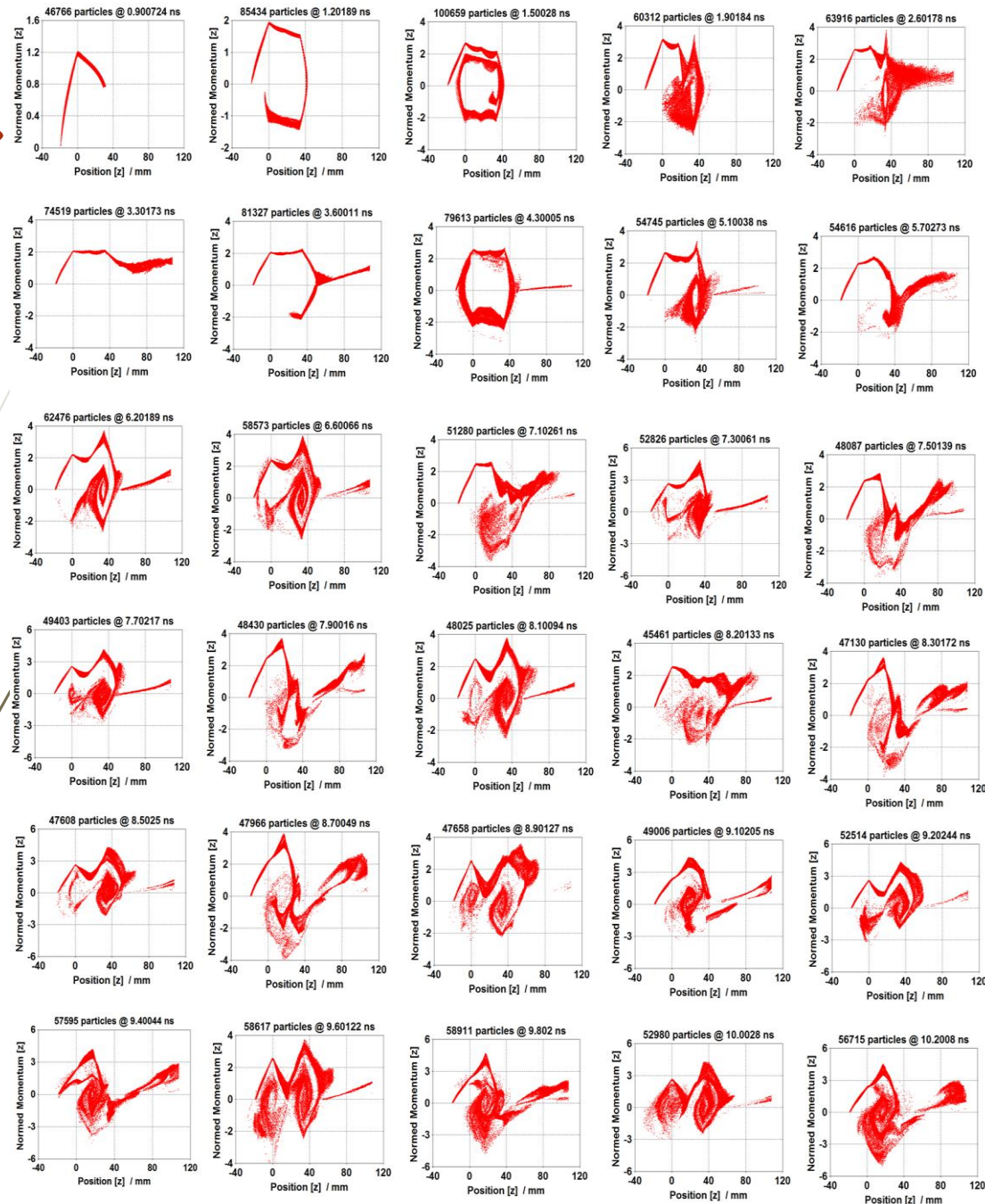


**Figure:** Plot of electron's momentum to visualize the process of virtual cathode formation in the reltron oscillator at different instant of time.

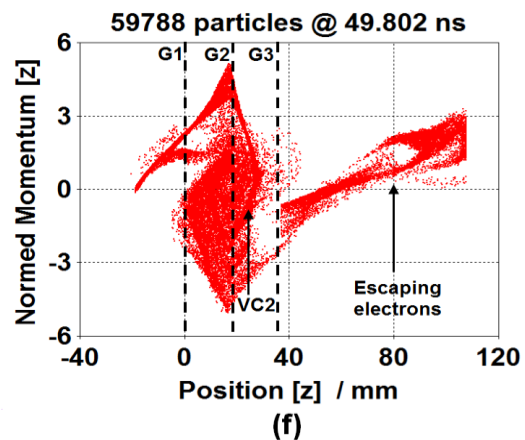
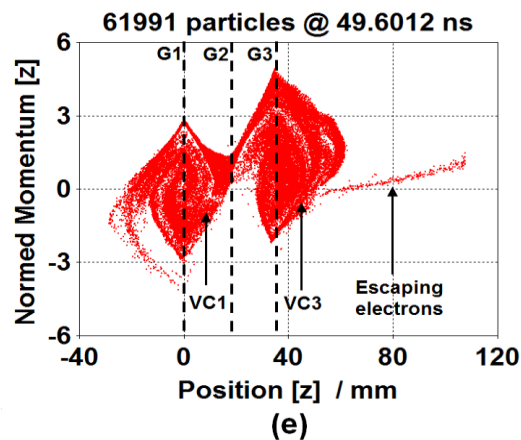
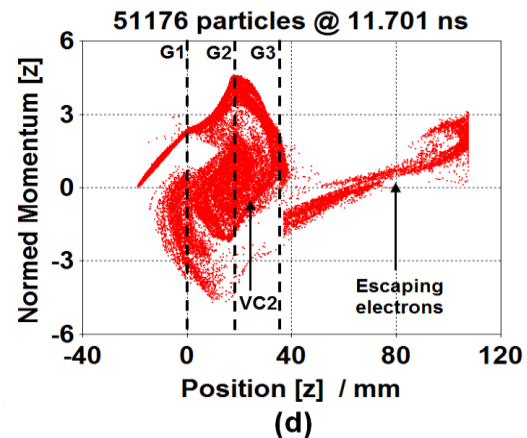
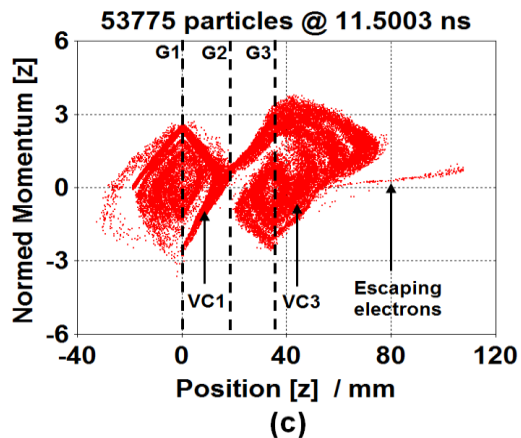
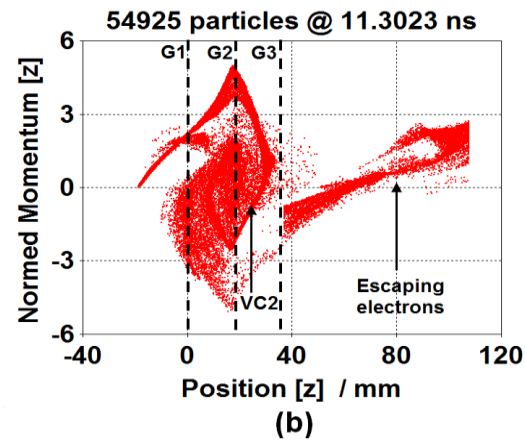
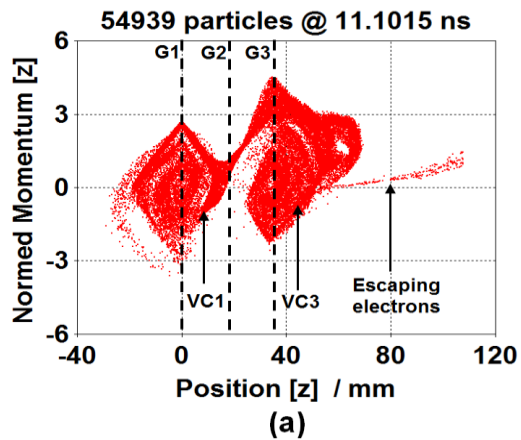


**Figure:** Plot of electron's normalized momentum at (a) 11.1 ns (b) 11.3 ns (c) 11.5 ns (d) 11.7 ns (e) 49.6 ns (f) 49.8 ns.

# Research Publications

75

## Patent:

1. **Manpuran Mahto** and Pradip Kumar Jain, “A Device with Improved Modulation Cavity for High Pulse Microwave Signal Generation and Method Thereof,” *Indian Patent Application No. 201611032924*, Date:27/09/2016.

# Journals:

76

1. **Manpuran Mahto** and Pradip Kumar Jain, “Design and Simulation Study of the HPM Oscillator-Reltron,” *IEEE Transactions on Plasma Science*, vol. 44, pp. 743–748, 2016.
2. **Manpuran Mahto** and Pradip Kumar Jain, “Oscillation Condition and Efficiency Analysis of the Reltron,” *IEEE Transactions on Plasma Science*, vol. 44, pp. 1056–1062, 2016.
3. **Manpuran Mahto** and P. K. Jain, “Electromagnetic Analysis of the HPM Oscillator - Reltron,” *AIP Physics of Plasmas*, vol. 23, p. 093118, 2016.
4. **Manpuran Mahto** and P. K. Jain, “Study of Virtual Cathodes Formation during Beam-Wave Interaction in the Reltron Oscillator,” *AIP Physics of Plasmas*, vol. 24, p. 093107, 2017.
5. **Manpuran Mahto** and Pradip Kumar Jain, “PIC Simulation Study of the Formation Mechanism of Periodic Virtual Cathodes in the Reltron,” *IEEE Transactions on Plasma Science*, vol. 46, pp. 518 - 523, 2018.
6. **Manpuran Mahto** and Pradip Kumar Jain, “Investigation of a Low-Impedance Reltron as a Gigawatt HPM Source,” *IEEE Transactions on Electron Devices*, vol. 66, pp. 1950 - 1953, 2019.
7. **Manpuran Mahto** and P. K. Jain, “Parametric Study of the Reltron Oscillators,” *Defence Science Journal*, vol. 69, pp. 448 - 452, 2019.

# Conferences:

77

1. **Manpuran Mahto** and P. K. Jain, “Reltron, A GigaWatt HPM Source - A Review”, *International Conference on Innovative Advancements in Engineering and Technology, IAET-2014*, JNU Jaipur, 7-8 March, 2014.
2. **Manpuran Mahto**, Chinta Santhosh, Gargi Dixit and P. K. Jain, “Analytical Study of Reltron Modulating Cavity”, *10th International Conference on Microwaves, Antenna, Propagation and Remote Sensing, ICMARS-2014*, ICRS Jodhpur, 9-12 December, 2014.
3. **Manpuran Mahto** and P. K. Jain, “ Beam Wave Interaction Studies of Gridless Reltron”, *National Conference on Recent Advances in Electronics & Computer Engineering, RAECE-2015*, IIT Roorkee, 13-15 February, 2015.
4. **Manpuran Mahto** and P. K. Jain, “Electromagnetic Analysis of Reltron Oscillator”, *National Workshop on Vacuum Electronic Devices and Applications, VEDA-2014*, DAVV Indore, 20-21 March, 2015.
5. **Manpuran Mahto** and P. K. Jain, “Simulation Study of Gridless Reltron”, *National Conference Emerging Trends in Vacuum Electronic Devices and Applications, VEDA-2015*, MTRDC Bangalore, 3-5 December, 2015.
6. **Manpuran Mahto** and P. K. Jain, “Electron Beam and RF Wave Interaction Mechanism in the Reltron Oscillator”, *11<sup>th</sup> International Conference on Industrial and Information Systems (ICIIS 2016)*, IIT Roorkee, 3-4 December, 2016.
7. Prabhakar Tripathi, **Manpuran Mahto** and P. K. Jain, “Simulation Study of Ku-Band Reltron Oscillator”, *National Conference on Emerging Trends in Vacuum Electronic Devices and Application*, IPR Gandhinagar, 16-18 March 2017.
8. **Manpuran Mahto** and P. K. Jain, “Parametric Study of Reltron Oscillators”, *VAMMAM-2018*, IIT Roorkee, 24-25 August, 2018.
9. **Manpuran Mahto** and P. K. Jain, “Exploration of Electromagnetic Behaviour of the Magnetically Coupled Cavities for High-Power Devices”, *Vacuum Electronic Devices and Application (VEDA)-2018*, IIT Guwahati, 22-24 November, 2018.
10. Neetu Kumari, **Manpuran Mahto** and P. K. Jain, “Study of Metamaterial Parameters using Retrieval Method”, *National Symposium on Vacuum Electronics Devices and Applications (VEDA-2019)*, NIT Patna, 21-23 November, 2019.
11. Garima Dubey, **Manpuran Mahto** and P. K. Jain, “Optimization Study OF S Band Reltron Oscillator”, *National Symposium on Vacuum Electronics Devices and Applications (VEDA-2019)*, NIT Patna, 21-23 November, 2019.
12. Garima Dubey, **Manpuran Mahto** and P. K. Jain, “Repetitive Pulse Operation of HPM Oscillator-Reltron”, *National Symposium on Vacuum Electronics Devices and Applications (VEDA-2019)*, NIT Patna, 21-23 November, 2019.



# Key References

78

- ▶ Miller, R. B., McCullough, W. F., Lancaster, K. T., and Muehlenweg, C. A., “Super-reltron theory and experiments,” *IEEE Transactions on Plasma Science*, 1992, v. 20, pp. 332–343.
- ▶ Marder, B. M., Clark, M. C., Bacon, L. D., Hoffman, J. M., Lemke, R. W., and Coleman, P. D., “The split-cavity oscillator: a high-power E-beam modulator and microwave source,” *IEEE Transactions on Plasma Science*, 1992, v. 20, pp. 312–331.
- ▶ Miller, R. B., Muehlenweg, C. A., Habiger, K. W., and Clifford, J. R., “Super-Reltron progress,” *IEEE Transactions on Plasma Science*, 1994, v. 22, pp. 701–705.
- ▶ Soh, S., Miller, R. B., Schamiloglu, E., and Christodoulou, C. G., “Dual-Mode Reltron,” *IEEE Transactions on Plasma Science*, 2012, v. 40, pp. 2083–2088.
- ▶ Soh, S., “Modeling, simulation and experimental study of the UNM low power reltron,” Ph. D. Thesis, The University of New Mexico, Albuquerque, New Mexico, 2012.
- ▶ Kim, H., Choi, J., Lee, B., Kim, J., and Lee, J., “MAGIC3D simulation of an ultra-compact, highly efficient, and high-power reltron tube,” *IEEE Transactions on Dielectrics and Electrical Insulation*, 2009, v. 16, pp. 961–966.
- ▶ Benford, J., Swegle, J. A., and Schamiloglu, E., *High Power Microwaves*, Taylor & Francis. CRC Press, 2007.

- Friedman, M., Krall, J., Lau, Y. Y., and Serlin, V., “Externally modulated intense relativistic electron beams,” *Journal of Applied Physics*, 1988, v. 64, pp. 3353-3379.
- Uhm, H. S., “A theoretical analysis of relativistic klystron oscillators,” *IEEE Transactions on Plasma Science*, 1994, v. 22, pp. 706–712.
- Friedman, M., Serlin, V., Drobot, A., and Seftor, L., “Self-modulation of an intense relativistic electron beam,” *Journal of Applied Physics*, 1984, v. 56, pp. 2459-2474.
- Lemke, R.W., “Linear stability of relativistic space-charge flow in a magnetically insulated transmission line oscillator,” *Journal of Applied Physics*, 1989, v. 66, pp. 1089-1094.
- Jiang, W., Masugata, K., and Yatsui, K., “Mechanism of microwave generation by virtual cathode oscillation”, *Physics of Plasmas*, 1995, v. 2, pp.982-986.
- Jiang, W. and Kristiansen, M., “Theory of the virtual cathode oscillator”, *Physics of Plasmas*, 2001, v. 8, pp.3781-3787.
- Champeaux, S., Gouard, P., Cousin, R., and Larour, J., “3-D PIC numerical investigations of a novel concept of multistage axial vircator for enhanced microwave generation”, *IEEE Transactions on Plasma Science*, 2015, v. 43, pp.3841-3855.



**Annexure II:**  
**Young Researcher's Talk-2 Slides**

# VED Webinar 2.0



## RF PULSE SHORTENING STUDIES OF HIGH POWER RELATIVISTIC BACKWARD WAVE OSCILLATOR USING MAGIC-PIC SIMULATIONS

Department of Electronics Engineering  
Indian Institute of Technology (BHU) Varanasi  
Varanasi – 221005.

Presented by

MUMTAZ ALI ANSARI  
Roll. No.-15091012

Supervisor

Dr. M. THOTTAPPAN

# Contents

- Design of an X-band Experimentally Tested RBWO by Gunin *et al.*
  - Simulations Results
  - RF Pulse Shortening Phenomena in RBWO at GW Power Level
    - Beam Degradation at Low Guiding Magnetic Field
    - High Field Electron Emission and Secondary Electron Emission
    - Collector Plasma
  - Combined Pulse Shortening Study
  - Conclusion

# Design of an X-band Experimentally Tested RBWO – [Gunin et al.]

➤ The X-band RBWO with cavity RR experimentally tested by Gunin *et al.* is modelled in MAGIC-3D as shown in Fig. 1.

Structural Parameters	Symbols	Values (mm)
Beam Radius	$r_b$	19.5
Mean Radius	$r_0$	23
Corrugation Depth	$r_1$	1.8
Period	$d$	13.50
Cavity Radius	$b$	29
Cavity Length	$L_c$	9
Drift Radius	$a$	25
Drift length	$L_{dr}$	21

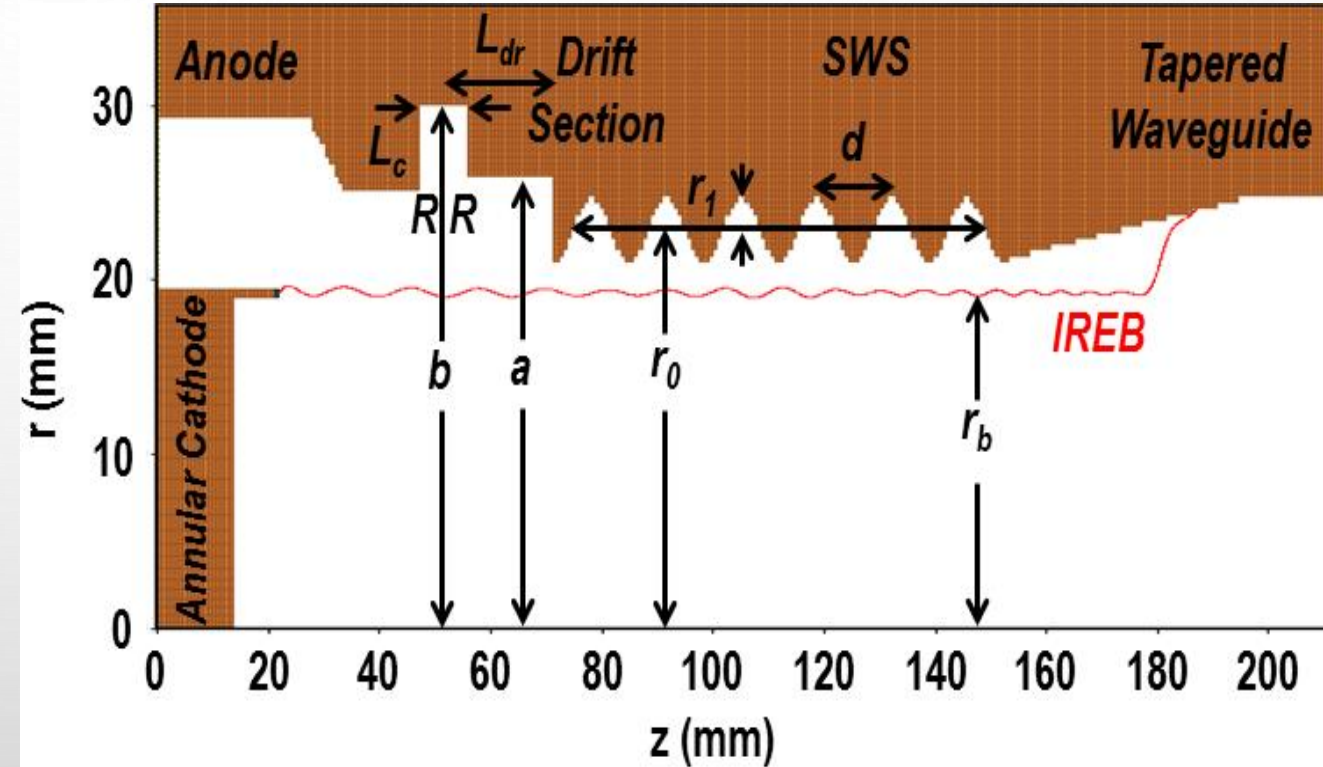


Fig. 1: Schematic of an X-band overmoded uniform RBWO



# Simulation Results

Electrical Parameters	Symbols	Values
DC Voltage	$V_0$	550 kV
Time Duration	-	100 ns
Beam Current	$I_b$	$\sim 6.1$ kA
Guiding Magnetic Field	$B_0$	0.61 T
RF Power	$P_0$	$\sim 800$ MW
Sat. Power Generation Time	$\tau$	$\sim 30$ ns
Frequency	$f_r$	$\sim 9.52$ GHz
Output Mode	-	$TM_{01}$

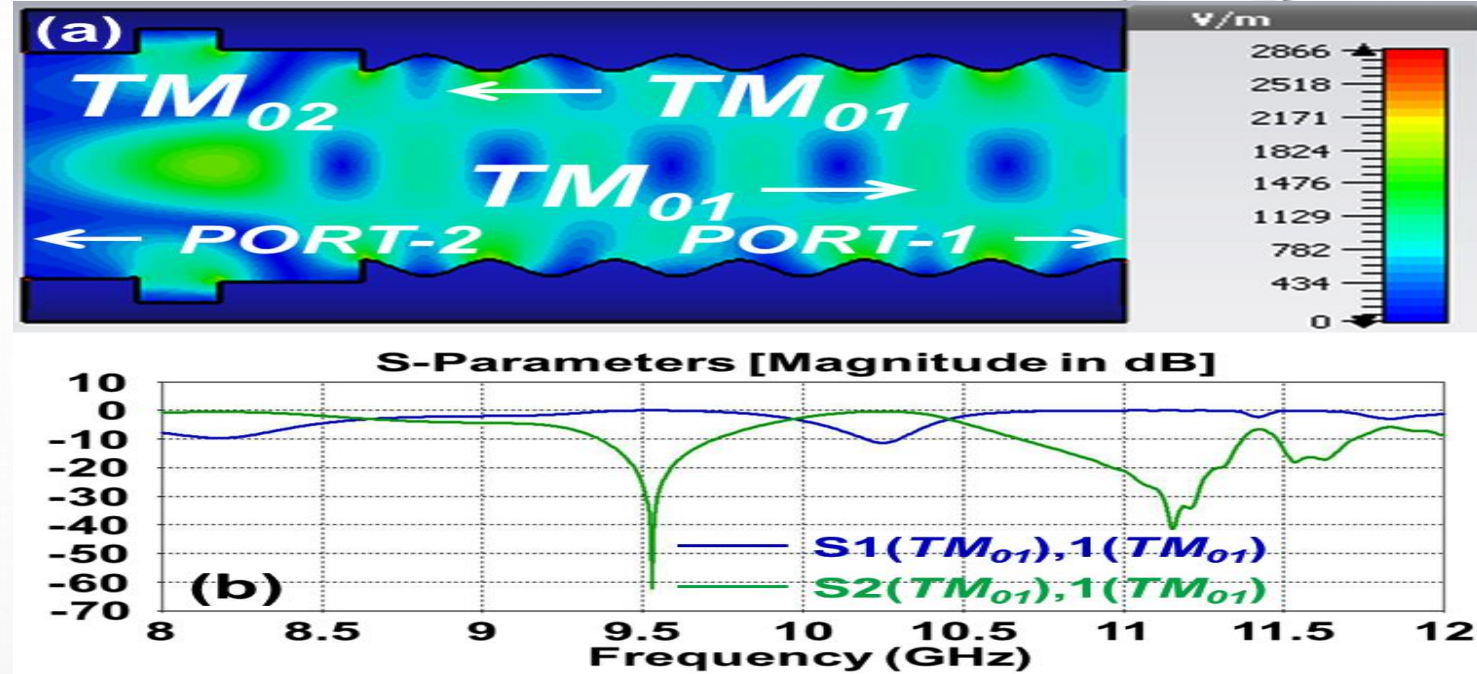


Fig. 2: (a) Cavity RR reflecting the  $TM_{01}$  mode and resonating in the  $TM_{02}$  mode and (b) S-parameter showing the reflection and transmission of the  $TM_{01}$  mode

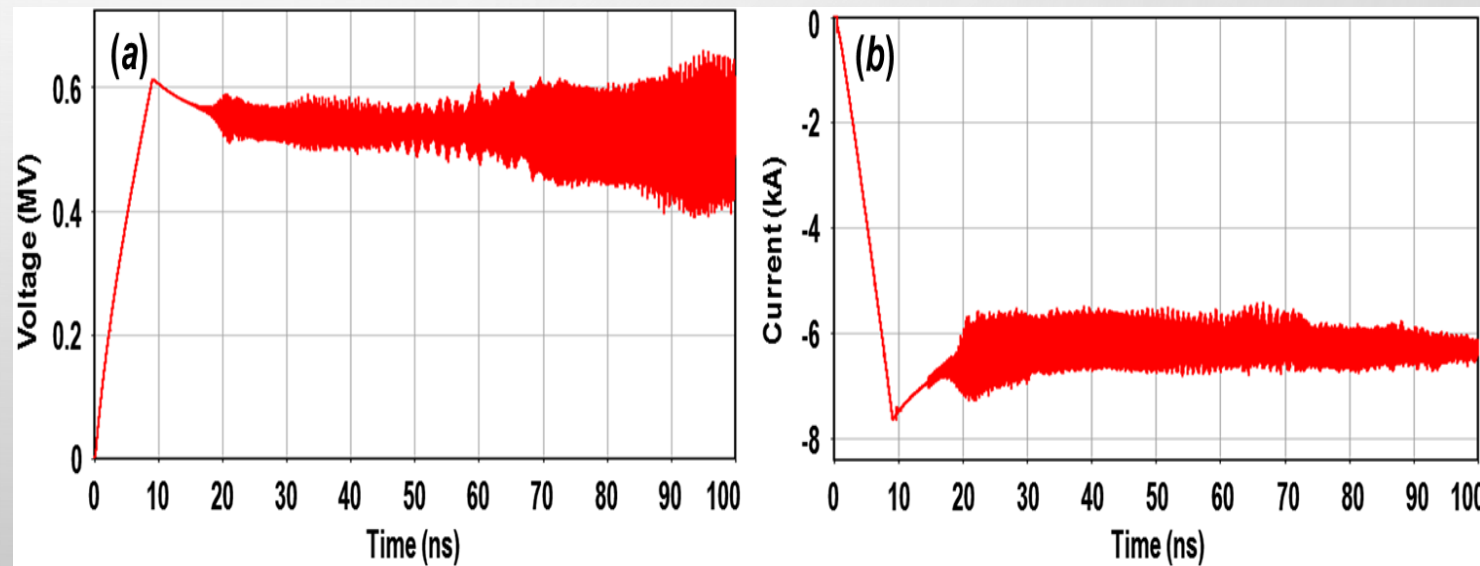
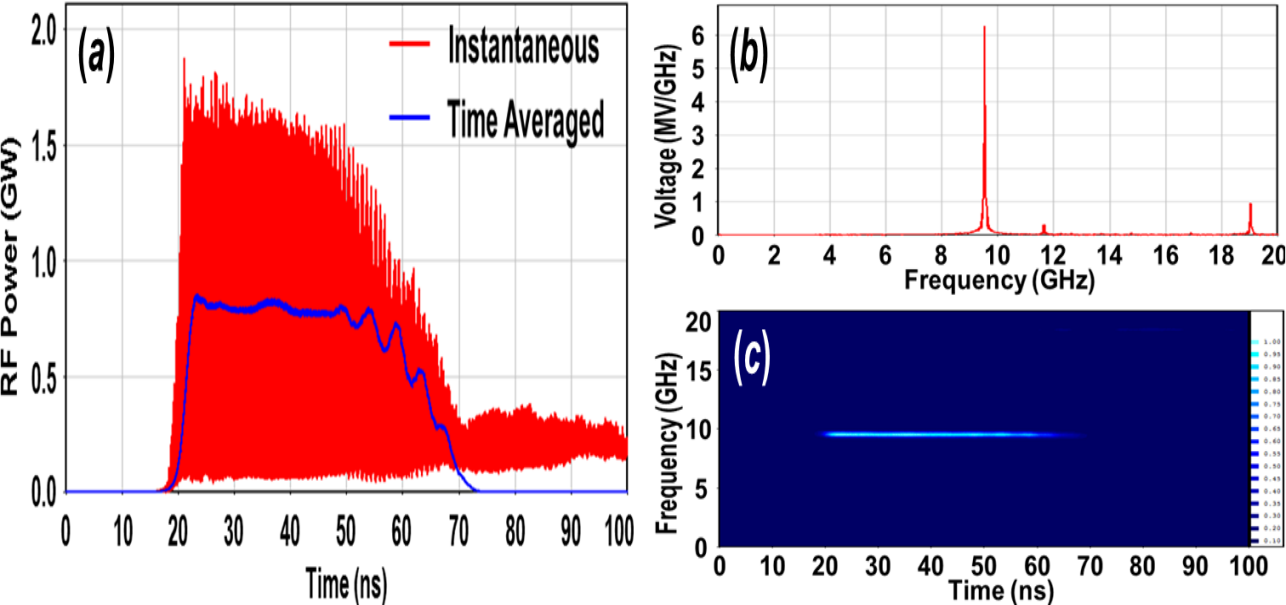
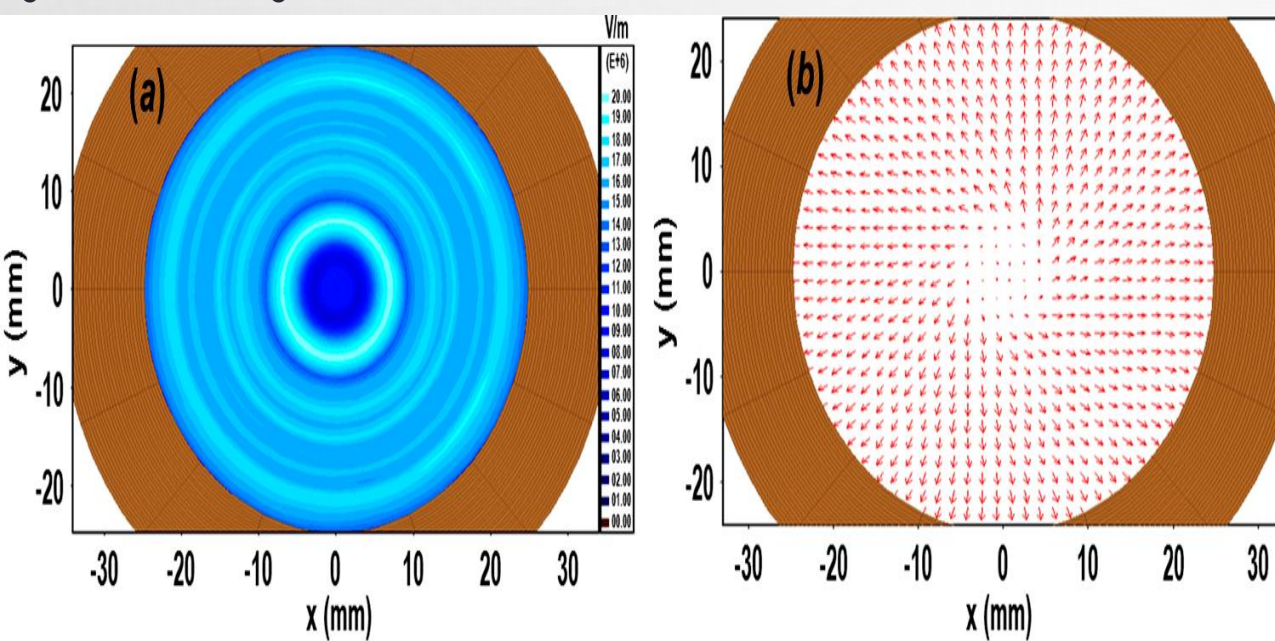


Fig. 3: (a) Modulated form of applied voltage, and (b) and modulated developed electron beam current



**Fig. 4:** (a) RF pulse power at 0.61T, (b) FFT, and (c) Frequency-Time plot of generated RF signal.



**Fig. 5:** E- field (a) contour and (b) vector plots of the desired  $TM_{01}$  mode.

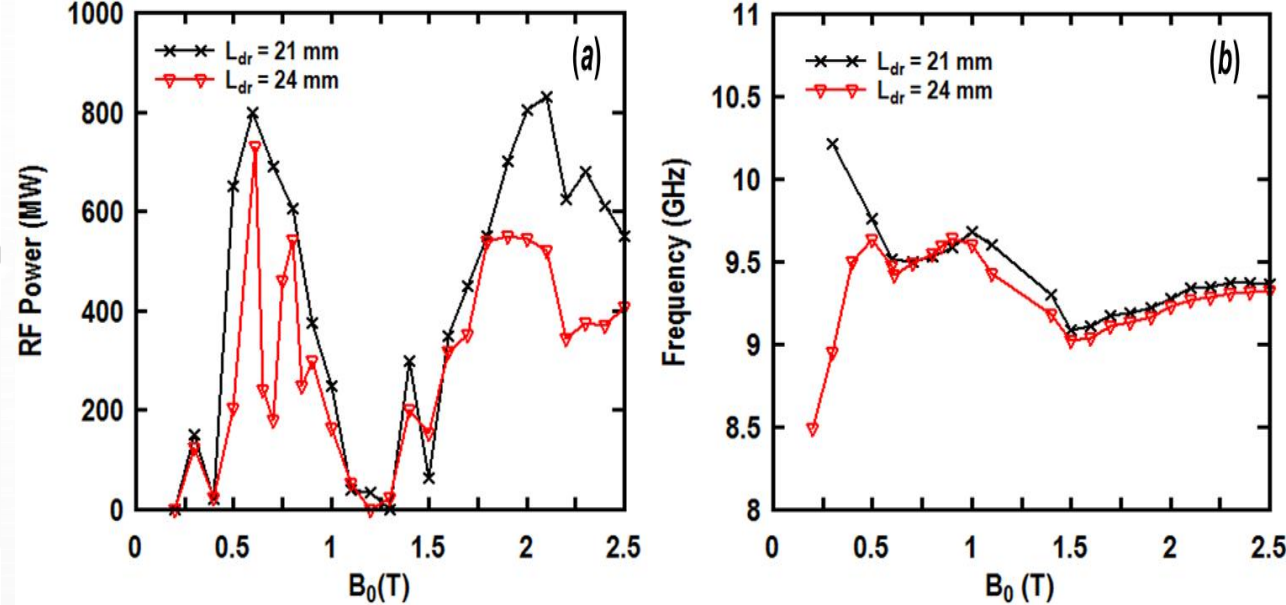


**Fig. 6:** (a) Dependence of RF power and (b) frequency on guiding magnetic field for different values of drift length.

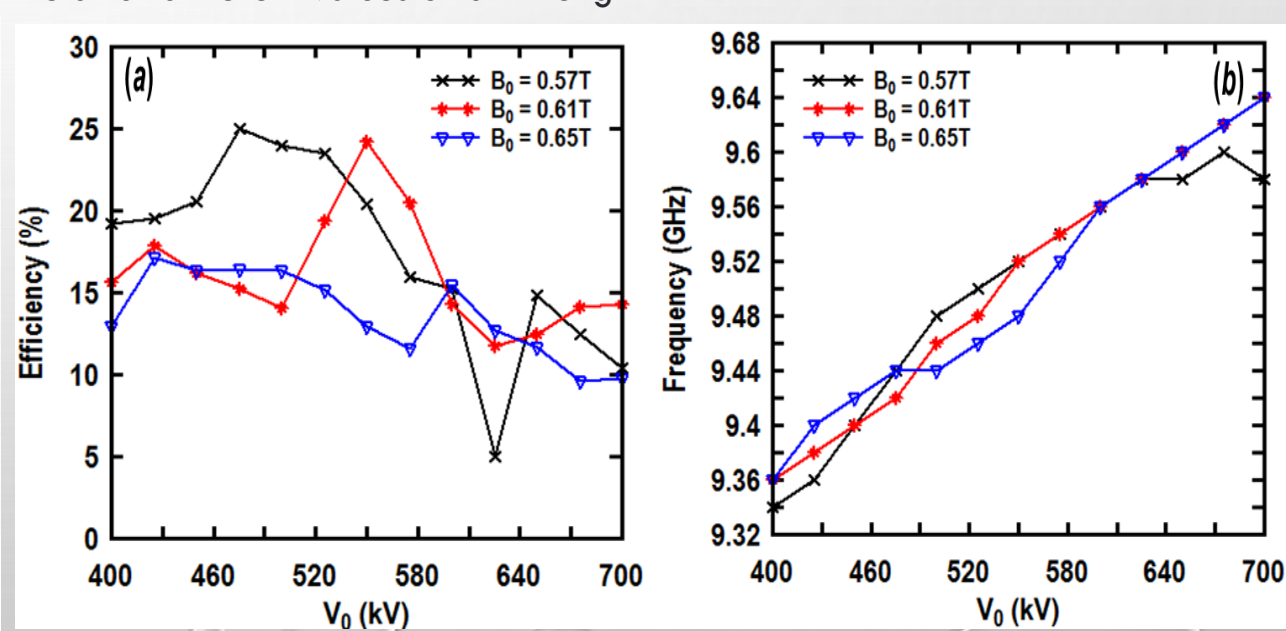


**Fig. 7:** (a) Dependence of conversion efficiency and (b) frequency on the diode voltage for different values of guiding magnetic field.



# RF Pulse Shortening Phenomena in RBWO at GW Power Level

- Pulse shortening is one of the most important and serious phenomena occurred in an HPM sources (RBWO) at low guiding magnetic field and GW level of RF power that restrict the power generation time less than 100 ns.
- Various causes of pulse shortening in linear beam HPM devices are:
  - Beam degradation at low guiding magnetic field
  - More than one RF mode excitation
  - Secondary Electron Emission
  - High Field Electron Emission
  - Anode Plasma Formation
  - Collector Plasma Formation
- However beam degradation along with collector plasma is an obvious phenomena which will occur at low guiding magnetic field of operation and can cause pulse shortening with higher probability

# Beam Degradation at Low Guiding Magnetic field

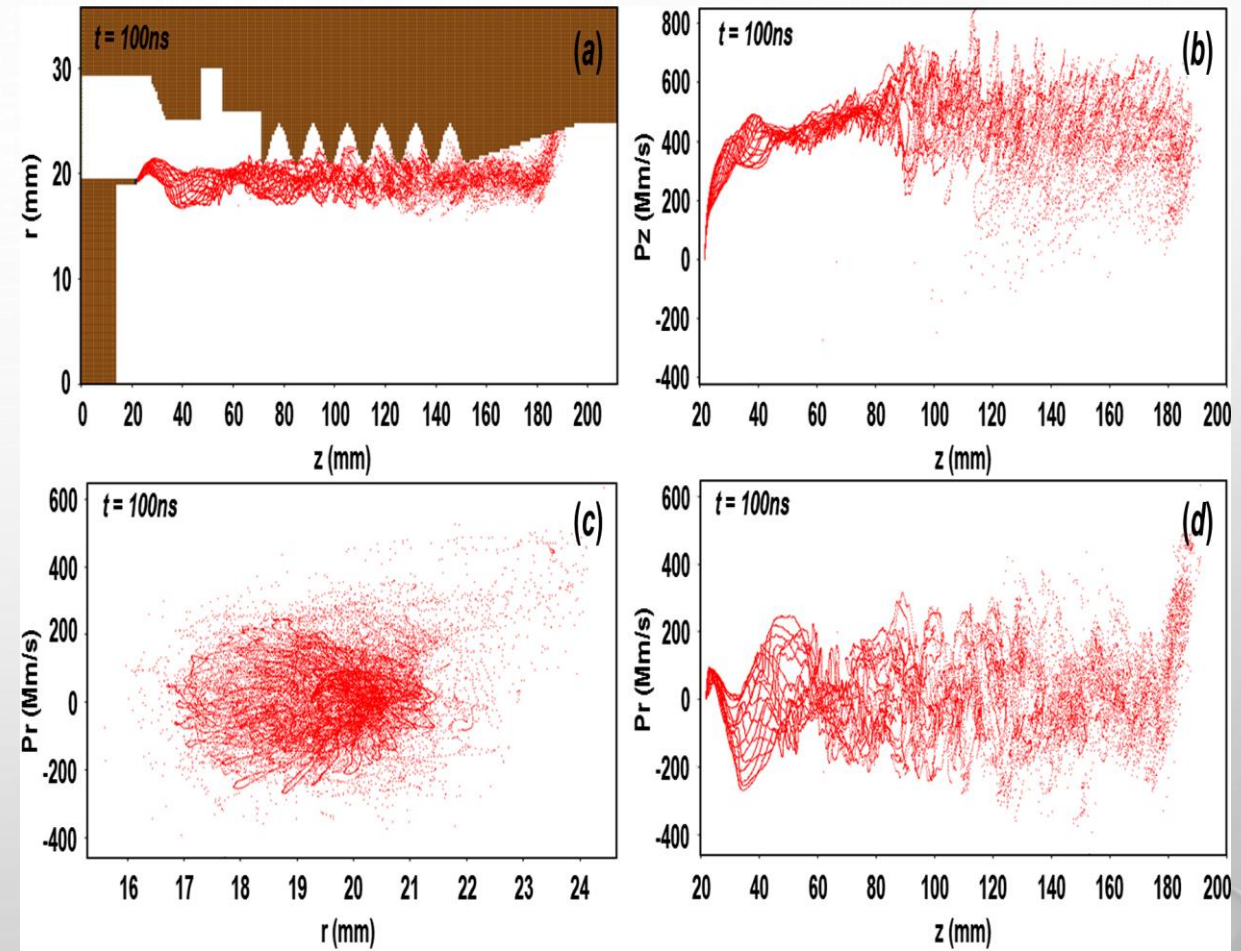
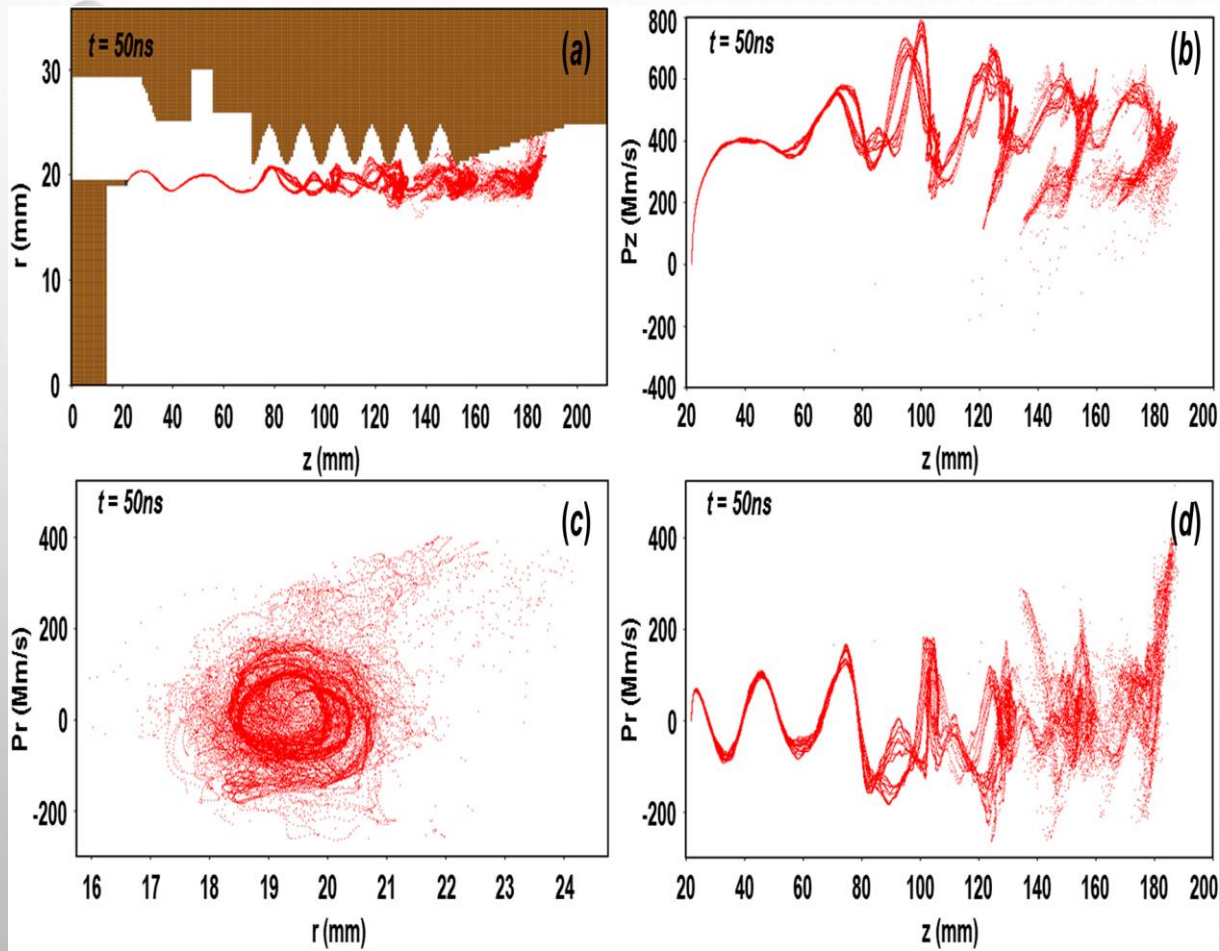


**Fig. 8:** (a) Deviation of electron beam trajectory, (b) axial momentum of electrons along the axis of SWS, and the transverse momentum of electrons Vs (c) radius and (d) axial length of SWS at low guiding magnetic field of 0.61 T at 50 ns.

**Fig. 9:** (a) Deviation of electron beam trajectory, (b) axial momentum of electrons along the axis of SWS, and the transverse momentum of electrons Vs (c) radius and (d) axial length of SWS at low guiding magnetic field of 0.61 T at 100 ns.



# High Field Electron Emission and Secondary Electron Emission

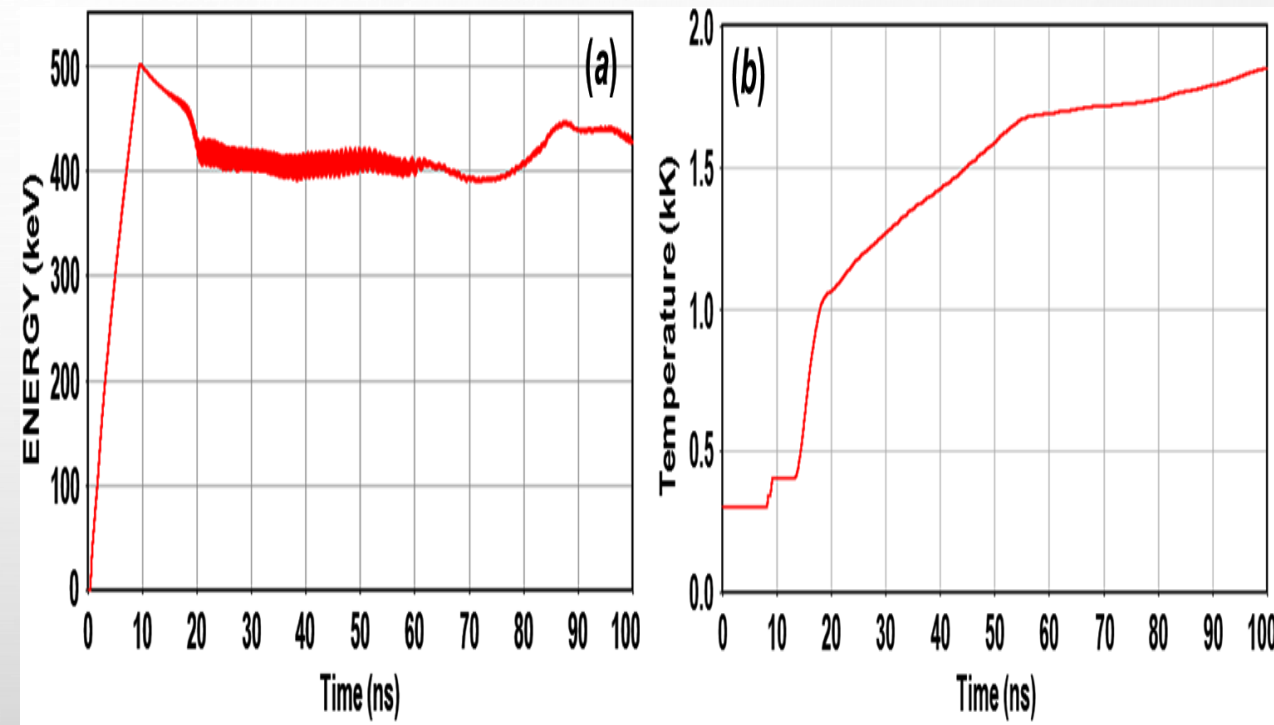
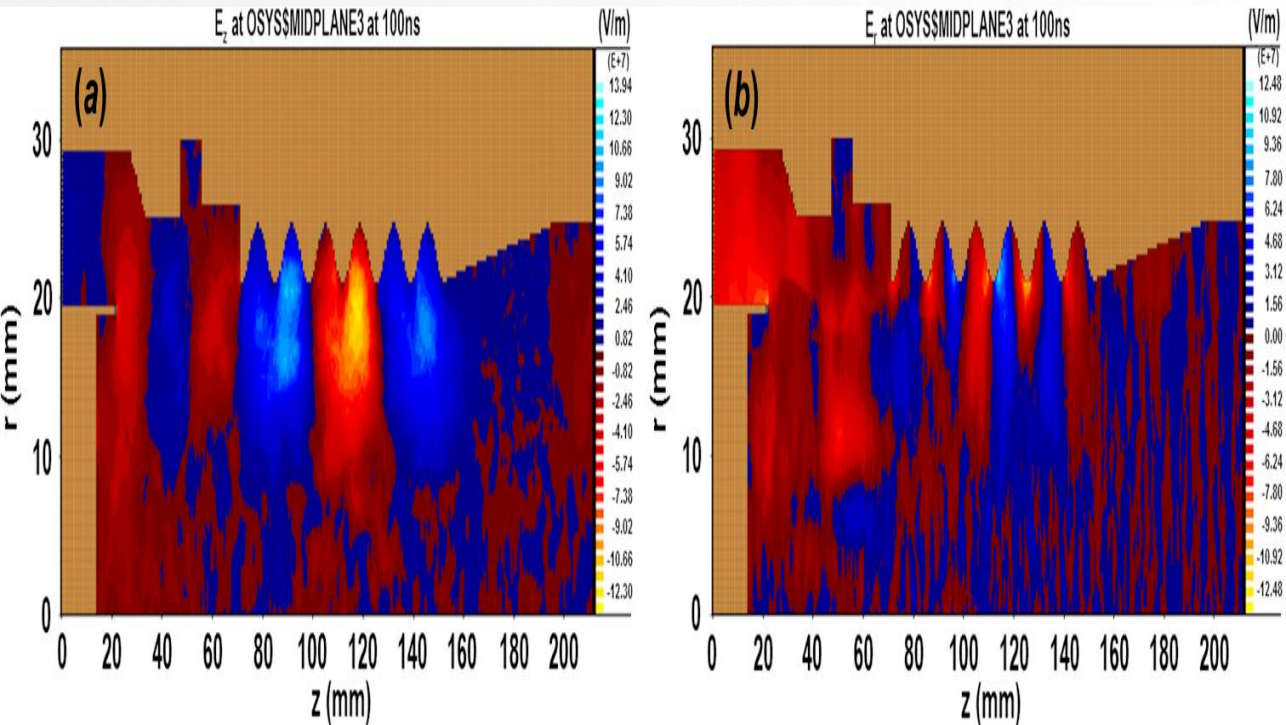


**Fig. 10:** Contour plot in the presence of beam showing (a) axial and (b) radial electric fields throughout the RBWO structure at 100ns.

**Fig. 11:** (a) Energy of primary collected electrons and (b) collector wall temperature at the beam dump due to primary electrons.

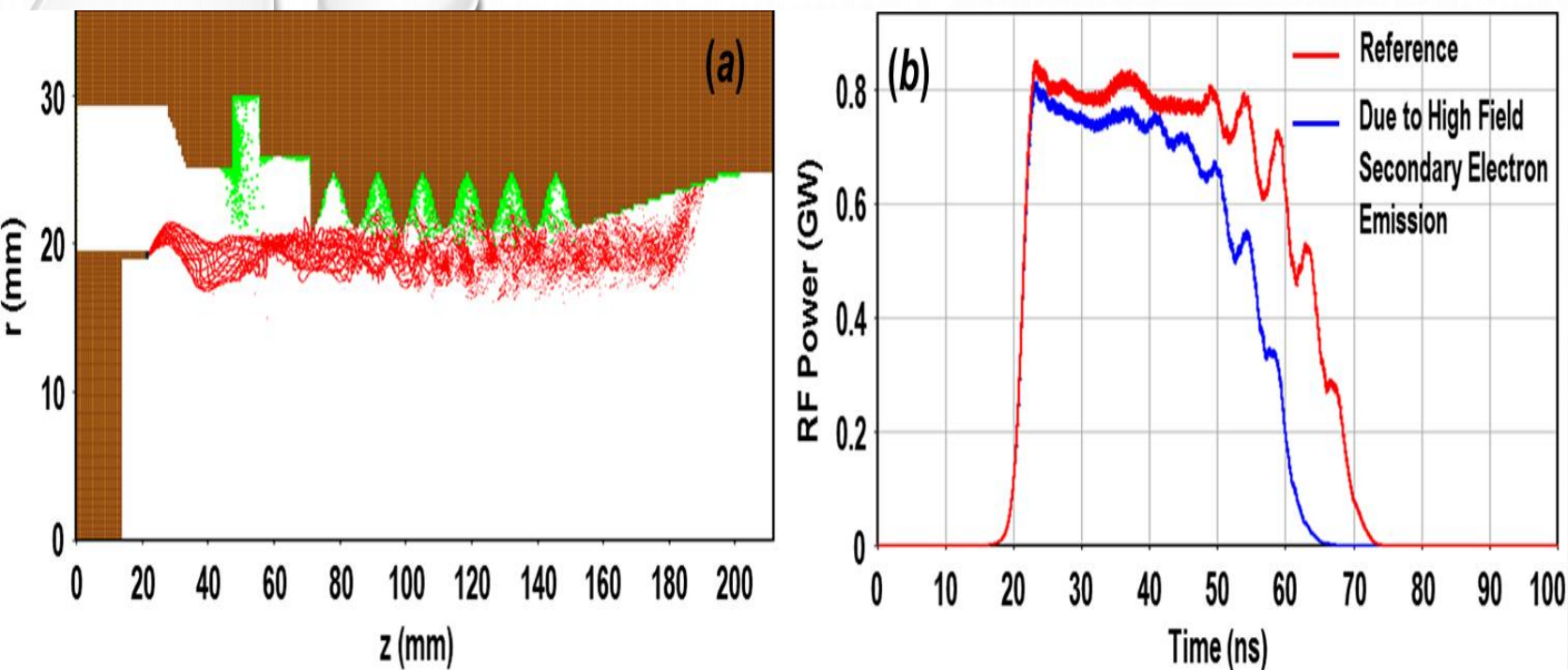


**Fig. 12:** (a) 2D Schematic showing primary electrons (red colour) and secondary electrons due to high field explosive emission (green colour), (b) Comparison of RF power.

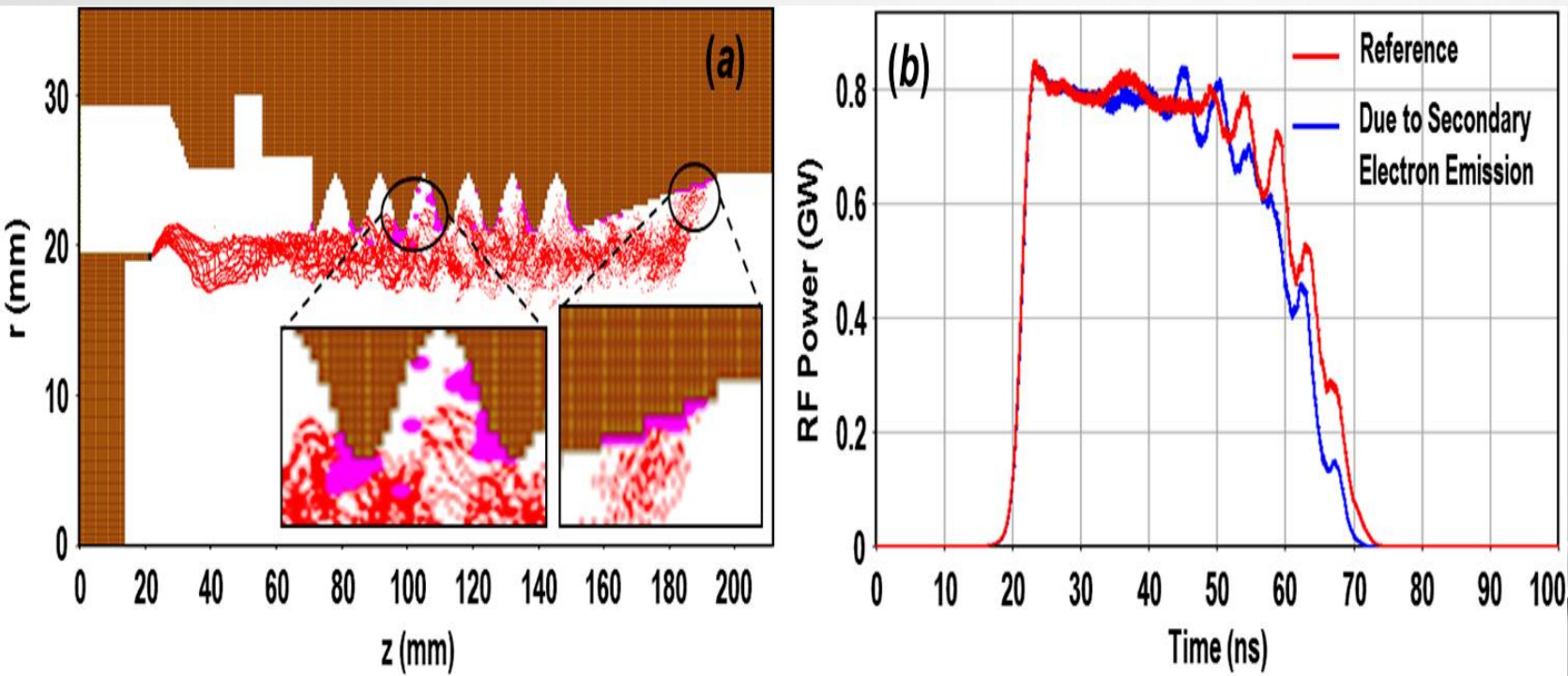


**Fig. 13:** (a) 2D Schematic showing primary electrons (red colour) and secondary electrons emitted due to incidence of primary electrons energy (pink colour), (b) Comparison of RF power.



# Collector Plasma

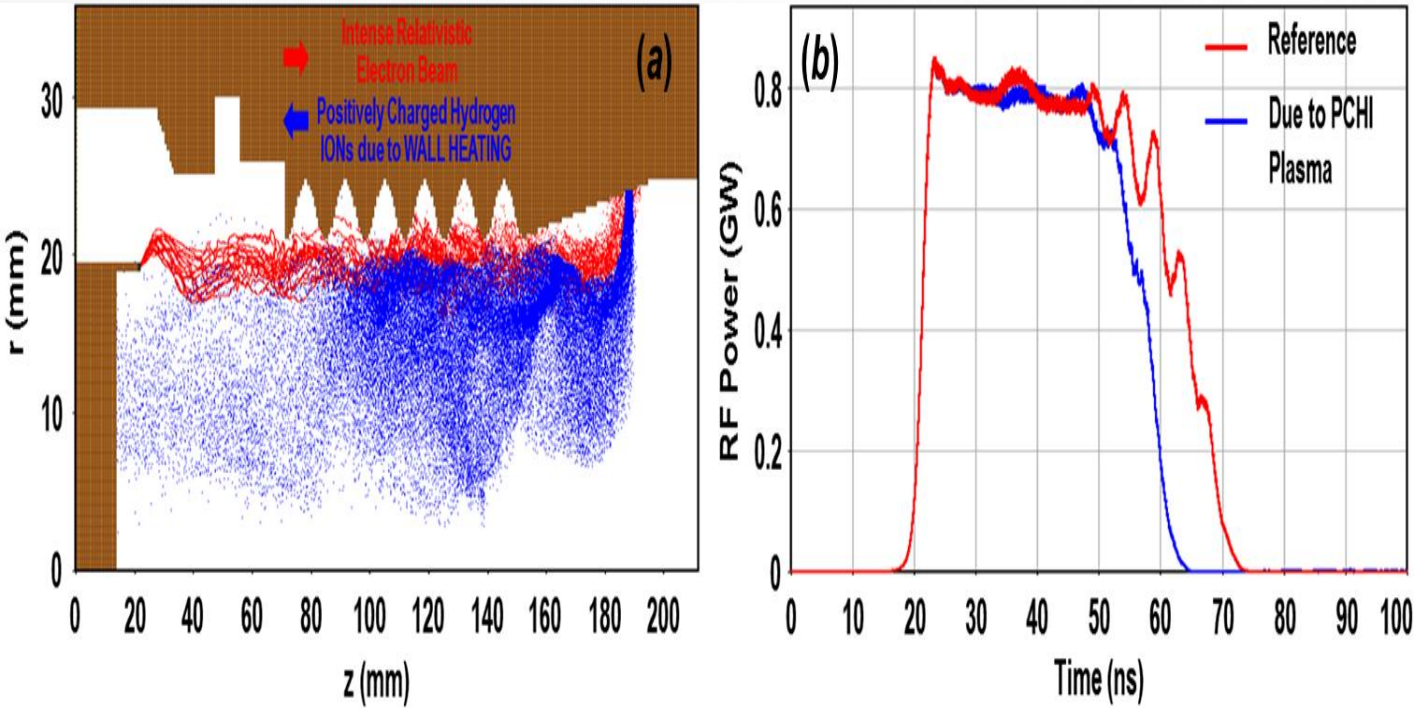


**Fig. 14:** (a) 2D Schematic showing primary electrons PCHI Plasma travelling from collector to cathode side, (b) Comparison of RF power.

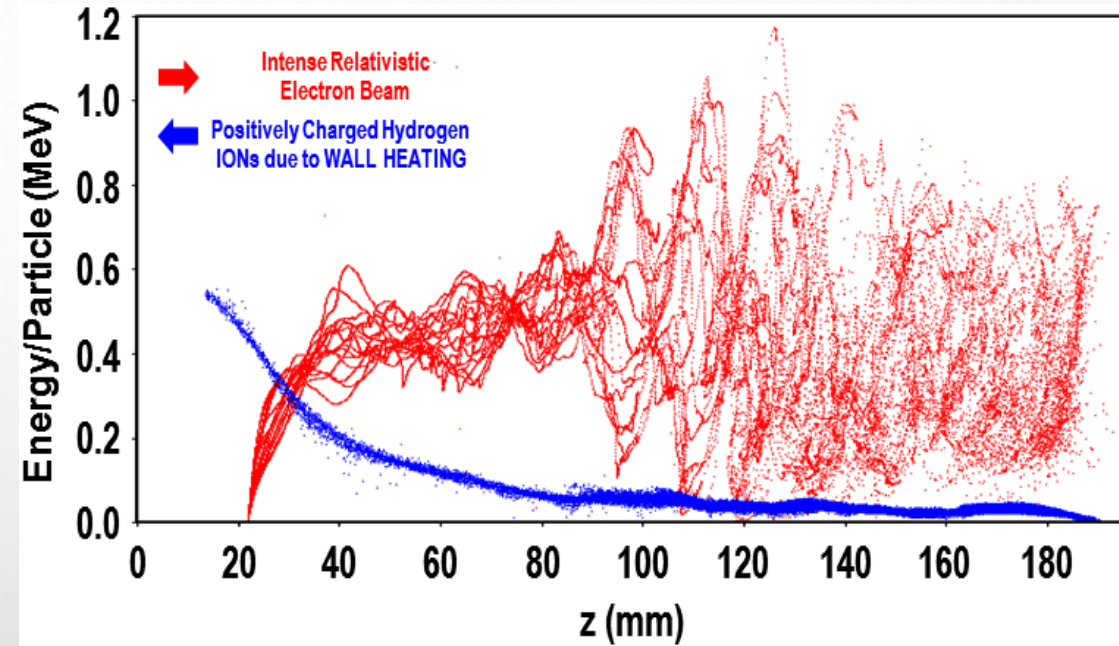


**Fig. 15:** Energy distribution of collector plasma (PCHI) and primary electron beam.

# Combined Pulse Shortening Study

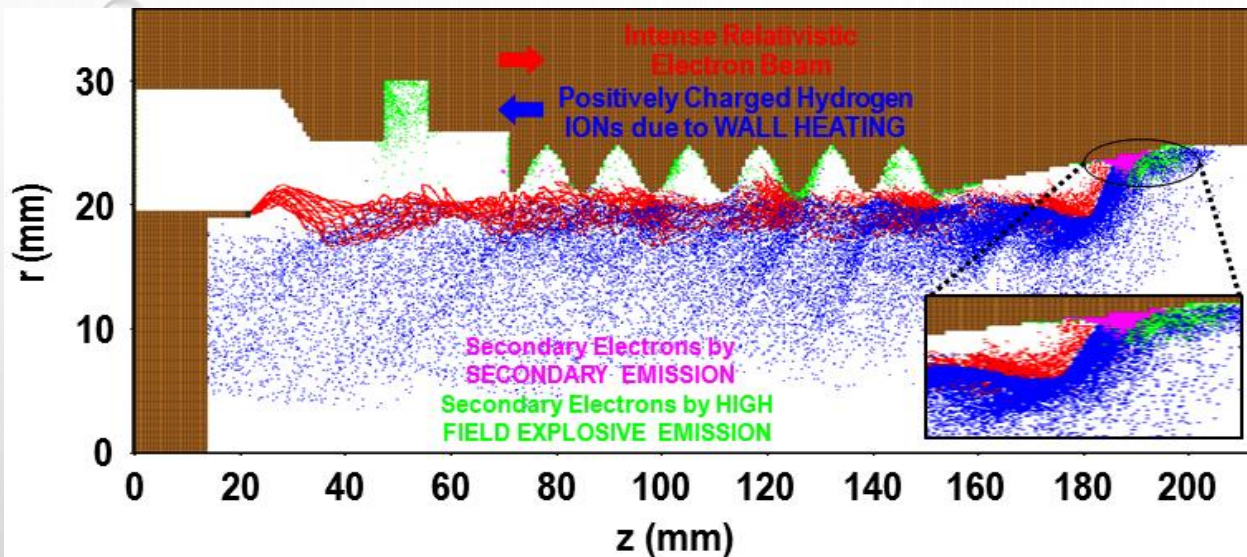


Fig. 16: 2D-schematic showing emission of all particles at 80 ns.

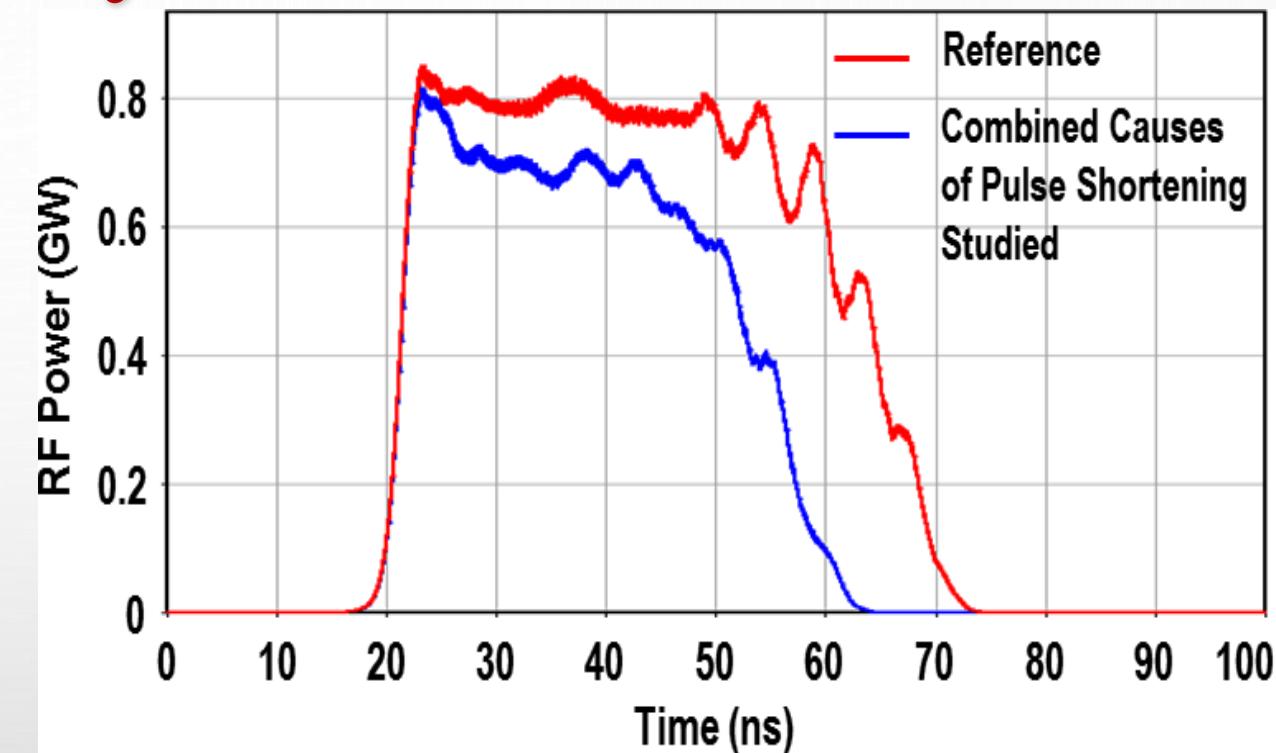
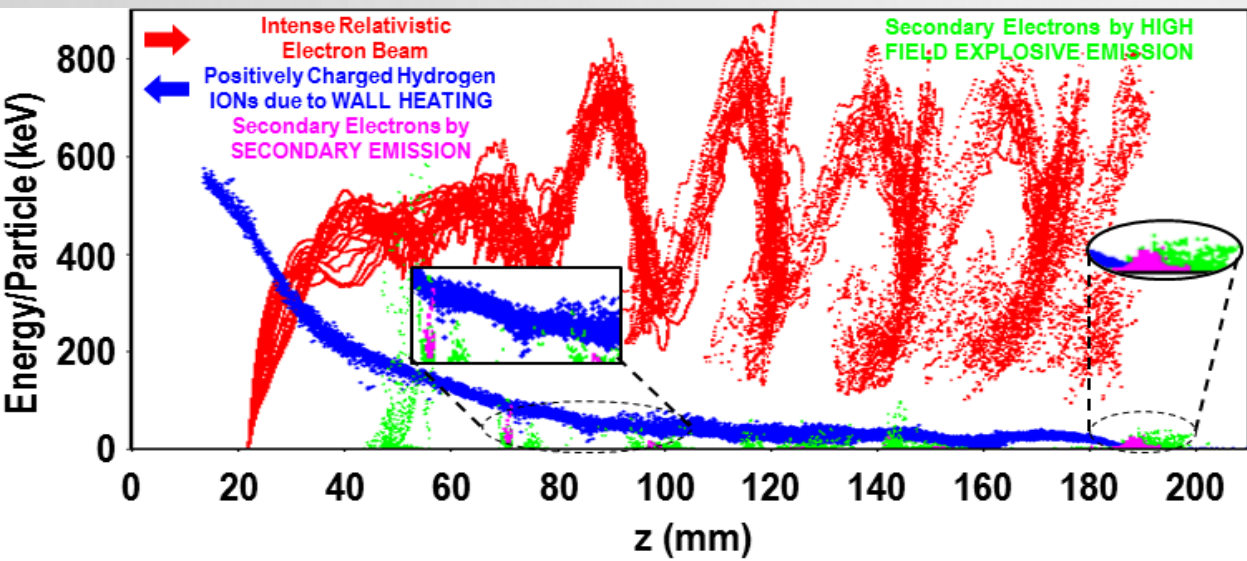


Fig. 18: Generated RF Power under the influence of all types of secondary electrons and positively charged hydrogen ions.

Fig. 17: Energy of all the emitted particles at 80 ns.



# Remedies for RF Pulse Shortening

## ➤ Structural modification of the device

- Smoothing of pointed structures
- Higher order mode operation of the device
- Overmoded RR
- Overmoded trapezoidal cavity RR
- Overmoded non-uniform SWS

## ➤ High guiding magnetic field

- Overcome beam degradation
- Reduce secondary electron emission
- No unwanted mode excitation

# Conclusion

- The PIC simulation of RBWO is compared with the experimentally tested RBWO and it is in good agreement with gunin *et al.*
- In addition to the validation of experimental data, the various causes of RF pulse shortening phenomena are constructed to analyse the effects over the generated RF power amplitude and duration.
- The saturated RF power of approximately 0.80 GW is generated for only 50 ns and ceases after approximately 73 ns due to degradation of the beam quality.
- RF power was additionally reduced by ~25 MW to ~ 0.775 GW and stopped after ~ 65 ns due to electrons emitting in a strong electric field from the RR and SWS surfaces.
- The generation time was further reduced by ~3 ns in addition to beam degradation and RF generation stops at ~70 ns, while there is no effect on RF power due to secondary electrons.
- Finally, the collector plasma (PCHI) further reduced the time of generation of saturated rf energy by ~9 ns and allowed the generation to disappear after ~64 ns.
- Finally, the combined study that includes all the mechanisms considered further reduced the generation of saturated RF by ~ 100 MW to ~ 0.70 GW for ~ 40 ns and the generation ended after ~ 63 ns.
- It was observed that RF generation greatly affected by beam degradation, high field electron emission and plasma formation.

# List of Publications

- M. A. Ansari And M. Thottappan, “Design and Simulation of Dual-band Nonuniform Relativistic Backward Wave Oscillator using a Bragg Structure as Its RF Circuit And Reflector-Cum-Mode Converter,” IEEE Transactions on Electron Devices, vol. 67, No. 4, pp. 1814-1818, April 2020.
- M.A. Ansari And M. Thottappan, “Studies of Pulse Shortening Phenomena and Their Effects on the Beam-wave Interaction in an RBWO Operating at Low Magnetic Field,” IEEE Transactions on Plasma Science, vol. 48, No. 2, pp. 0426-0432, Feb. 2020.
- M.A. Ansari And M. Thottappan, “Design and Performance Analyses of High Efficiency X-band Relativistic Backward Wave Oscillator Using an Improved Resonant Reflector Under Low Guiding Magnetic Field,” IEEE Transactions on Plasma Science, vol. 47, No. 4, pp. 1754-1761, Apr. 2019.
- M.A. Ansari And M. Thottappan, “Analysis, Design, And 3D-simulation of a High Efficiency Overmoded Non-uniform Relativistic Backward Wave Oscillator,” IEEE Transactions On Electron Devices, vol. 65, No. 3, pp. 1158-1163, March 2018.
- V. Venkata Reddy, M.A. Ansari And M. Thottappan, “Simulation Investigations of High Power Overmoded Relativistic Backward Wave Oscillator with Trapezoidal Resonant Reflector,” Defense Science Journal – Communicated.



# References

- R. J. Barker and E. Schamiloglu, *high-power microwave sources and technologies*. New York: IEEE Press/John Wiley and Sons, 2001.
- J. Benford, J. A. Swegle, and E. Schamiloglu, *high power microwaves*, 3<sup>rd</sup>. New York: Taylor & Francis, 2016.
- B. N. Basu, *electromagnetic theory and applications in beam-wave electronics*. Singapore, New Jersey, London, Hong Kong: World Scientific Publishing Co. Inc., 1996.
- S. H. Gold, G. S. Nusinovich, and S. H. Gold, “review of high-power microwave source research review of high-power microwave source research,” vol. 3945, no. 1997, 2013.
- M. Abrams, “dawn of the e-bomb,” *IEEE Spectr.*, Vol. 40, pp. 24–30, 2003.
- J. A. Swegle, “starting conditions for relativistic backward wave oscillators at low currents,” *the Phys. Fluids*, vol. 30, no. 4, pp. 1201–1211, 1987.
- R. Alan Kehs, Alan Bromborsky, B. G. Ruth, S. E. Graybill, W. W. Destler, Y. C. Carmel, M. C. Wang, “A high power backward wave oscillator driven by a relativistic electron beam,” *IEEE Trans. Plasma Science*, vol. 13, no. 6, pp. 559–562, Dec. 1985.
- J. A. Swegle, R. A. Anderson, J. F. Camacho, B. R. Poole, M. A. Rhodes, E. T. Rosenbury, and D. L. Shaeffer, “scaling studies and time-resolved microwave measurements on a relativistic backward-wave oscillator,” *IEEE Trans. Plasma Sci.*, Vol. 21, pp. 714–724, 1993.
- L. D. Moreland, E. Schamiloglu, R. W. Lemke, A. M. Roitman, S. D. Korovin, and V. V. Rostov, “enhanced frequency agility of high power relativistic backward wave oscillators,” *IEEE Trans. Plasma Sci.*, Vol. 24, no. 3, pp. 28–85, Jun. 1996.
- Gunin et al., “Relativistic X-band BWO with 3-GW output power,” *IEEE Trans. Plasma Sci.*, Vol. 26, no. 3, pp. 326–331, Jun. 1998.
- B. Levush, T.M. Antonsen, A. Bromborsky, W. Lou, and Y. Carmel, “theory of relativistic backward-wave oscillators with end reflections,” *IEEE Trans. Plasma Sci.*, Vol. 20, pp. 263–280, 1992.
- A. N. Vlasov, A. S. Ilyin, Y. Carmel, and S. Member, “Cyclotron effects in relativistic backward-wave oscillators operating at low magnetic fields,” vol. 26, no. 3, pp. 605–614, 1998.
- J. Benford and G. Benford, “Survey of pulse shortening in high-power microwave sources,” *IEEE Trans. Plasma Sci.*, Vol. 25, no. 2, pp. 311–317, 1997.
- D. M. Goebel, “Pulse Shortening causes in High Power BWO and TWT microwave sources,” *IEEE Trans. Plasma Sci.*, Vol. 26, no. 3, pp. 263–274, 1998.
- J. Zhang et al., “Successful Suppression of Pulse Shortening in an X-band Overmoded Relativistic Backward-Wave Oscillator with pure  $TM_{01}$  mode output,” *IEEE Trans. Plasma Sci.*, Vol. 43, no. 2, pp. 528–531, Feb. 2015.



## **Annexure IV**

### **Typical WhatsApp Chats with Thinkers in VED**

24/08/2020, 19:41 - Dr. Vishal Kesari:

Dear Colleagues,

On behalf of the editorial team, I thank all the members of group for providing the data for proceedings of webinar#1.

Please find the proceeding attached.

I will be happy in receiving suggestions to improve the proceedings of upcoming webinars.

Thanks and regards,

Vishal Kesari

24/08/2020, 20:03 - Dr. SN Joshi CEERI:

Dear Dr Vishal,

Thanks a lot for bringing the proceedings of the 1st Webinar held on Aug.1, 2020. I thank you and entire editorial team for meticulous efforts in bringing these proceedings.

With best wishes,

24/08/2020, 20:24 - Dr. BK Shukla IPR Gandhinagar: Thank you Vishal, you have done most difficult job. It is well written.

24/08/2020, 20:57 - BNBasu Prof: Great work done, Vishal! Congratulations! Excellent document for Webinar#1 Resolution/Proceedings!

24/08/2020, 21:25 - RK Gupta CEERI: Great work Dr Vishal n team for releasing proceedings in such a short time.

24/08/2020, 20:07 - Dr. Vishal Kesari: Thanks Sir for best wishes and appreciation. It's all teamwork. Thank you very much for all the guidance. It's all due to combined efforts by all the contributors, editorial team, and group members.

24/08/2020, 21:00 - Dr. Chandra Shekhar CEERI:

<https://zeenews.india.com/india/drdo-identifies-108-systems-subsystems-to-be-designed-developed-by-indian-industry-only-2305066.html>

25/08/2020, 18:38 - Dr. Vishal Kesari: IEEE AP MTT Joint Chapter, Gujarat Section is organizing a webinar on "Brazing Technology for Microwave Vacuum Electron Devices-Vacuum and Hydrogen Brazing" as per below details:

1. Date: Saturday, August 29,2020
2. Time: 1430hrs-1600hrs
3. Online link: <https://meet.google.com/ebe-wdwn-tdu>
4. Speaker: Shri R.P.Singh, M/S Lucas Milhaupt, USA

The chosen topic will be helpful for both students and professionals as ever-growing opportunity in India in the field of Brazing (used in many industries & applications like: RF & Microwave Vacuum Electron Devices, Automobile, Air-conditioning, Mechanical structures etc.)

Hence, you are requested to circulate this webinar flyer so that the academic, scientific and industrial community can take advantage of the experience & knowledge of speaker.

Please request participants to drop an email to this ID for information.

On Behalf of IEEE Chapter!  
Contact: [ieeeapmttamd@gmail.com](mailto:ieeeapmttamd@gmail.com)

25/08/2020, 18:42 - BNBasu Prof: GREAT OPPORTUNITY

25/08/2020, 19:57 - Dr. SN Joshi CEERI: Yes Prof. Basu, I agree with you. It is still a critical area in the area of Vacuum Devices.  
Thanks Dr Vishal for sharing the link.

25/08/2020, 20:27 - Dr. Vishal Kesari: Most welcome Sir. It is also one of the objectives of this group to post /circulate the announcement of relevant conference/seminar/ workshop/ webinar.

27/08/2020, 08:48 - Dr. Lalit Kumar: VIRTUAL ICOPS2020 - Status Update, Acceptance Letter and Registration Fee Posted By Rajdeep Singh Rawat Posted Date 8/26/2020 5:46:28 PM Audience All Users Dear ICOSP2020 Participants Thank you for your support and participation in Virtual ICOPS2020. Status Update - As of now we have 955 abstracts submitted for Virtual ICOPS2020; 873 accepted and carried forward from earlier submission deadline in January 2020 and 82 new submissions. We have 8 Plenary and 91 Invited Speakers for our programme. Tomorrow, 27 August is the last day for Abstract submission. Acceptance Letter - Please note that the acceptance letter for the abstracts, which were accepted during the last round, can be self-generated from the abstract submission system. You just need to login to your account on Abstract Submission portal and click on "My

**Proceedings Second Webinar**  
**Expert Talk (Magnetron) & Researchers' Talk Series (Reltron and Relativistic BWO)**

Abstract" and the download the letter from the link for "Acceptance Letter".  
Registration Fee - Please proceed to pay the reduced registration fee at the earliest, before 30 September, if you wish to avail the early bird discount. Looking forward for your continued support and participation. Thanks and Best regards Professor Rajdeep Singh Rawat General Chair, ICOPS2020

28/08/2020, 23:47 - Dr. Vishal Kesari:

Webinar: Modeling RF and Microwave Heating with COMSOL

Respected Dr. Kesari,

You are invited to attend our live webinar on how to model RF and microwave heating with the COMSOL Multiphysics ® software on September 10 at 3 p.m. IST.

During this webinar, you will see how simulation with COMSOL Multiphysics ® allows you to extend your RF models to include effects such as temperature rise, structural deformations, and fluid flow. We will discuss how to model microwave and RF heating in antennas, circuit boards, living tissue, and devices that combine metallic and lossy dielectric domains. The webinar will include a live demo and a Q&A session.

For more information and to register, visit: <http://comsol.co.in/c/azab>

Feel free to forward this information to colleagues with similar interests. I look forward to seeing you there!

Best regards,  
Aditi Karandikar  
COMSOL  
Phone: 080-6738 3622; Email: [aditi@comsol.com](mailto:aditi@comsol.com)

29/08/2020, 17:28 - Dr. Vishal Kesari:

Dear Colleagues,

Today some of us attended a webinar on "Brazing Technology for Microwave Vacuum Electron Devices-Vacuum and Hydrogen Brazing" organized by IEEE AP MTT Joint Chapter, Gujarat Section. The speaker was Shri R P Singh from M/s Lucas Milhaupt, USA. The talk was quite interesting. Some details included in his talk are attached herewith.

Regards,

Vishal Kesari

29/08/2020, 17:28 - Dr. Vishal Kesari:  
File attached: Brazing Fundamentals \_ Lucas Milhaupt.pdf

**Proceedings Second Webinar**

**Expert Talk (Magnetron) & Researchers' Talk Series (Reltron and Relativistic BWO)**

29/08/2020, 17:57 - +91 99220 92509: The Webinar was very informative and had good discussion. I am very grateful to the Speaker Shri R.P singh sir, Dr Lalit Kumar sir & organizers.

From - Panacea Medical Technologies Pvt. Ltd.

29/08/2020, 20:15 - Dr. SN Joshi CEERI: Thanks Vishal for organising this webinar. It was quite informative, however, I expected more attendees.

## **Annexure V:**

**Brazing Fundamentals from M/s Lucas  
Milhaupt, USA**

**(open literature:**

**<https://www.lucasmilhaupt.com/EN/Brazing-Academy/Brazing-Fundamentals.htm>)**

# BRAZING PROCESS FUNDAMENTALS: HOW TO BRAZE IN SIX STEPS

---

## THE IMPORTANCE OF PROPER BRAZING PROCEDURES

Brazing is ideally suited for joining of dissimilar metals and is performed at relatively low temperature. We've said that a brazed joint "makes itself"—or that capillary action, more than operator skill, insures the distribution of the filler metal into the joint. But even a properly-designed joint can turn out imperfectly if the correct brazing process steps are not followed. These brazing procedures boil down the brazing process to six basic steps.

How to braze? There are six fundamentals of brazing that every brazer should follow to ensure consistent and repeatable joint quality, strength, hermeticity, and reliability. They are generally simple to perform (some may take only a few seconds), but none of them should be omitted from your brazing operation if you want to end up with sound, strong, neat-appearing joints.

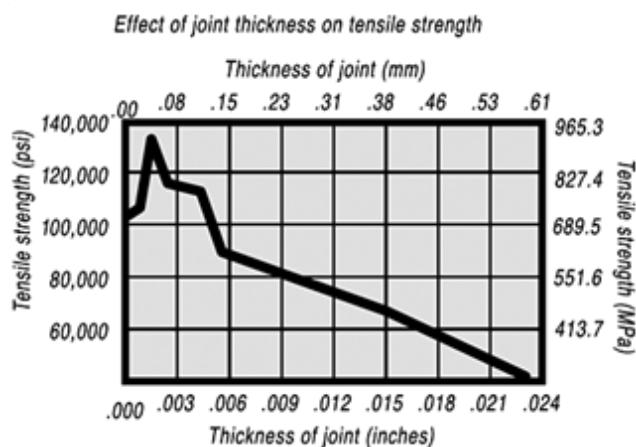
For the sake of simplicity, we'll discuss these six brazing process steps mainly in terms of "manual brazing," that is, brazing with hand-held torch and hand-fed filler metal. But everything said about manual brazing applies as well to mass production brazing. The same brazing process steps must be taken, although they may be performed in a different manner.

For more on the uses of brazing, [watch this video](#).

# BRAZING PROCESS STEP 1: GOOD FIT AND PROPER CLEARANCES

Brazing, as we've seen, uses the principle of capillary action to distribute the molten filler metal between the surfaces of the base metals. Therefore, during the brazing process, you should take care to maintain a clearance between the base metals to allow capillary action to work most effectively. This means, in almost all cases— a close clearance.

The following chart is based on brazing butt joints of stainless steel, using Easy-Flo® filler metal. It shows how the tensile strength of the brazed joint varies with the amount of clearance between the parts being joined.



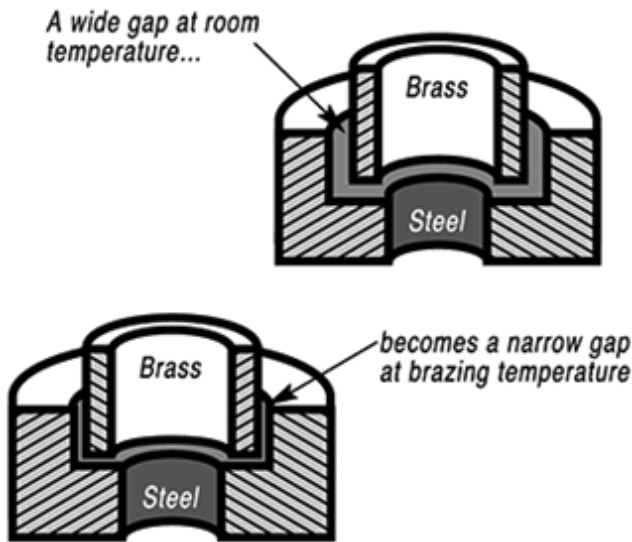


Note that the strongest joint (135,000 psi/930.8 MPa) is achieved when the joint clearance is .0015" (.038mm.)

When the clearance is narrower than this, it's harder for the filler metal to distribute itself adequately throughout the entire joint and joint strength is reduced.

Conversely, if the gap is wider than necessary, the strength of the joint will be reduced almost to that of the filler metal itself. Also, capillary action is reduced, so the filler metal may fail to fill the joint completely again lowering joint strength.

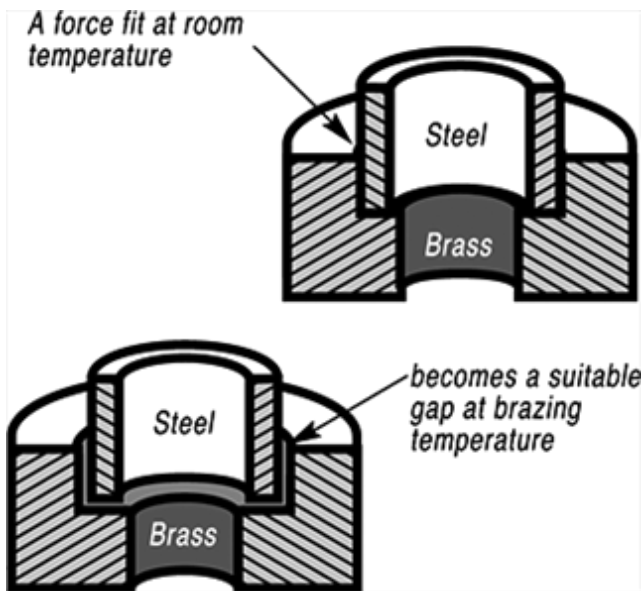
So the ideal clearance for a brazed joint, in the example above, is in the neighborhood of .0015" (.038mm.) But in ordinary day-to-day brazing, you don't have to be this precise to get a sufficiently strong joint.



Capillary action operates over a range of clearances, so you get a certain amount of leeway. Look at the chart again, and see that clearances ranging from .001" to .005" (.025 mm to .127 mm) still produce joints of 100,000 psi (689.5 MPa) tensile strength.

If you're joining two flat parts, you can simply rest one on top of the other.

The metal-to-metal contact is all the clearance you'll usually need, since the average "mill finish" of metals provides enough surface roughness to create capillary "paths" for the flow of molten filler metal. (Highly polished surfaces, on the other hand, tend to restrict filler metal flow.)



However, there's a special factor you should consider carefully in planning your joint clearances. Brazed joints are made at brazing temperatures, not at room temperature. So you must take into account the "coefficient of thermal expansion" of the metals being joined. This is particularly true of tubular assemblies in which dissimilar metals are joined.

As an example, let's say you're brazing a brass bushing into a steel sleeve. Brass expands, when heated, more than steel. So if you machine the parts to have a room temperature clearance of .002"-.003" (.051 mm-.076 mm), by the time you've heated the parts to brazing temperatures the gap may have closed completely! The answer? Allow a greater initial clearance, so that the gap at brazing temperature will be about .002"-.003" (.051 mm-.076 mm.).

Of course, the same principle holds in reverse. If the outer part is brass and the inner part steel, you can start with virtually a light force fit at room temperature. By the time you reach brazing temperature, the more rapid expansion of the brass creates a suitable clearance.

For more information on good fit and proper clearance, watch our video [here!](#)

## How much allowance should you make for expansion and contraction?

It depends on the nature and sizes of the metals being joined and the configuration of the joint itself. Although there are many variables involved in pinpointing exact clearance tolerances for each situation, keep in mind the principle involved—different metals expand at different rates when heated. To help you in planning proper clearances in brazing dissimilar metals, the chart on the opposite page furnishes the coefficient of thermal expansion for a variety of metals and alloys.

## Comparison Of Materials: Coefficient Of Thermal Expansion

Material	10 <sup>-6</sup> in./in.°/°F		10 <sup>-5</sup> in./in.°/°C		Material	10 <sup>-6</sup> in./in.°/°F		10 <sup>-5</sup> in./in.°/°C	
	High	Low	High	Low		High	Low	High	Low
Zinc & its Alloys <sup>c</sup> .....	19.3	10.8	3.5	1.9	Martensitic Stainless Steels <sup>c</sup> .....	6.5	5.5	1.2	1.0
Lead & its Alloys <sup>c</sup> .....	16.3	14.4	2.9	2.6	Nitriding Steels <sup>d</sup> .....	6.5	—	1.2	—
Magnesium Alloys <sup>b</sup> .....	16	14	2.8	2.5	Palladium <sup>c</sup> .....	6.5	—	1.2	—
Aluminum & its Alloys <sup>c</sup> .....	13.7	11.7	2.5	2.1	Beryllium <sup>b</sup> .....	6.4	—	1.1	—
Tin & its Alloys <sup>c</sup> .....	13	—	2.3	—	Chromium Carbide Cermet <sup>c</sup> .....	6.3	5.8	1.1	1.0
Tin & Aluminum Brasses <sup>c</sup> .....	11.8	10.3	2.1	1.8	Thorium <sup>b</sup> .....	6.2	—	1.1	—
Plain & Leaded Brasses <sup>c</sup> .....	11.6	10	2.1	1.8	Ferritic Stainless Steels <sup>c</sup> .....	6	5.8	1.1	1.0
Silver <sup>c</sup> .....	10.9	—	2.0	—	Gray Irons (cast) <sup>c</sup> .....	6	—	1.1	—
Cr-Ni-Fe Superalloys <sup>d</sup> .....	10.5	9.2	1.9	1.7	Beryllium Carbide <sup>d</sup> .....	5.8	—	1.0	—
Heat Resistant Alloys (cast) <sup>d</sup> .....	10.5	6.4	1.9	1.1	Low Expansion Nickel Alloys <sup>c</sup> .....	5.5	1.5	1.0	.3
Nodular or Ductile Irons (cast) <sup>c</sup> .....	10.4	6.6	1.9	1.2	Beryllia & Thoria <sup>a</sup> .....	5.3	—	.9	—
Stainless Steels (cast) <sup>d</sup> .....	10.4	6.4	1.9	1.1	Alumina Cermets <sup>d</sup> .....	5.2	4.7	.9	.8
Tin Bronzes (cast) <sup>c</sup> .....	10.3	10	1.8	1.8	Molybdenum Disilicide <sup>c</sup> .....	5.1	—	.9	—
Austenitic Stainless Steels <sup>c</sup> .....	10.2	9	1.8	1.6	Ruthenium <sup>b</sup> .....	5.1	—	.9	—
Phosphor Silicon Bronzes <sup>c</sup> .....	10.2	9.6	1.8	1.7	Platinum <sup>c</sup> .....	4.9	—	.9	—
Coppers <sup>c</sup> .....	9.8	—	1.8	—	Vanadium <sup>b</sup> .....	4.8	—	.9	—
Nickel-Base Superalloys <sup>d</sup> .....	9.8	7.7	1.8	1.4	Rhodium <sup>b</sup> .....	4.6	—	.8	—
Aluminum Bronzes (cast) <sup>c</sup> .....	9.5	9	1.7	1.6	Tantalum Carbide <sup>d</sup> .....	4.6	—	.8	—
Cobalt-Base Superalloys <sup>d</sup> .....	9.4	6.8	1.7	1.2	Boron Nitride <sup>d</sup> .....	4.3	—	.8	—
Beryllium Copper <sup>c</sup> .....	9.3	—	1.7	—	Columbium & its Alloys .....	4.1	3.8	.7	.68
Cupro-Nickels & Nickel Silvers <sup>c</sup> .....	9.5	9	1.7	1.6	Titanium Carbide <sup>d</sup> .....	4.1	—	.7	—
Nickel & its Alloys <sup>d</sup> .....	9.2	6.8	1.7	1.2	Steatite <sup>c</sup> .....	4	3.3	.7	.6
Cr-Ni-Co-Fe Superalloys <sup>d</sup> .....	9.1	8	1.6	1.4	Tungsten Carbide Cermet <sup>c</sup> ..	3.9	2.5	.7	.4
Alloy Steels <sup>d</sup> .....	8.6	6.3	1.5	1.1	Iridium <sup>b</sup> .....	3.8	—	.7	—
Carbon Free-Cutting Steels <sup>d</sup> .....	8.4	8.1	1.5	1.5	Alumina Ceramics <sup>c</sup> .....	3.7	3.1	.7	.6
Alloy Steels (cast) <sup>d</sup> .....	8.3	8	1.5	1.4	Zirconium Carbide <sup>d</sup> .....	3.7	—	.7	—
Age Hardenable Stainless Steels <sup>c</sup> .....	8.2	5.5	1.5	1.0	Osmium and Tantalum <sup>b</sup> .....	3.6	—	.6	—
Gold <sup>c</sup> .....	7.9	—	1.4	—	Zirconium & its Alloys <sup>b</sup> .....	3.6	3.1	.6	.55
High Temperature Steels <sup>d</sup> ..	7.9	6.3	1.4	1.1	Hafnium <sup>b</sup> .....	3.4	—	.6	—
Ultra High Strength Steels <sup>d</sup> ..	7.6	5.7	1.4	1.0	Zirconia <sup>a</sup> .....	3.1	—	.6	—
Malleable Irons <sup>c</sup> .....	7.5	5.9	1.3	1.1	Molybdenum & its Alloys .....	3.1	2.7	.6	.5
Titanium Carbide Cermet <sup>d</sup> .....	7.5	4.3	1.3	.8	Silicon Carbide <sup>a</sup> .....	2.4	2.2	.4	.39
Wrought Irons <sup>c</sup> .....	7.4	—	1.3	—	Tungsten <sup>b</sup> .....	2.2	—	.4	—
Titanium & its Alloys <sup>d</sup> .....	7.1	4.9	1.3	.9	Electrical Ceramics <sup>c</sup> .....	2	—	.4	—
Cobalt <sup>d</sup> .....	6.8	—	1.2	—	Zircon <sup>c</sup> .....	1.8	1.3	.3	.2
					Boron Carbide <sup>a</sup> .....	1.7	—	.3	—
					Carbon and Graphite <sup>c</sup> .....	1.5	1.3	.3	.2

<sup>a</sup> Values represent high and low sides of a range of typical values. (\* or mm/mm)  
<sup>b</sup> Value at room temperature only.  
<sup>c</sup> Value for a temperature range between room temperature and 212-750° F/100-390° C.  
<sup>d</sup> Value for a temperature range between room temperature and 1000-1800° F/540-980° C.  
<sup>e</sup> Value for a temperature range between room temperature and 2200-2875° F/1205-1580° C.  
 Reprinted with permission from "Materials Selector," Reinhold Publishing Co., Penton/IPC.

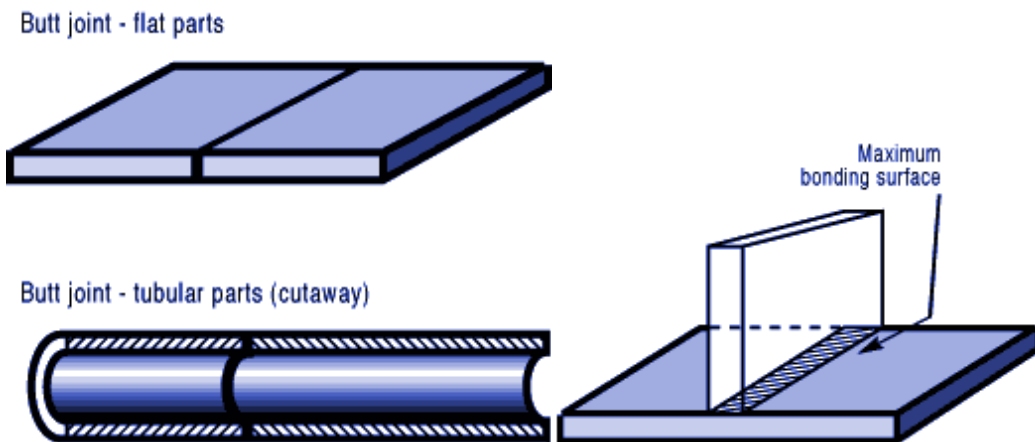
## Proper Joint Clearance

There are only two basic types - the butt and the lap. The rest are essentially modifications of these two. Let's look first at the butt joint, both for flat and tubular

parts.

## Designing Butt Joints

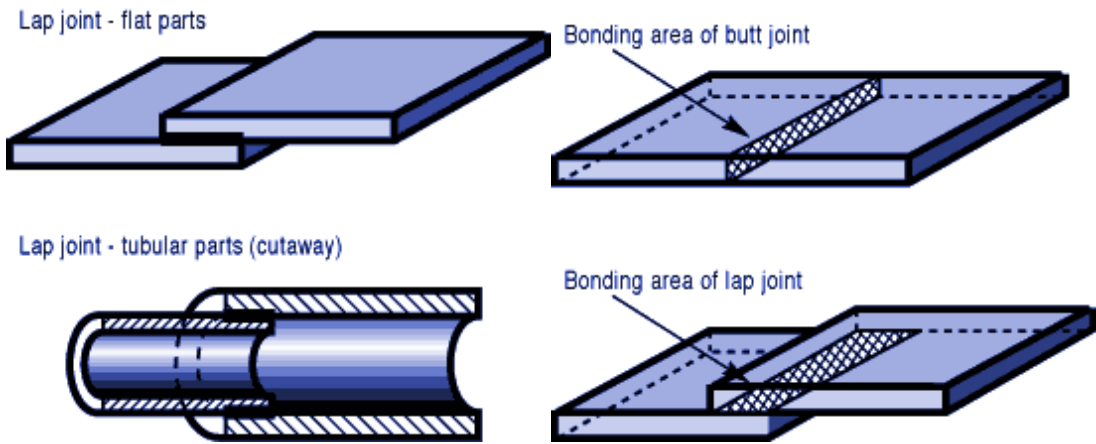
As you can see, the butt joint gives you the advantage of a single thickness at the joint. Preparation of this type of joint is usually simple, and the joint will have sufficient tensile strength for most applications. However, the strength of the butt joint does have limitations. It depends on the amount of bonding surface, and in a butt joint the bonding area can't be any larger than the cross-section of the thinner member.



## Designing Lap Joints

The first thing you'll notice is that, for a given thickness of base metals, the bonding area of the lap joint can be larger than that of the butt joint and usually is. With larger bonding areas, lap joints can usually carry larger loads.

The lap joint doubles the thickness at the joint, but in many applications (plumbing connections, for example) this reinforcement of the joint is preferable. Resting one flat member on the other is usually enough to maintain a uniform joint clearance. And, in tubular joints, nesting one tube inside the other holds them in proper alignment for brazing. However, suppose you want a joint that has the advantages of both types; single thickness at the joint combined with maximum tensile strength. You can get this combination by designing the joint as a butt-lap joint.

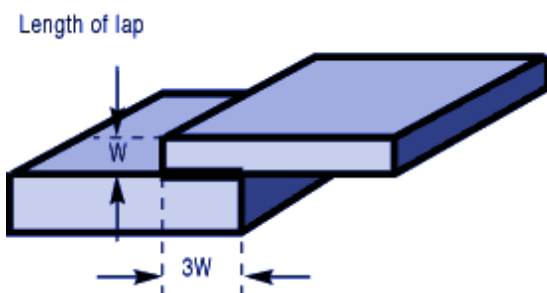


## Conclusion

True, the butt-lap is usually a little more work to prepare than straight butt or lap, but the extra work can pay off. You wind up with a single thickness joint of maximum strength. And the joint is usually self-supporting when assembled for brazing.

## Figuring the proper length of lap

Obviously, you don't have to calculate the bonding area of a butt joint. It will be the cross-section of the thinner member. A good rule of thumb is to design the lap joint to be three times as long as the thickness of the thinner joint member.



A longer lap may waste brazing filler metal without a corresponding increase in joint strength. And a shorter lap will lower the strength of the joint. For most applications, you're on safe ground with the "rule of three." More specifically, if

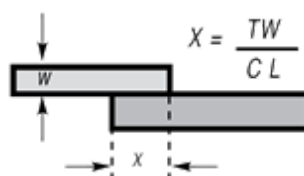
you know the approximate tensile strengths of the base members, the lap length required for optimum joint strength in a silver brazed joint is as follows:

Tensile strength of weakest member	Lap length = factor x W (W = thickness of weakest member)
35,000 psi - 241.3 MPa	2 x W
60,000 psi - 413.7 MPa	3 x W
100,000 psi - 689.5 MPa	5 x W
130,000 psi - 896.3 MPa	6 x W
175,000 psi - 1,206.6 MPa	8 x W

## Figuring length of lap for joints

If you have a great many identical assemblies to braze, or if the joint strength is critical, it will help to figure the length of lap more exactly, to gain maximum strength with minimum use of brazing materials. The formulas given below will help you calculate the optimum lap length for flat and for tubular joints.

### Flat joints



X = Length of lap

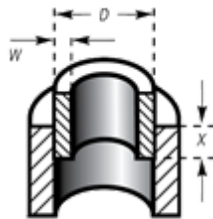
T = Tensile strength of weakest member

W = Thickness of weakest member

C = Joint integrity factor of .8

L = Shear strength of brazed filler metal

## Tubular joints



$$X = \frac{W (D-W) T}{C L D}$$

X = Length of lap area

W = Wall thickness of weakest member

D = Diameter of lap area

T = Tensile strength of weakest member

C = Joint integrity factor of .8

L = Shear strength of brazed filler metal

## Designing to distribute stress

When you design a brazed joint, obviously you aim to provide at least minimum adequate strength for the given application. But in some joints, maximum mechanical strength may be your overriding concern. You can help ensure this degree of strength by designing the joint to prevent concentration of stress from weakening the joint.

### Spread the stress

Figure out where the greatest stress falls, then impart flexibility to the heavier member at this point, or add strength to the weaker member. When you're designing a joint for maximum strength, use a lap to increase joint area rather than a butt, and design the parts to prevent stress from being concentrated at a



single point. There is one other technique for increasing the strength of a brazed joint, frequently effective in brazing small-part assemblies. You can create a stress-distribution fillet, simply by using a little more brazing filler metal than you normally would, or by using a more "sluggish" alloy. Usually you don't want or need a fillet in a brazed joint, as it doesn't add materially to joint strength. It pays to create the fillet when contributing to spreading joint stresses.

## Designing for service conditions

In many brazed joints, the chief requirement is strength. And we've discussed various ways of achieving joint strength. But there are frequently other service requirements which may influence the joint design or filler metal selection. For example, you may be designing a brazed assembly that needs to be electrically conductive. A silver brazing filler metal, by virtue of its silver content, has very little tendency to increase electrical resistance across a properly-brazed joint. But you can further insure minimum resistance by using a close joint clearance, to keep the layer of filler metal as thin as possible. In addition, if strength is not a prime consideration, you can reduce length of lap. Instead of the customary "rule of three," you can reduce lap length to about 1-1/2 times the cross-section of the thinner member.

If the brazed assembly has to be pressure-tight against gas or liquid, a lap joint is almost a must since it withstands greater pressure than a butt joint. And its broader bonding area reduces any chance of leakage. Another consideration in designing a joint to be leak proof is to vent the assembly. Providing a vent during the brazing process allows expanding air or gases to escape as the molten filler metal flows into the joint. Venting the assembly also prevents entrapment of flux in the joint. Avoiding entrapped gases or flux reduce the potential for leak paths. If possible, the assembly should be self-venting. Since flux is designed to be displaced by molten filler metal entering a joint, there should be no sharp corners or blind holes to cause flux entrapment. The joint should be designed so that the flux is pushed completely out of the joint by the filler metal. Where this is not possible, small holes may be drilled into the blind spots to allow flux escape. The joint is completed when molten filler metal appears at the outside surface of these drilled holes.

To maximize corrosion-resistance of a joint, select a brazing filler metal containing such elements as silver, gold or palladium, which are inherently corrosion-resistant. Keep joint clearances close and use a minimum amount of filler metal, so that the finished joint will expose only a fine line of brazing filler metal to the atmosphere. These are but a few examples of service requirements that may be demanded of your brazed assembly. As you can see both the joint design and filler metal selection must be considered.

If you'd like to watch a hands on demonstration of good fit and proper clearance, [check out this video](#).

# BRAZING PROCESS STEP 2: CLEANING THE METALS



Capillary action will work properly only when the surfaces of the metals are clean. If they are “contaminated”—coated with oil, grease, rust, scale or just plain dirt—those contaminants have to be removed. If they remain, they will form a barrier between the base metal surfaces and the brazing materials. An oily base metal, for example, will repel the flux, leaving bare spots that oxidize under heat and result in voids. Oil and grease will carbonize when heated, forming a film over which the filler metal will not flow. And brazing filler metal won’t bond to a rusty surface.

Cleaning the metal parts is seldom a complicated job, but it has to be done in the right sequence. Oil and grease should be removed first, because an acid pickle solution aimed to remove rust and scale won’t work on a greasy surface. (If you try to remove rust or scale by abrasive cleaning before getting rid of the oil, you’ll wind up scrubbing the oil, as well as fine abrasive powder, more deeply into the surface.)

Start by getting rid of oil and grease. In most cases you can do it very easily either by dipping the parts into a suitable degreasing solvent, by vapor degreasing, or by alkaline or aqueous cleaning. If the metal surfaces are coated with oxide or scale, you can remove those contaminants chemically or mechanically. For chemical removal, use an acid pickle treatment, making sure that the chemicals are compatible with the base metals being cleaned, and that no acid traces remain in crevices or blind holes. Mechanical removal calls for

abrasive cleaning. Particularly in repair brazing, where parts may be very dirty or heavily rusted, you can speed the cleaning process by using a grinding wheel, or file or metallic grit blast, followed by a rinsing operation.

Once the parts are thoroughly clean, it's a good idea to flux and braze as soon as possible. That way, there's the least chance for recontamination of surfaces by factory dust or body oils deposited through handling.

For more on properly cleaning the metals, check out this [blog post](#) or this [video](#).

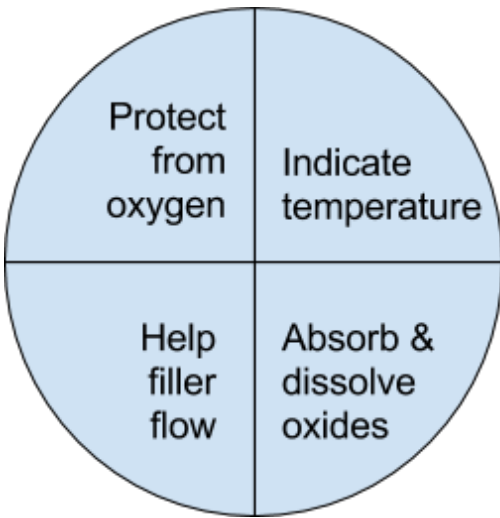
# BRAZING PROCESS STEP 3: FLUXING THE PARTS

## Why Brazing Requires Flux

Flux is a chemical compound applied to the joint surfaces before brazing. Its use, with a few exceptions, is crucial in the atmospheric brazing process. Heating a metal surface accelerates the formation of oxides, the result of chemical combination between the hot metal and oxygen in the air. If you don't stop these oxides from forming, they'll inhibit the brazing filler metal from wetting and bonding to the surfaces.

A coating of flux on the joint area guards the surfaces from the air, preventing oxide formation. It also dissolves and absorbs any oxides that form throughout heating or that were not completely removed in the cleaning process.

Understanding the functions and stages of flux will help you achieve strong, quality joints in your operation.



## Flux Application

You can apply flux as long as you cover the joint surfaces completely. Flux traditionally is made in a paste, so it's usually most convenient to brush it on. But as production quantities increase, it may be more effective to apply the flux by dipping or dispensing a pre-measured deposit of high-viscosity dispensable flux from an applicator gun. Why dispensable flux? Many companies find the repeatable deposit size improves joint consistency, and because typically less flux is used, the amount of residue entering the waste stream is also reduced. [Watch our new technical video](#) for an in-depth look at the four functions of flux.

## When do you flux and how do you choose?

Typically just before brazing, if possible. That way the flux has least chance to dry out and flake off, or get knocked off the parts in handling. Which flux do you use? Choose the one formulated for the specific metals, temperatures and conditions of your brazing application. There are fluxes formulated for practically every need; for example - fluxes for brazing at very high temperatures (in the 2000°F/1093°C area), fluxes for metals with refractory oxides, fluxes for long heating cycles, and fluxes for dispensing by automated machines.

The addition of metallic boron changes white flux to black. Black flux is beneficial for fast induction heating, may provide better protection in a high-temperature brazing operation, and can be helpful with high-liquidus filler metals.



Boron-modified black flux can help ensure a successful braze joint when brazing large parts over an extended period of heating time, or with base materials that require extra care to reduce tenacious oxides. Lucas Milhaupt's technical staff demonstrates the difference between white versus black flux in this video.

Fortunately for your inventory, general-purpose fluxes, such as Handy & Harman's Handy Flux, are suitable for most typical brazing jobs.

## How much flux do you use?

Enough to last throughout the entire heating cycle. Keep in mind that the larger and heavier the pieces brazed, the longer the heating cycle will take - so use more flux. (Lighter pieces, of course, heat up faster and require less flux.) As a general rule, don't skimp on the flux. It's your insurance against oxidation. Think of the flux as a sort of blotter. It absorbs oxides like a sponge absorbs water. An insufficient amount of flux will quickly become saturated and lose its effectiveness. A flux that absorbs less oxides not only insures a better joint than a totally saturated flux, but it is a lot easier to wash off after the brazed joint is completed.

Flux can also act as a temperature indicator, minimizing the chance of overheating the parts. Handy & Harman's Handy Flux, for example, becomes completely clear and active at 1100°F/593°C. At this temperature, it looks like water and reveals the bright metal surface underneath - telling you that the base metal is just about hot enough to melt the brazing filler metal. In this video, we'll show you how Handy® Flux appears during the brazing process.

## Handy Flux temperature indicator chart

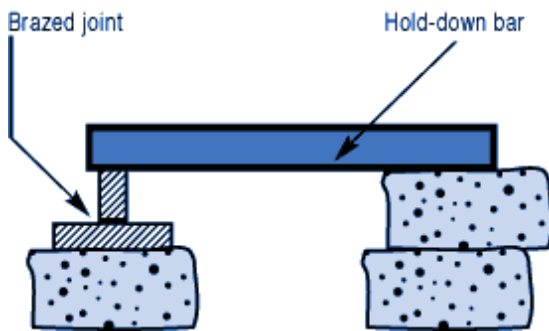
Temp	Appearance Of flux
------	--------------------

Temp	Appearance Of flux
212°F (100°C)	Water boils off
600°F (315°C)	Flux becomes white and slightly puffy, starts to "work"
800°F (425°C)	Flux lies against surface and has a milky appearance
1100°F (593°C)	Flux is completely clear and active, looks like water. Bright metal surface is visible underneath. Test the temperature by touching brazing filler metal to base metal. If brazing filler metal melts, assembly is at proper temperature for brazing.

Fluxing is an essential step in the brazing operation, aside from a few exceptions. You can join copper to copper without flux, by using a brazing filler metal specially formulated for the job, such as Handy & Harman's Sil-Fos or Fos-Flo 7. (The phosphorus in these alloys acts as a fluxing agent on copper.) You can also omit fluxing if brazing occurs in a controlled atmosphere (i.e. a gaseous mixture contained in an enclosed space, usually a brazing furnace). The atmosphere (such as hydrogen, nitrogen or dissociated ammonia) completely envelops the assemblies and, by excluding oxygen, prevents oxidation. Even in controlled atmosphere brazing you may find that a small amount of flux improves the wetting action of the brazing filler metal.

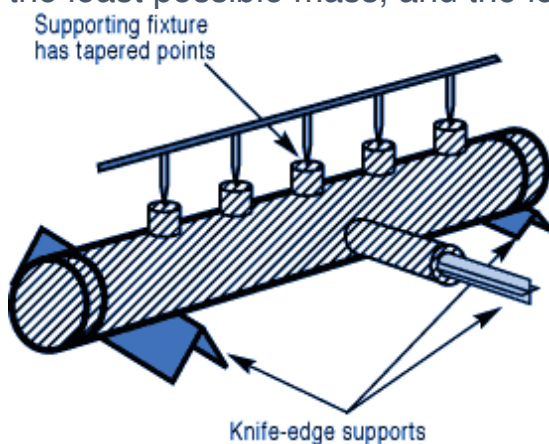
For more tips on proper fluxing, [watch this video](#).

# BRAZING PROCESS STEP 4: ASSEMBLY FOR BRAZING



The parts of the assembly are cleaned and fluxed. Now you have to hold them in position for brazing. Be sure they remain in correct alignment during the heating and cooling cycles, so that capillary action can do its job. If the shape and weight of the parts permit, the simplest way to hold them together is by gravity. Or give gravity a helping hand by adding additional weight.

If you have a number of assemblies to braze and their configuration is too complex for self-support or clamping, use a brazing support fixture. Design it for the least possible mass, and the least contact with the parts of the assembly.

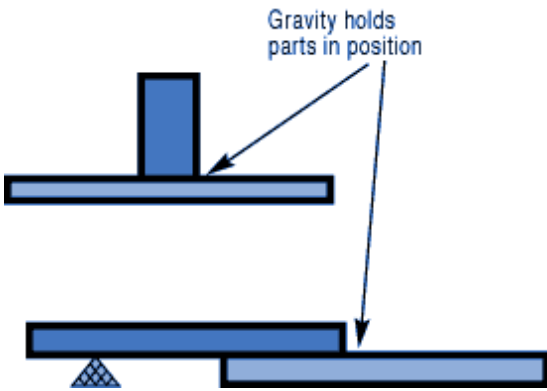


(A cumbersome fixture that contacts the assembly broadly will conduct heat away from the joint area.)

Use pinpoint and knife-edge design to reduce contact to the minimum.

Try to use materials in your fixture that are poor heat conductors, such as stainless steel, Inconel or ceramics. Since these are poor conductors, they draw the least heat away from the joint.

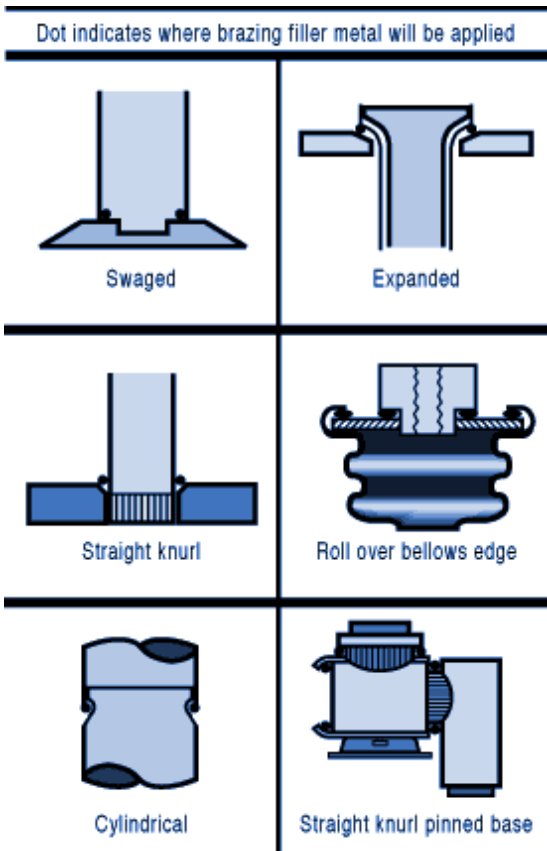




Choose materials with compatible expansion rates so you won't get alterations in assembly alignment during the heating cycle.

If you're planning to braze hundreds of identical assemblies, think in terms of designing the parts themselves for self-support during the brazing process. At the initial planning stage, design mechanical devices that will accomplish this purpose, and that can be incorporated in the fabricating operation. Typical devices include crimping, interlocking seams, swaging, peening, riveting, pinning, dimpling or knurling.

Sharp corners should be minimized in mechanically held assemblies; corners can impede capillary action and should be slightly rounded to aid the flow of filler metal. A simple mechanical holding device is the best, since its only function is to hold the parts together while the permanent joint is made by brazing.



## Fixture Facts

A fixture is built to cradle, hold or secure an assembly to be joined. Proper fixtures should meet these criteria:

- Allow easy insertion of assembly components and easy removal of the brazed assembly
- Support assembly components to permit expansion and contraction during heating and cooling
- Support the assembly at points away from the heat zone (preventing the fixture from becoming a heat sink)
- Permit the flame to be directed around the entire joint area, so the alloy can flow throughout the joint
- Use gravity to assist capillary action
- Maintain alignment and dimensional stability until the alloy solidifies
- Be sufficiently flexible to accommodate other similar assemblies

## Better Joint Design

An axiom of metal joining is that proper joint design is the path to efficient fixturing. Brazeing experts at Lucas Milhaupt offer these tips for improving your joint design:

- Make component pieces of the assembly self locating, so the fixture only supports and cradles the components.
- Allow space for the filler metal to flow and for flux to be forced out of the joint.

Example Problem: Where a tube enters a fitting or casting, some manufacturers use a press fit to keep externally applied alloy from reaching the bottom of the joint, where it might plug a hole in the fitting. Unfortunately, molten flux reaches the bottom of the blind hole and is trapped there, as alloy melts and tries to enter the joint. The alloy cannot displace the flux, so heavy flux inclusions and poor joint quality result.

Example Solution: Use a slip fit and a buried preform in the hole. The alloy is induced by heat to flow to the top of the joint, pushing the flux out. This leaves the hole open and results in a sound joint. Take into account the expansion and contraction characteristics of the metals being joined. If possible, design the joint so the higher-expansion material is the outer member of the joint. (It will expand more than the inner member, providing clearance where the filler metal will flow.)

Silver brazeing is a cost-effective method for joining metals, especially when joints are designed for maximum brazeing efficiency and fixtures are designed as described. Many products manufactured today could be redesigned for brazeing to reduce manufacturing costs. Even though silver is expensive, it represents a small percentage of total assembly costs.

## Fixturing Tips

Lucas Milhaupt engineers offer these ideas for improving manufacturing efficiency with fixturing:

- Construct fixtures from 300-series, non-magnetic stainless steel for better corrosion resistance and dimensional stability (other ideas include Inconel and some ceramics).
- When fixturing for furnace brazing, hold the mass of the fixture to a minimum. (Payoff is dependent on lb/hr through the furnace; increased weight = reduced fuel efficiency.)
- When fixturing for induction heating, keep fixtures away from the work coil, so they will not act as heat sinks or interfere with the magnetic field.
- Avoid use of springs for bringing parts back to dimensional alignment. If they are required, keep them out of the heat zone, so they will not be affected by flux residue or oxidation.

Fixture design is a key factor in achieving quality flame-brazed or soldered joints. In addition, proper joint design is the path to efficient fixturing.

Combining improvements to both these areas can result in better-quality joints, increase operating efficiency and reduce costs.

Get a more in-depth look of proper assembly [in this video](#).

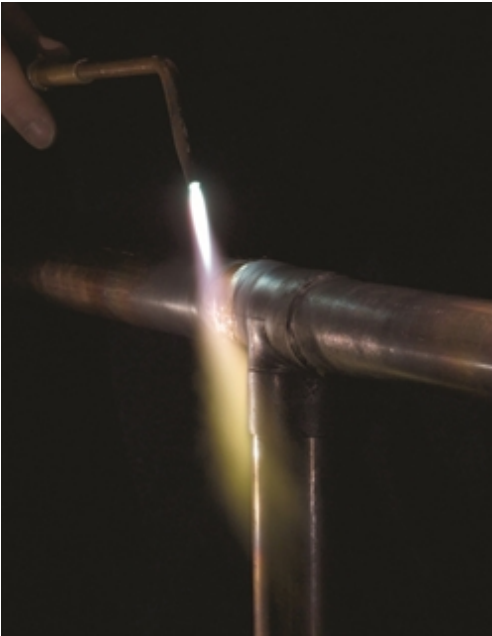
# **BRAZING PROCESS STEP 5: BRAZING THE ASSEMBLY: HEATING METHODS**

The fifth step is the actual accomplishment of the brazing joint. It involves heating the assembly to brazing temperature, and flowing the filler metal through the joint.

## **Brazing Heating Methods**

There are four main types of brazing heating methods: torch or manual brazing, induction brazing, resistance brazing, and vacuum brazing. The heating method most commonly used in brazing a single assembly is the hand held torch, therefore most of this guide will focus on manual brazing practices and principles. However, if you need assistance with furnace brazing, please see our furnace atmosphere blog.

First, apply heat broadly to the base metals. If you're brazing a small assembly, you may heat the entire assembly to the flow point of the brazing filler metal. If you're brazing a large assembly, you heat a broad area around the joint.



All you have to keep in mind is that both metals in the assembly should be heated as uniformly as possible so they reach brazing temperature at the same time. When joining a heavy section to a thin section, the “splash-off” of the flame may be sufficient to heat the thin part. Keep the torch moving at all times. When joining heavy sections, the flux may become transparent—which is at 1100°F (593°C)—before the full assembly is hot enough to receive the filler metal.

In torch brazing, a variety of fuels are available—natural gas, acetylene, propane, propylene, etc., combusted with either oxygen or air. The most popular is still the oxy/acetylene mixture. When it comes to safely brazing with oxy-acetylene torches, let's look at two important aspects: safety equipment, plus procedures for safe operation. This is serious business: arc rays and sparks can result in loss of sight, fume inhalation can lead to lung damage, and other accidents can cause burns, fires, or explosions.

## Oxy-acetylene Torch Safety Equipment

In addition to gloves, eye protection, and related safety gear, these are the important elements:

**Cylinders** - Oxygen and acetylene are kept in separate cylinders and not combined until the torch tip is ignited. Oxygen cylinders, typically painted green, contain oxygen compressed up to 2,200 psi (pounds per square inch). Oxygen is a stable compound by nature, but any oil or grease which comes in contact with the oxygen will burst into flames. Therefore, keep hands and gloves free of these materials before handling cylinders. Acetylene gas cylinders are compressed at only about 250 psi, which is much lower than oxygen tanks. However, unlike oxygen, acetylene is rather unstable and, therefore, should not be introduced into the torch above 15 psi. As an extra precaution, cylinder valves should be open no more than 1.5 turns, in the event an operator must close a valve quickly.

**Regulators** - Installed on the cylinder, regulators control both the pressure of the cylinder and the outlet pressure leading to the torch. Turn keys or knobs on the regulators allow adjustment of the outlet pressure. Again, the setting should be no more than 15 psi for acetylene. Consult the torch manufacturer for proper pressure settings for acetylene and oxygen.

**Check Valves** - From the regulator, the two gases travel through check valves, which ensure that the gases can be shut off in the event of backflow.

Alternatively, check valves can be placed between the gas hoses and the torch. Please note that check valves can stop reverse gas flow, but they cannot stop flame in the event of a flashback.

**Flashback Arrestors** - Flashback arrestors prevent fire from flowing back into the cylinders, which will otherwise lead to an explosion. Flashback arrestors contain cut-off valves with low melting points. When triggered by flame, they readily shut off the gas supply and thus extinguish the flame. Both check valves and flashback arrestors should be tested or changed regularly to ensure they are working properly.

## Oxy-acetylene Torch Safe Operation

In addition to using safety equipment, workers should practice safe operation to prevent flashbacks. Keep acetylene and oxygen separate until the torch is ignited. When starting a torch, the acetylene valve should be opened first. Next, the torch should be ignited, and then oxygen can be introduced. Please note that opening both gas valves prior to ignition can cause gas backflow into either gas hose, leaving the system vulnerable to flashback.

After use, it is critical that both gas lines be emptied separately-one at a time-through the torch. If this "bleeding" of gas lines is done simultaneously for oxygen and acetylene, any pressure difference between the gas lines will cause backflow of one gas into the other line, so this should be avoided.

Flashbacks can also be caused by brazing with multiple torches, simultaneously, on one part. If using dual torches to heat both sides of a part, do not aim the

torches at each other, but rather, angle each torch toward the part. If one torch should cause flashback in the other, operators will hear a loud hissing sound and should immediately turn off the gas by closing first the acetylene valve and then the oxygen valve.

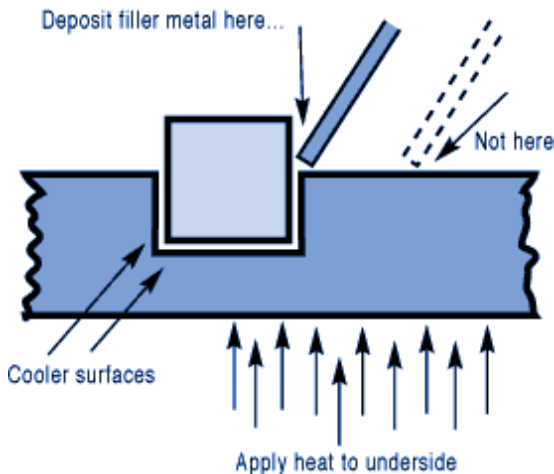
## Flux Changes During Brazing Process

Some metals are good conductors—and consequently carry off heat faster into cooler areas. Others are poor conductors and tend to retain heat and overheat readily. The good conductors will need more heat than the poor conductors, simply because they dissipate the heat more rapidly.

In all cases, your best insurance against uneven heating is to keep a watchful eye on the flux. If the flux changes in appearance uniformly, the parts are being heated evenly, regardless of the difference in their mass or conductivity.

## Depositing Filler Metals

You've heated the assembly to brazing temperature. Now you are ready to deposit the filler metal.



In manual brazing, all this involves is carefully holding the rod or wire against the joint area. The heated assembly will melt off a portion of the filler metal, which will instantly be drawn by capillary action throughout the entire joint area.

You may want to add some flux to the end of the filler metal rod— about 2” to 3” (51 mm to 76 mm)— to improve the flow. This can be accomplished by either brushing on or dipping the rod in flux. On larger parts requiring longer heating time, or where the flux has become saturated with much oxide, the addition of fresh flux on the filler metal will improve the flow and penetration of the filler metal into the joint area.

However, there is one small precaution to observe. Molten brazing filler metal tends to flow toward areas of higher temperature. In the heated assembly, the outer base metal surfaces may be slightly hotter than the interior joint surfaces. So take care to deposit the filler metal immediately adjacent to the joint. If you



deposit it away from the joint, it tends to plate over the hot surfaces rather than flow into the joint. In addition, it's best to heat the side of the assembly opposite the point where you're going to feed the filler metal. In the example above, you heat the underside of the larger plate, so that the heat draws the filler metal down fully into the joint. (Always remember—the filler metal tends to flow toward the source of heat.)

## General Safety In Brazing

In brazing, there is always the possibility of dangerous fumes and gases rising from base metal coatings, zinc and cadmium-bearing filler metals, and from fluorides in fluxes. The following well-tested precautions should be followed to guard against any hazard from these fumes.



**1. Ventilate confined areas:** Use ventilating fans and exhaust hoods to carry all fumes and gases away from work, and air supplied respirators as required.

**2. Clean base metals thoroughly:** A surface contaminant of unknown composition on base metals may add to fume hazard and may cause a too rapid breakdown of flux, leading to overheating and fuming.

**3. Use sufficient flux:** Flux protects base metals and filler metal during the heating cycle. Full flux coverage reduces fuming. Also, consult your SDS regarding specific hazards associated with brazing flux.

**4. Heat metals broadly:** Heat the base metals broadly and uniformly. Intense localized heating uses up flux, increases danger of fuming. Apply heat only to



base metals, not to filler metal. (Direct flame on filler metal causes overheating and fuming.)

**5. Know your base metals:** A cadmium coating on a base metal will volatilize and produce toxic fume during heating. Zinc coatings (galvanized) will also fume when heated. Learn to recognize these coatings. It is recommended that they be removed before parts are heated for brazing.

**6. Know your filler metals:** Be especially careful not to overheat assembly when using filler metals that contain cadmium. Consult Pages 34-37 or the Safety Data Sheet (SDS) for maximum recommended brazing temperatures of a specific filler metal. The filler metal carries a warning label. Be sure to look for it and follow the instructions carefully.

[Watch this video](#) for a closer look at the proper heating methods for brazing.

## BRAZING PROCESS STEP 6: CLEANING THE BRAZED JOINT

After you've brazed the assembly, you have to clean it. And cleaning is usually a two-step operation. First— removal of the flux residues. Second— pickling to remove any oxide scale formed during the brazing process.

### Flux Removal

Flux removal is a simple, but essential operation. (Flux residues are chemically corrosive and, if not removed, could weaken certain joints.) Since most brazing fluxes are water soluble, the easiest way to remove them is to quench the assembly in hot water (120°F/50°C or hotter). Best bet is to immerse them while they're still hot, just making sure that the filler metal has solidified completely before quenching. The glass-like flux residues will usually crack and flake off. If they're a little stubborn, brush them lightly with a wire brush while the assembly is still in the hot water.

Depending on your brazing process, you may need to perform post-braze joint cleaning to remove residual flux. This step can be crucial since most fluxes are corrosive, such as the pictured refrigeration line corrosion.

## Reasons to Remove Flux

Let's examine five reasons why post-braze flux removal is important:

1. You cannot inspect a joint that is covered with flux.
2. Flux can act as a bonding agent and may be holding the joint together, without successful brazing. This joint would fail during service.
3. In pressure service, flux may mask pinholes in a braze joint, even though it withstands a pressure test. The joint would leak soon after being placed into service.
4. Flux is hygroscopic, so residual flux attracts available water from the environment. This leads to corrosion.
5. Paint or other coatings do not stick to areas covered with residual flux.

## Methods for Flux Removal

After brazing, flux forms a hard, glass-like surface and can be difficult to remove. What is the best cleaning method? You can remove excess flux by various means; the most cost-effective approaches involve water.

Industry flux standards focus on water-based fluxes. AMS 3410 and AMS 3411 stipulate that all fluxes conforming to these specifications should be soluble in water at 175°F/79°C or less after brazing. Therefore, brazing fluxes are typically designed to dissolve in water.

The most common methods for post-braze flux removal are:

### Soaking/wetting

Use hot water with agitation in a soak tank to remove excess flux immediately following the braze operation, and then dry the assembly. When soaking is not possible, use a wire brush along with a spray bottle or wet towel. When using a soak bath of any kind, change the solution periodically to avoid saturating the cleaning solution.

### Quenching

This process induces a thermal shock that cracks off residual flux. When quenching a brazed part in hot water, take care to avoid compromising the braze joint. Quench only after the braze filler metal has solidified to avoid cracks or rough braze joints. Note that quenching can affect base material mechanical properties. Do not quench materials with large differences in coefficients of thermal expansion to avoid cracks in the base materials and tears within the braze alloy.

You can use more elaborate methods of removing flux as well—an ultrasonic cleaning tank to speed the action of the hot water, or live steam. Additional cleaning methods include:

- Steam lance cleaning - This process employs superheated steam under pressure to dissolve and blast away flux residue.
- Chemical cleaning - You can use an acidic or basic solution, generally with short soak times to avoid deteriorating the base materials. For chemical soaks, monitor the pH level to determine when to change the solution.
- Mechanical cleaning - Clean residue from brazed joints with a wire brush or by sandblasting. Be advised that soft metals-including aluminum-require extra care, as they are vulnerable to the embedding of particles.

Always ensure that your cleaning method is compatible with base metal properties. Some metal groups achieve a desired effect from a special treatment after cleaning. Stainless-steel and aluminum parts, for example, may benefit from chemical immersion to improve surface corrosion resistance.



The only time you run into trouble removing flux is when you haven't used enough of it to begin with, or you've overheated the parts during the brazing process. Then the flux becomes totally saturated with oxides, usually turning green or black. In this case, the flux has to be removed by a mild acid solution. A 25% hydrochloric acid bath (heated to 140-160°F/60-70°C) will usually dissolve the most stubborn flux residues. Simply agitate the brazed assembly in this solution for 30 seconds to 2 minutes. No need to brush. A word of caution, however—acid solutions are potent, so when quenching hot brazed assemblies in an acid bath, be sure to wear a face shield and gloves.

After you've gotten rid of the flux, use a pickling solution to remove any oxides that remain on areas that were unprotected by flux during the brazing process. The best pickle to use is generally the one recommended by the manufacturer of the brazing materials you're using. Highly oxidizing pickling solutions, such as bright dips containing nitric acid, should be avoided if possible, as they attack the silver filler metal. If you do find it necessary to use them, keep the pickling time very short.

## Recommended pickling solutions for post-braze removal of oxides

Application	Formulation	Comments
Oxide removal from copper, brass, bronze, nickel silver and other copper alloys containing high percentages of copper.	10 to 25% hot sulphuric acid with 5-10% potassium dichromate added.	Pickling can be done at same time flux is removed. Will work on carbon steels, but if pickle is contaminated with copper, the copper will plate out on the steel and will have to be removed mechanically, This sulphuric pickle will remove copper or cuprous oxide stains from copper alloys. It is an oxidizing pickle, and will discolor the silver filler metal, leaving it a dull gray.

Application	Formulation	Comments
Oxide removal from irons and steels.	A 50% hydrochloric acid solution, used cold or warm. More diluted acid can be used (10-25%) at higher temperatures (140-160°F/60-70°C.)	A mixture of 1 part hydrochloric acid to 2 parts water can be used for Monel and other high nickel alloys. Pickling solution should be heated to about 180°F/80°C. Mechanical finishing is necessary for bright finishes. This HCl pickle is not like bright dips on nonferrous metals.
Oxide removal from stainless steels and alloys containing chromium.	20% sulphuric acid, 20% hydrochloric acid, 60% water, used at 170-180°F (75-80°C.)	This pickle is followed directly by a 10% nitric dip, and then a clean water rinse.
	20% hydrochloric acid, 10% nitric acid, 70% water, used at about 150°F (65°C.)	This pickle is more aggressive than the sulphuric-hydrochloric mixture listed above, and will etch both the steel and the filler metal.

**Note:** The pickles recommended above will work with any of the standard silver filler metals, and no specific instructions are required for the individual filler metals. The phos-copper and silver-bearing phos-copper filler metals are different, and then only when used on copper without flux. In this case, a hard

copper phosphate slag forms in small globules on the metal surface. Prolonged pickling in sulphuric acid will remove this slag, but a short pickle in 50% hydrochloric acid for a few minutes is more effective. When the brazed joint is to be plated or tinned, the removal of the slag is absolutely essential. A final mechanical cleaning, therefore, is advisable for work which is to be plated.

## Post-Cleaning Inspection of Brazed Joints

Depending on your brazing process, you may need to perform post-braze joint cleaning to remove residual flux. This step is crucial for several reasons; including the corrosive nature of most fluxes and the possibility that excess flux could contribute to joint failure. The most common cleaning methods involve water-specifically soaking/wetting and quenching.

## Discontinuities During Joint Inspection

Examining finished joints may be the final step in the brazing process, but inspection procedures should be incorporated into the design stage. Your methodology will depend on the application, service and end-user requirements plus regulatory codes and standards.

Define your acceptance criteria for any discontinuity with considerations for shape, orientation, location (surface or subsurface) and relationship to other discontinuities. Be sure to state acceptance limits in terms of minimum requirements.

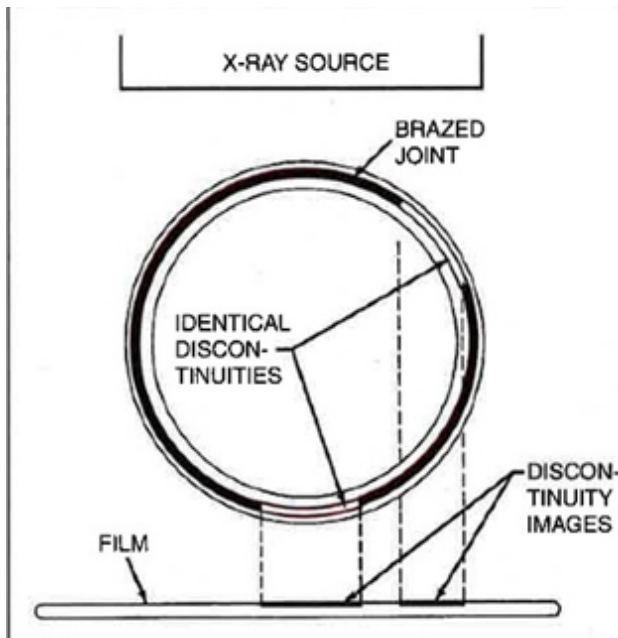
Common discontinuities of brazed joints, identified through nondestructive examination, include:

- Voids or porosity - an incomplete flow of brazing filler metal which can decrease joint strength and allow leakage-often caused by improper cleaning, incorrect joint clearance, insufficient filler metal, entrapped gas or thermal expansion.
- Flux entrapment - resulting from insufficient vents in the joint design-preventing the flow of filler metal and reducing joint strength as well as service life
- Discontinuous fillets - areas on the joint surface where the fillet is interrupted-usually discovered by visual inspection
- Base metal erosion (or alloying) - when the filler metal alloys with the base metal during brazing-movement of the alloy away from the fillet may cause erosion and reduce joint strength
- Unsatisfactory surface condition or appearance - excessive filler metal or rough surfaces-may act as corrosion sites and stress concentrators, also interfering with further testing

- Cracks - reducing strength and service life of the joint-may also be caused by liquid metal embrittlement.

## Brazed Joint Examination Methods: Nondestructive testing methods

Nondestructive testing methods of checking quality and specification conformance include:

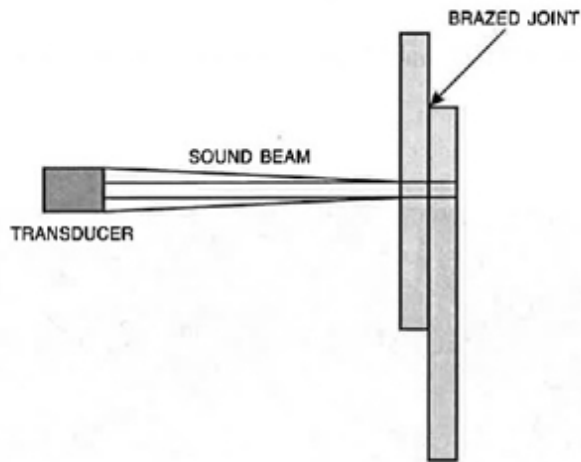


**Visual examination** - with or without magnification-for evaluating voids, porosity, surface cracks, fillet size and shape, discontinuous fillets plus base metal erosion (not internal issues such as porosity and lack of fill)

**Leak testing** - for determining gas- or liquid-tightness of a brazement. Pressure (or bubble leak) testing involves the application of air at greater-than-service pressures. Vacuum testing is useful for refrigeration equipment and detection of minute leaks, employing a mass spectrometer and a helium atmosphere.

**Radiographic examination** - useful in detecting internal flaws, large cracks and braze voids, if thickness and X-ray absorption ratios permit delineation of the brazing filler metal-cannot verify a proper metallurgical bond (pictured right)





**Proof testing** - subjecting a brazed joint to a one-time load greater than the service level-applied by hydrostatic methods, tensile loading or spin testing

**Ultrasonic examination** - a comparative method for evaluating joint quality, in immersion mode or contact mode-involves reflection of sound waves by surfaces, using a transducer to emit a pulse and receive echoes (pictured to the right)

**Liquid penetrant examination** - dye and fluorescent penetrants may detect cracks open to the surface of joints-not suitable for inspection of fillets, where some porosity is always present

**Acoustic emission testing** - evaluating the extent of discontinuity-using the premise that acoustic signals undergo a frequency or amplitude change when traveling across discontinuities

**Thermal transfer examination** - detects changes in thermal transfer rates due to discontinuities or unbrazed areas-images show brazed areas as light spots and void areas as dark spots

## Brazed Joint Examination Methods: Destructive testing methods

There are also several destructive and mechanical testing methods, often used in random or lot testing:

**Peel testing** - useful for evaluating lap joints and production quality control for general quality of the bond plus presence of voids and flux inclusions-where one member is held rigid while the other is peeled away from the joint

**Metallographic examination** - testing the general quality of joints-detecting porosity, poor filler metal flow, base metal erosion and improper fit

**Tension and shear testing** - determines strength of a joint in tension or in shear-used during qualification or development rather than production

**Fatigue testing** - testing the base metal plus the brazed joint-a time-consuming and costly method

**Impact testing** - determines the basic properties of brazed joints-generally used in a lab setting

**Torsion testing** - used on brazed joints in production quality control-for example, studs or screws brazed to thick sections

## Failed Brazing Inspection

The size, complexity and severity of the application determine the best inspection method, and several methods may be required. If you are unable to develop an accurate and dependable method of inspecting a critical brazed joint, consider revisiting your joint design to allow adequate inspection.

Examining finished joints may be the final step in the brazing process, but inspection procedures should be incorporated into the design stage. Both nondestructive and destructive methods may be employed, depending on the application, service and end-user requirements plus regulatory codes and standards.

Once the flux and oxides are removed from the brazed assembly, further finishing operations are seldom needed. The assembly is ready for use, or for the application of an electroplated finish. In the few instances where you need an ultra-clean finish, you can get it by polishing the assembly with a fine emery cloth. If the assemblies are going to be stored for use at a later time, give them a light rust-resistant protective coating by adding a water soluble oil to the final rinse water.

[Watch this video](#) for more on how to properly clean joints.